Organization and consequences of functional responses in microglia upon activation of the TLR4 complex

Dissertation

for the award of the degree

"Doctor rerum naturalium" (Dr. rer. nat.)

in the Molecular Medicine Study Program

at the Georg-August University Göttingen

submitted by

Hana Janova

Born in Prague, Czech Republic

Göttingen, 2014

Members of the Thesis Committee

Supervisor

Prof. Dr. Uwe-Karsten Hanisch
Department of Neuropathology
University Medicine Göttingen, University of Göttingen

Second member of the Thesis Committee

Prof. Dr. Wolfgang Brück
Department of Neuropathology
University Medicine Göttingen, University of Göttingen

Third member of the Thesis Committee

Prof. Dr. Dr. Hannelore Ehrenreich
Department of Clinical Neurosciences
Max Planck Institute for Experimental Medicine, Göttingen

Date of Disputation:

Affidavit

I hereby declare that I have written my Ph.D. thesis entitled "**Organization and Consequences of Functional Responses in Microglia upon Activation of the TLR4 complex**" independently and with no other sources and aids than quoted. This thesis has not been submitted elsewhere for any academic degree.

Göttingen, July 2014

_____
(Signature)

Abstract

Microglia are resident macrophage-like cells of the central nervous system (CNS) which constantly survey the tissue for signs of homeostatic disturbance. As the major immunocompetent effector cells in the brain parenchyma, they express a large variety of receptors for pathogen-associated molecular patterns (PAMPs). Among them, Toll-like receptor (TLR) 4 allows microglia to respond not only to bacterial infection but also to damage. Stimulation of TLR4 by bacterial lipopolysaccharide (LPS) as well as self-derived damage-associated molecular patterns (DAMPs) released upon tissue impairment triggers signaling via both TRIF- and MyD88-dependent routes. The ultimate secretion of cytokines and chemokines attracts and instructs peripheral immune cells to enable protection of the CNS as well as promotion of tissue regeneration. We show here that the TLR4 co-receptor CD14 is an essential gatekeeper for mounting immune reactions in the CNS to LPS and *E.coli* administration as well as upon mechanical trauma and ischemic stroke. Unlike extraneural macrophages, microglia employ CD14 to gain extreme sensitivity to very small amounts of LPS. At the same time, CD14 protects microglia from overshooting responses to high doses of LPS, thereby especially preventing an excessive production of the neutrophil chemoattractant CXCL1. Accordingly, CD14 supports the recruitment of monocytes and neutrophils into the CNS as challenged by low doses of LPS, while simultaneously preventing an augmented neutrophil influx upon exposure to high amounts of LPS or *E.coli*. Importantly, we demonstrate a mandatory requirement of CD14 in DAMP-triggered and TLR4-mediated immune reactions. CD14 deficiency (in *cd14$^{-/-}$* conditions) or block (e.g. by an antibody) completely abrogates microglial responses triggered by plasma fibronectin (as a representative DAMP) and impairs leukocyte infiltrations following traumatic CNS injury. Upon ischemic CNS injury, *cd14$^{-/-}$*mice do not only display fewer monocytes in the brain but also an enlarged stroke size. Notably, we found that interferon (IFN) β is a key element in the CD14-mediated containment of CXCL1 synthesis, suggesting a negative CD14/TLR4→TRIF→IFNβ→INAR1→Jak feedback loop on the MyD88-driven chemokine induction. Finally, even though CD14 orchestrates TLR4-mediated responses to infectious and non-infectious stimuli, its expression is under the control of various TLR ligands and cytokines. Thus, CD14-controlled functions of microglia are themselves subject to a versatile control by other CNS-resident and incoming peripheral cells. These regulations will allow for an incorporation or the exclusion of the damage-sensing capacity of the TLR4 complex during CNS responses to most diverse pathological scenarios.

Zusammenfassung

Mikroglia sind residente Makrophagen-artige Zellen des Zentralnervensystems (ZNS), die das Gewebe kontinuierlich auf Anzeichen homöostatischer Störungen überwachen. Als die wesentlichen immunkompetenten Effektorzellen im Hirnparenchym exprimieren sie eine Vielzahl von Rezeptoren für pathogen-assoziierte molekulare Strukturmuster (*pathogen-associated molecular patterns*, PAMPs). Zu diesen Rezeptoren zählt der *Toll-like receptor* (TLR) 4, der nicht nur Reaktionen der Mikroglia auf bakterielle Infektionen, sondern auch auf Gewebe?Schädigungen ermöglicht. Stimulation des TLR4 mit bakteriellem Lipopolysaccharid (LPS) und endogenen schädigung-sassoziierten molekularen Strukturen (*damage-associated molecular patterns*, DAMPs), die durch Gewebebeeinträchtigung freigesetzt werden, löst sowohl TRIF- als auch MyD88-abhängige Signalkaskaden aus. Die damit induzierte Freisetzung von Zytokinen und Chemokinen rekrutiert und instruiert periphere Immunzellen für eine Protektion und unterstützende Geweberegeneration des ZNS. Wir zeigen hier, dass der TLR4-Korezeptor CD14 ein essenzieller *gate keeper* für die Generierung von Immunantworten im ZNS ist, die durch LPS oder *E. coli*-Verabreichung, aber auch durch mechanisches Trauma und ischämischen Schlaganfall ausgelöst werden. In gewissem Gegensatz zu extraneuralen Makrophagen nutzen Mikroglia CD14 zur Erlangung einer extremen Sensitivität gegenüber sehr geringen LPS-Mengen. Gleichzeitig schützt CD14 Mikroglia vor überschießenden Reaktionen auf hohe LPS-Dosen und verhindert dabei insbesondere die exzessive Produktion von CXCL1, eines chemoattraktiven Signals für neutrophile Granulozyten. Entsprechend unterstützt CD14 die ZNS-Rekrutierung von Monozyten und Neutrophilen durch niedrige LPS-Dosen, während es die verstärkte Einwanderung von Neutrophilen durch hohe Dosen von LPS oder *E. coli* verhindert. Als eine besonders wichtige Funktion beschreiben wir dabei die absolute CD14-Abhängigkeit DAMP-ausgelöster und TLR4-vermittelter Immunreaktionen. CD14-Defizienz (unter *cd14*^{-/-}-Bedingungen) oder CD14 Blockade (durch Antikörper) löschen mikrogliale Reaktionen, die durch Plasma-Fibronektin (als repräsentatives DAMP-Molekül) ausgelöst werden können, komplett aus und beeinträchtigen die Leukozyten-Infiltration nach ZNS-Trauma. Bei einer ischämischen ZNS-Schädigung weisen *cd14*^{-/-}-Mäuse im Gehirn nicht nur weniger Monozyten auf, sondern gleichzeitig ein vergrößertes Infarktvolumen. Wir konnten für Interferon (IFN) β eine Schlüsselfunktion in der CD14-vermittelten Eindämmung der CXCL1-Synthese darstellen, die auf eine negative CD14/TLR4→TRIF→IFNβ→INAR1→Jak- Rückkopplung für MyD88-getriebene Chemokine schließen lässt. Obwohl CD14 somit TLR4-vermittelte Reaktionen auf infektiöse und nicht-infektiöse Agenzien orchestriert, wird seine Expression durch verschiedene TLR-Liganden und Zytokine reguliert. Letztlich unterliegen damit CD14-kontrollierte Funktionen selbst einer komplexen Kontrolle durch ZNS-residente

und eingewanderte periphere Zellen. Diese Regulationen können über die Einbeziehung oder den Ausschluss der Kapazitäten des TLR4-Komplexes für eine Schadenserkennung während der ZNS-Reaktionen in unterschiedlichsten pathologischen Szenarien entscheiden.

Table of Contents

List of Figures

List of Tables

Abbreviations

APC	-	antigen presenting cell
APC	-	allophycocyanin
Aβ	-	amyloid β
BBB	-	blood brain barrier
BMDM	-	bone marrow-derived macrophages
BTK	-	Bruton's tyrosine kinase
CCR2	-	C-C chemokine receptor
CD	-	cluster of differentiation
CLR	-	C-type lectin receptor
CNS	-	central nervous system
CpG	-	cytosin-phosphatidyl-guanin
CSF	-	cerebrospinal fluid
CXC_3CR1	-	CX3C-chemokine receptor 1
CXCL	-	chemokine (C-X-C motif) ligand
CXCR	-	chemokine (C-X-C motif) receptor
DAMP	-	damage/danger-associated molecular pattern
DC	-	dendritic cell
ds	-	double-stranded
DsRed	-	*Discosoma* red fluorescent protein
ECM	-	extracellular matrix
ELISA	-	enzyme-linked immunosorbent assay
FACS	-	fluorescence-activated cell sorting
FITC	-	fluorescein isothiocyanate
FN	-	fibronectin
FSC	-	forward scatter
G-CSFR	-	granulocyte colony-stimulating factor receptor
GFAP	-	glial fibrillary acidic protein
GPI	-	glycosylphophatidylinositol
HMGB1	-	high mobility group protein
Hsp	-	heat shock protein

Iba-1	-	ionized calcium-binding adaptor molecule 1
IFN	-	interferon
IFNAR	-	IFN-α/β receptor
IL	-	interleukin
IRF	-	interferon regulatory factor
ISGF3	-	IFN-stimulated gene (ISG) factor 3
ISRE	-	IFN-stimulated response elements
LBP	-	LPS binding protein
LLR	-	leucin rich repeats
LPS	-	lipopolysaccharide
LTA	-	lipoteichoic acid
Ly-6C	-	lymphocyte antigen 6C
Ly-6G	-	lymphocyte antigen 6G
Mac3	-	macrophage antigen 3
MAL	-	MyD88 adaptor-like
MALP-2	-	macrophage-activating lipopeptide 2
MAPK	-	mitogen activated protein kinase
MCAO	-	middle cerebral artery occlusion
mCD14	-	mebrane CD14
MD-2	-	myeloid differentiation factor-2
ME	-	module EigenGene
MFI	-	median fluorescence intensity
MHC	-	major histocompatibility complex class molecules
Myb	-	myeloblastosis
NETs	-	neutrophil extracellular traps
NF-κB	-	nuclear factor κB
NK cells	-	natural killer cells
NLR	-	NOD-like receptor
NO	-	nitric oxide
PAMP	-	pathogen associated molecular pattern
PE	-	phycoerythrin
PerCP	-	peridinin chlorophyll

pFN	-	plasma fibronectin
PGE2	-	prostaglandin E2
PLC	-	phospholipase C
PRR	-	pattern-recognition receptor
qRT-PCR	-	quantitative real time PCR
RLR	-	RIG-I-like receptor
ROS	-	reactive oxygen species
sCD14	-	soluble CD14
ss	-	single-stranded
SSC	-	side scatter
STAT	-	signal transducer and activator of transcription
Syk	-	spleen tyrosine kinase
TICAM	-	TIR domain-containing adaptor molecule
TIR	-	Toll-interleukin (IL)-1
TIRAP	-	TIR domain containing adaptor protein
TLR	-	Toll-like receptor
TNF	-	tumor necrosis factor
TRAM	-	TRIF-related adaptor molecule
TRIF	-	TIR-domain-containing adaptor-inducing interferon-β
WGCN	-	weighted gene co-expression network analysis
wt	-	wildtype

1. Introduction

1.1 Innate immunity

Vertebrates have developed a sophisticated immune system that enables them to survive in a world of microbes which can even trigger life-threatening diseases. This system comprises innate and adaptive immunity. Innate immunity is responsible for the first very quick response. However, it is not as specific as the adaptive immunity and offers only limited memory. The main components of innate immunity are physical barriers (e.g. epithelial layers), circulating effector proteins (e.g. complement), cytokines and cells carrying a range of functions for the recognition and elimination of infectious agents. The lastly mentioned cells include neutrophils, monocytes, macrophages, dendritic cells (DCs) and natural killer (NK) cells that play crucial roles in the immediate sensing of pathogens which invaded the body. They also guarantee that an adaptive immune response can be initiated. As effector cells, and establishing first measures of host defense, they offer mechanisms of killing as well as clearing pathogens and, after their elimination, restore the lost tissue homeostasis. Moreover, cells of the innate immunity can also respond to signs of danger which do not only arise from infection but also from tissue injury and cell impairment.

1.2 Neutrophils – the first line of defense

Neutrophils are generated in the bone marrow from myeloid precursors throughout life. In healthy conditions, they circulate in the blood stream for a short period (12.5 hours for mouse cells and 5.4 days for human neutrophils) (Pillay et al., 2010), after which they are eventually cleared from the circulation in the liver, spleen and bone marrow (Kolaczkowska and Kubes, 2013). However, their life span can be prolonged several times during inflammation, so that they can also contribute to the resolution of inflammation (Ortega-Gómez et al., 2013). Neutrophils are the first line of defense against bacterial and fungal pathogens. Their release from the bone marrow pool and migration to the site of inflammation are accomplished by signals through CXC-chemokine receptor 2 (CXCR2) (i.e. the receptor for the chemokines chemokine CXC ligand (CXCL) 1 and 2), granulocyte colony-stimulating factor receptor (G-CSFR) and Toll-like receptors (TLRs) (Borregaard, 2010). Neutrophils eliminate the pathogens either intracellularly or extracelullarly. Intracellular degradation is executed after a phagocytosis by antibacterial proteins (cathepsins, defensins, lactoferrin and lysozyme) and reactive oxygen species (ROS). Neutrophils kill the extracellular microorganisms by antibacterial proteins released into the extracellular milieu or by breaking down their nuclear contents and creating NETs (neutrophil

extracellular traps) (Brinkmann et al., 2004). Neutrophils are on one hand necessary for successful clearance of a quickly spreading infection. On the other hand, their high toxicity can also be detrimental, causing tissue damage, especially during processes of sterile inflammation (Chen and Nunez, 2010). Therefore, neutrophil recruitment must be kept under tight control.

During the last decades, many studies have been addressing the toxic as well as the beneficial character of neutrophils. For the tracking and monitoring purposes, an antibody against Ly-6G turned out to be a suitable tool. This receptor is specifically expressed by neutrophils that can be thereby easily distinguished from other cells in the blood or within inflammatory tissues (Fleming et al., 1993).

1.3   Monocytes

Monocytes are a subpopulation of mononuclear leukocytes with a bean-shaped nucleus, which are derived from precursors in the bone marrow. After a series of maturational steps, they are released into the bloodstream, from where they can transmigrate into a variety of tissues and differentiate into resident macrophages or DCs. Two major subtypes of murine monocytes are distinguishable on the basis of their surface receptor expression (Geissmann et al., 2003). Inflammatory monocytes express high levels of Ly-6C and CC-chemokine receptor 2 (CCR2), but low levels of CX3C-chemokine receptor 1 (CX_3CR1, also known as the fractalkine receptor). They egress from the bone marrow and migrate to the site of infection and inflammation in a CCR2-dependent manner, following the gradient of the chemokines CC ligand (CCL) 2 and 7 (Tsou et al., 2007). Here, they then mediate microbicidal activity — they phagocytose foreign particles, including pathogens, and produce a variety of cytokines and chemokines. The second principal monocyte subpopulation, referred as patrolling monocytes, expresses high levels of CX_3CR1 and low levels of CCR2 as well as Ly-6C. Patrolling monocytes are less motile. They rather adhere and migrate along the luminal surface of endothelial cells and serve as intravascular housekeepers (Auffray et al., 2007; Carlin et al., 2013). However, patrolling monocytes may also rapidly infiltrate into the damaged site, depending on various stimuli (Auffray et al., 2007). In the absence of inflammation, Ly-6C^{hi} monocytes can return to the bone marrow and there differentiate into Ly-6C^{lo} monocytes (Sunderkötter et al., 2004). In the human system, other receptors have been used for a classification of monocytes into two major subclasses, namely CD14 and CD16 (Shi and Pamer, 2011). CD14^{hi}CD16$^-$ cells have been called classical monocytes, since their phenotype matches the original description of monocytes. The CD14$^+$CD16$^+$ monocytes express in addition CD32 and high amounts of major histocompatibility complex (MHC) class II molecules (Gordon and Taylor, 2005).

1.4   Inflammation, chemoattraction, transmigration and resolution of inflammation

Inflammation is a patho/physiological process that is necessary for an elimination of infectious agents, clearance of damaged tissue as well as subsequent resolution and restoration of homeostasis. Monocytes/monocyte-derived macrophages, neutrophils and resident macrophages all contribute to the inflammatory cascade. The resident macrophages work as sentinel cells that react to tissue damage and/or pathogen invasion in their neighborhood by regulating the infiltration of leukocytes via expression of cytokines and chemokines as well as by increasing the permeability of local blood vessels (Shi and Pamer, 2011; Soehnlein and Lindbom, 2010). Neutrophils, as the first line of defense, follow chemotactic molecules, which are bound to the endothelium via glycoaminoglycans (Sadik et al., 2011). During recruitment to the site of inflammation, neutrophils undergo a series of steps involving tethering, rolling, adhesion, crawling and finally transmigration. Neutrophils infiltrate within a couple of hours and they do not only eliminate the pathogens, but also produce and modify chemokines to emphasize the call for monocytes. Monocytes are recruited as the second line of defense after 1-3 days (Kantari et al., 2008), and they follow the same paradigm of leukocyte extravasation as neutrophils. Once the neutrophils, monocytes and local macrophages have removed the inflammatory stimuli, the inflammation must be resolved to prevent additional tissue damage that could lead to chronic inflammation. Resolution of inflammation is a complex process in which further neutrophil influx is stopped, the remaining neutrophils die by apoptosis and these dead cells are actively cleared by the infiltrated monocytes and local macrophages. The ingestion of apoptotic cells by macrophages leads to a switch in their phenotype from a pro- to an anti-inflammatory orientation (Ortega-Gómez et al., 2013). Reprogrammed macrophages will thus stop killing the tissue-resident cells and start to produce growth factors, which enable restoration of the damaged tissue.

1.5   Resident macrophages

Resident marcrophages are distributed throughout the body and their phenotype is adapted to the needs of their environment, e.g. in bones (osteoclasts), the lung (alveolar macrophages), interstitial connective tissue (histiocytes), the liver (Kupffer cells), the spleen (marginal-zone and metallophilic macrophages) as well as the central nervous system (CNS), which harbors or associates with the parenchymal microglia, the perivascular cells as well as the meningeal and choroid plexus macrophages (Murray and Wynn, 2011).

1.6   Microglia

Microglia are the principal innate immune cells of the CNS, serving a wide range of functions as housekeepers, sensors and effectors under normal healthy as well as disease conditions (Hanisch and Kettenmann, 2007; Kettenmann et al., 2011). They have been generally considered as the resident macrophages of the CNS, accounting for 5-20% of all cells in the parenchyma, but varying in density and features depending on their location (Gertig and Hanisch, 2014; Hanisch, 2013; Kim et al., 2000; Lawson et al., 1990). In comparison to mononuclear innate immune cells of the blood, they are derived from the primitive myeoloid progenitors emerging from the extra-embryonic yolk sac before day 8 (Ginhoux et al., 2010). This process happens in a Myb-independent manner (Schulz et al., 2012) via transcription factor PU.1- and interferon regulatory factor (IRF) 8-dependent pathways (Kierdorf et al., 2013). After settling in the CNS, they are maintained by local proliferation of resident progenitors, independent of replenishment by circulating monocytic precursors (Elmore et al., 2014).

Under normal physiological conditions, microglia have extended, branched processes (having caused the description by a 'ramified' appearance), which are used in a highly motile fashion to constantly survey the CNS, thereby looking for signs of disturbance (Nimmerjahn et al., 2005) and nursing synaptic connections (Wake et al., 2009).

Apart from being innate immune cells, they contribute to the postnatal development and the plasticity of the neuronal circuitry. Microglia remove redundant synaptic material in a process called synaptic pruning (Paolicelli et al., 2011; Schafer et al., 2012). In the adult hippocampus, unchallenged microglia phagocytose the apoptotic stem and progenitor cells in the subgranule zone (SGZ) that were pruned and thus not integrated into hippocampal circuitry to participate in some forms of learning and memory, mood regulation, and fear conditioning (Kempermann, 2008; Parkhurst et al., 2013; Sierra et al., 2010; Tremblay et al., 2011; Zhan et al., 2014).

Upon tissue injury or infection, microglia shift their phenotype from monitoring guards toward executive immune cells (Eggen et al., 2013; Hanisch and Kettenmann, 2007). For that, they undergo morphological and molecular changes enabling them to produce a variety of cytokines, chemokines, lipid mediators, enzymes, ROS and nitric oxide (NO) (Hanisch, 2012). This halts infection spread as well as enables clearance of neurotoxic factors and debris. Once the stimuli are too intense or chronic, microglia are not able to eliminate the source of danger on their own and they attract immune cells from the periphery (like neutrophils and monocytes) (London et al., 2013a). Microglia can be distinguished from these freshly incoming cells by flow cytometry on the basis of lower CD45 expression. However, within few days, monocytes differentiate into macrophages, which are phenotypicaly similar to the 'activated'

microglia. In the past, these newly recruited monocytes were considered to replenish the microglial pool and to become functional microglia, referred as „blood-derived microglia" (Bechmann et al., 2005; Priller et al., 2001; Simard et al., 2006). However, only recently advanced technologies have been able to demonstrate that newly incoming cells have specific non-redundant functions and that they do not remain in the brain to form new microglia properly (Ajami et al., 2007; Hashimoto et al., 2013).

In neuropathologies, microglia were previously considered to be predominantly neurotoxic and tissue-damaging (Block et al., 2007; Schwartz et al., 2006), but new studies clearly show also their beneficial contributions. For instance, they facilitate oligodendrogenesis during multiple sclerosis (Butovsky et al., 2006) and protect the neurons from ischemic damage (Neumann et al., 2006). Actually, microglial activation and activities are primarily protective and beneficial, and it is only their acute excessive, chronic or maladapted action that associates with a failure to protect or to foster detrimental cascades (Hanisch, 2012; Hanisch and Kettenmann, 2007). Moreover, novel functions under normal conditions have been postulated, such as a participation in the myelin turnover (Fitzner et al., 2011), and it is becoming clear that these cells have a fundamental impact on the functionality of the CNS, even including higher levels of brain functions (Zhan et al., 2014).

Considering their immune nature, microglia can also serve on demand as antigen presenting cells (APCs) via upregulation of MHC I and II as well as co-stimulatory molecules CD80 and CD86 (B7.1 and B7.2).

These very heterogenous and sometimes contradictory roles of microglia in infection and homeostasis could be partially explained by considering the existence of different responder subtypes of microglia, a concept still awaiting further investigation (Gertig and Hanisch, 2014; Hanisch, 2013).

1.7 Toll-like receptors

Innate immune cells are able to rapidly respond once they face danger. This feature is allowed by expression of germline-encoded pattern-recognition receptors (PRRs), which recognize molecular determinants known as pathogen-associated molecular patterns (PAMPs). They comprise structural motifs that are shared and conserved among multiple pathogens. In contrast to variable receptors of adaptive immune cells (like the B and T cell receptors), PRRs are encoded by complete genes without a clonal variety and without any gene re-arrangements. PRRs cover several receptor families, such as membrane-bound C-type lectin receptors (CLRs), NOD-like receptors (NLRs) and RIG-I-like receptors (RLRs) (Kawai and Akira, 2011). However, the best-characterized PRRs, in terms of known ligands and signaling mechanisms, are members of the Toll-like receptor (TLR) family. Thus far, 13 TLRs have been

described in mice and 11 in humans. TLRs are type I transmembrane proteins with an extracellular and intracellular domain. The extracellular domain contains leucine-rich repeats and is responsible for ligand binding. The cytosolic Toll-interleukin(IL)-1 receptor (TIR) domain enables signal transduction (Akira et al., 2006). TLRs are expressed on the cell surface (TLR1, TLR2, TLR4, TLR5 and TLR6) and in intracellular compartments (TLR3, TLR7, TLR8, and TLR9). Intracellular location of TLRs allows the innate cells to sense the nucleic acids of viruses and bacteria, or such material within infected cells upon their phagocytic uptake. Lipoproteins and peptidoglycan are recognized by TLR1, TLR2 and TLR6, double-stranded (ds) RNA by TLR3, lipopolysaccharide (LPS) by TLR4, flagellin by TLR5, single-stranded (ss) RNA by TLR7 and TLR8 and DNA (e.g., cytosin-phosphatidyl-guanin, CpG) by TLR9 (Hanke and Kielian, 2011). The ligands for TLR10 and TLR11 are still unknown. Some TLRs interact with each other, such as TLR2-TLR1 and TLR2-TLR6. This heterodimerization can then change the specificity of each separate partner and thereby enlarge the repertoire of accepted ligands while sharing signaling outcomes. Other heterodimerizations were reported for TLR4 and TLR2 as well as TLR6 (Stewart et al., 2010; Wang et al., 2014).

Binding of a ligand to a TLR initiates downstream signaling events, which depend on the particular TLR as well as on TIR domain-containing sorting and signaling adaptor molecules, namely myeloid differentiation primary response 88 (MyD88), TIR domain containing adaptor protein (TIRAP)/MyD88 adaptor-like MAL, TIR-domain-containing adaptor-inducing interferon-β (TRIF) and TRIF-related adaptor molecule (TRAM)/TIR domain-containing adaptor molecule 2 (TICAM-2) (Akira et al., 2006; Kawai and Akira, 2010). MyD88 is an adaptor protein used by all TLRs except for TLR3. It leads to the activation of kinases and transcription factors, such as mitogen activated protein kinase (MAPK) and nuclear factor κB (NF-κB), culminating in a production of pro-inflammatory cytokines, e.g. tumor necrosis factor (TNF) α or interleukin (IL) 6, and chemokines, e.g. CCL2 or CXCL1. TLR3 and TLR4 recruit the adaptor protein TRIF in an alternative pathway that leads via activation of NF-κB and interferon regulatory factor (IRF) 3 to the induction of type I interferons, i.e. IFNα/IFNβ, and additional pro-inflammatory chemokines, like CCL5. TLRs also contribute to the adaptive immunity, since they trigger expression of co-stimulatory molecules on APCs (e.g., DCs and macrophages) and drive the production of cytokines, such as IL-12 that are necessary for successful activation, differentiation and proliferation of T cells (Hertz et al., 2001; Pasare and Medzhitov, 2004). In the CNS, microglia express most of the TLRs (TLR1-4 and TLR6-9), however, also neurons, astrocytes and oligodendrocytes are equipped with selected TLRs (Kielian, 2009).

1.8 TLR4

TLR4 was the first member of the TLR family to be discovered. In contrast to other TLRs, TLR4 recruits both MyD88 and TRIF adaptor molecules for signaling. This is achieved indirectly, via the sorting proteins TIRAP/MAL and TRAM/TICAM-2, respectively. In the periphery, TLR4 is widely expressed on innate immune cells (such as macrophages, monocytes, DCs or neutrophils) and non-immune cells, like endothelial cells. Small amounts are also found on adaptive immune cells (T and B cells) (McGettrick and O'Neill, 2007). In the CNS, microglia are the only cells that have been definitely confirmed to have TLR4 (Lehnardt et al., 2003; McGettrick and O'Neill, 2007).

LPS, the cell wall component of Gram-negative bacteria, is the best known PAMP that triggers an immune response via TLR4 signaling (Beutler and Rietschel, 2003). LPS exists in different variants (chemotypes) that are parts of miscellaneous bacterial strains. LPS structures can differ by acylation and phosphorylation. Moreover, based on the complexity of the O-polysaccharide moiety as bound to the lipid A trunk of the structure and associating with the colony morphology, one can distinguish S ("smooth") and R ("rough") LPS chemotypes (Raetz and Whitfield, 2002). Induction of cyto- and chemokines is a most prominent functional result of LPS binding to TLR4. Each of the released factors may depend on the recruitment of one or both of the adaptor proteins to a varying extent. For instance, in microglia, TNFα, IL-6, IL-12p40 and CXCL1 are strictly MyD88-dependent, while others, like CCL2 or CCL5, are more promiscuous, using both MyD88 and TRIF adaptors (Regen et al., 2011).

The recognition of a LPS structure and its subsequent signaling are not held by TLR4 alone. TLR4 forms a complex with other proteins. LPS binding protein (LBP) binds in the plasma avidly LPS aggregates and transfers them to the co-receptor CD14 (Wright et al., 1990). CD14 extracts the monomeric molecules of LPS and presents them to the TLR4-MD2 complex, thereby forming a 'm' shaped 2:2:2 TLR4, myeloid differentiation factor-2 (MD-2) and LPS complex (Park and Lee, 2013). Apart from these directly involved proteins, TLR4 interacts further with different non-TLR proteins, including integrins (CD11b), Fc receptors or chemokine receptors (e.g. CXCR4) (Ling et al., 2014; Triantafilou and Triantafilou, 2002) and also other TLR receptors (e.g. TLR2 or TLR6) (Stewart et al., 2010; Wang et al., 2014).

1.9 CD14 as a TLR4 co-receptor

CD14 is a 55 kDa glycoprotein which was initially identified on human monocytes as a surface marker of myeloid lineage cells (Goyert et al., 1986). CD14 exists in two forms, as a membrane-anchored and as a soluble variant. The surface-expressed mCD14 is glycosylphophatidylinositol (GPI)-anchored, and its expression was identified also on tissue macrophages (such as microglia, Kupffer cells and peritoneal,

lung or spleen macrophages), DCs, neutrophils and gingival fibroblasts (Gautier et al., 2012; Landmann et al., 2000). The soluble form of CD14 (sCD14) is present in the serum (in human blood at 2-3 µg/ml) and extravascular fluids (Tapping and Tobias, 2000). sCD14 is liberated as the 55 kDa form by escape from GPI anchoring, or as the 49 kDa version upon proteolytic cleavage (Landmann et al., 2000). During infection, the expression of mCD14 by cells is induced and the concentration of sCD14 in the blood and cerebrospinal fluid (CSF) can get elevated. Epithelial and endothelial cells can utilize the sCD14-LBP complex instead of mCD14 (as they lack expression of the latter) to thereby respond to LPS (Pugin et al., 1993).

Due to the same number of leucin rich repeats (LRR) motifs, mouse CD14 forms a dimer that has a horseshoe-like shape very similar to TLR4. The human form of CD14 has structural similarities to the mouse counterpart, but it purifies and crystallizes as a monomer and has an expanded N-terminal pocket with different rim residues (Kelley et al., 2013).

CD14 was initially described as a chaperon for LPS binding to the TLR4-MD2 complex, which enables the immune cells to initiate the signaling already at picomolar concentrations of LPS (Gioannini et al., 2004). The role of CD14 was demonstrated for the TLR4-TIRAP-MyD88-dependent signaling that is induced from the plasma membrane and that leads to the production of pro-inflammatory cytokines (e.g. TNFα) via NF-κB activation. Subsequently, and with an involvement of spleen tyrosine kinase (Syk) and phospholipase (PL)Cγ2, CD14 facilitates the endocytosis of the whole TLR4 complex, allowing for the second wave of signaling from the endosomal compartment (Zanoni et al., 2011), which is TRAM-TRIF-dependent and culminates in IFNβ production (Kagan et al., 2008; Kawai et al., 2001). The internalization of the TLR4 complex with LPS is dynamin- and clathrin-dependent, and monomeric G-protein Rab11a was found to be involved in the recruitment of TLR4 to phagosomes (Husebye et al., 2006, 2010; Kagan et al., 2008).

In peritoneal macrophages, CD14 not only enhanced the sensitivity to track low amounts of LPS, but it also helped to distinguish between S- and R-LPS variants (Gangloff et al., 2005), with distinct signaling consequences (Jiang et al., 2005). In the absence of CD14, these cells could not induce the TRIF-dependent production of IFNβ in response to any of the LPS chemotypes, and also irrespective of the concentration. In contrast, R-LPS could still elicit induction of TNFα via the TIRAP-MyD88-dependent pathway (Jiang et al., 2005). In contrast, our group found that in the absence of CD14, microglia maintained the induction of cyto- and chemokines to higher doses of S-LPS, as well as to R-LPS chemotypes. The analyses of the total release by CD14-deficient microglia (isolated from c$d14^{-/-}$ mice) even revealed an extensive production of some of the factors (CXCL1, IL-6, IL-12p40 and TNFα), while

others (CCL2, CCL3 and CCL5) were produced at the same level in both genotypes (Regen et al., 2011). Interestingly, this work also revealed that microglia acquire the ability to distinguish between S- and R-LPS forms as part of their postnatal development (Scheffel et al., 2012). These findings contribute to the notion that the CD14/TLR4 complex may have distinct features in microglia as compared to extraneural macrophage populations.

Even though mCD14 is a GPI-anchored protein with no expected direct link to cytosolic signaling, TLR4-independent signal transduction was required for calcium mobilization in DCs (Zanoni et al., 2009). This calcium influx was a prerequisite for further nuclear factor of activated T-cells (NFAT) activation, which regulated production of IL-2 and prostaglandin E2 (PGE2) and was dependent of an induction of Src and PLCγ2 activation (Zanoni et al., 2009). These findings show the diverse role of CD14 in the organization of responses to LPS as triggered through TLR4.

However, CD14 can also serve as a partner of TLR1, 2, 3, 6, 7 and 9 (Akashi-Takamura and Miyake, 2008; Baumann et al., 2010; Lee et al., 2006; Weber et al., 2012; Yoshimura et al., 1999; Zanoni and Granucci, 2013a). As a TLR1/2 co-receptor, CD14 binds microbial products, such as lipoteichoic acid (LTA) or synthetic triacylated lipoprotein Pam_3CSK_4, and mediates TLR2-induced NF-κB activation from endosomal compartments following to a clathrin/dynamin-dependent endocytosis (Brandt et al., 2013). Only the CD14-mediated uptake of poly(I:C), bacterial DNA cytosin-phosphatidyl-guanin (CpG) and ssRNA could lead to TLR3, TLR7 and TLR9 response, respectively (Baumann et al., 2010; Lee et al., 2006).

The role of CD14 *in vivo* during Gram-negative infectious diseases and LPS administration depends on the affected tissue (region) and the strength of the challenge. Injection of LPS or *E.coli* into the peritoneum of *cd14*^{-/-} mice did not lead to septic shock, as in the case of wild-type (wt) mice (Haziot et al., 1996), which is then probably accompanied by higher numbers of *E.coli* found in the bloodstream and tissue samples, as seen in the animals injected with anti-CD14 antibody (Opal et al., 2003). In another sepsis model (cecal ligation and puncture model), the mortality of animals was not affected by a knockout of CD14, but still a phenotype was manifested upon measurement of lower pro-inflammatory cyto- and chemokine levels in the blood, compared to the wt situation (Ebong et al., 2001). Furthermore, mice deficient in CD14 or treated with anti-CD14 antibody (anti-CD14 Ab) were not able to respond to LPS treatment, which resulted in attenuated pulmonary edema and lower neutrophil recruitment (Knapp et al., 2006; Tasaka et al., 2003). The neutrophil influx into lungs of *cd14*^{-/-} mice was also lower, accompanied by less TNFα after low-dosed LPS treatment. However, high amounts of S-LPS led to the opposite result, with more TNFα and neutrophils in the lungs of *cd14*^{-/-} mice than in their wt counterparts (Anas et al., 2010). Similarly, CD14 was necessary in infection with low doses of *Klebsiella*

pneumonia (*K. pneumonia)* to trigger TNFα production and neutrophil infiltration, that enabled bacteria clearance and survival of the animals. In contrast, anti-CD14 Ab did not affect the outcome after infection with high doses of bacteria (Roy et al., 2001).

In the Gram-positive infection, CD14 apparently binds cell wall components of Gram-positive bacteria (like LTA) and interacts with TLR2 (Schröder et al., 2003; Yoshimura et al., 1999). Soluble CD14 as well as membrane CD14 were shown to be necessary for a successful colonization of the respiratory tract by *Streptococcus pneumoniea (S.pneumonia)* (Dessing et al., 2007). In *cd14$^{-/-}$* mice, higher levels of CXCR2 receptors on neutrophils and increased CXCL2 production were induced after subarachnoidal injection of *S. pneumoniea*. This resulted in excessive neutrophil infiltration in the cerebrospinal fluid and subsequent higher mortality in comparison to wt animals (Echchannaoui et al., 2005).

The interaction of CD14 with TLR9 was necessary for a release of IL-6 and IL-1β after the injection of bacterial DNA CpG into the peritoneum. Also here, CD14 was controlling the amount of CXCL1 and subsequently the number of immigrated neutrophils, while the levels of CCL2 and attracted monocytes in the peritoneum were the same in both genotypes (Baumann et al., 2010).

1.10 Damage-associated molecular patterns and sterile inflammation

The TLR system, however, can also react to injury in the absence of infectious stimuli by recognition of damage- or danger associated molecular patterns (DAMPs)(Matzinger, 1994, 2002; Mosser and Edwards, 2008). DAMPs are endogenous factors that under physiological conditions serve various functions, but do not primarily alarm the immune system. They gain the immunologic relevance upon tissue injury and cell impairment, when they leave their physiological compartment (nucleus, cytosol, plasma) and further also become more vulnerable to oxidation or aggregation (Hanisch, 2013; Rubartelli and Lotze, 2007). Immune responses to DAMPs lead to sterile inflammation, a process that is similar to that triggered by PAMPs. Since the tissue injury can often come with an infection, the fueling of sterile acute inflammation may prepare the system for eradication of the incoming pathogens. Further steps allow for the resolution of inflammation and wound repair. However, persistent (chronic) sterile inflammation can have devastating consequences, particularly in the CNS, where it can contribute to the development or aggravation of neurodegenerative and/or autoimmune diseases, such as in Alzheimer´s disease (AD), Parkinson's disease (PD) or multiple sclerosis (MS), and their respective animal models, such as experimental autoimmune encephalomyelitis (EAE), as a model of MS (Buchanan et al., 2010; Midwood et al., 2009; Stewart et al., 2010).

The TLR4 complex was shown to interact with intracellular DAMPs that are released from necrotic cells, such as high mobility group protein B1 (HMGB1), heat shock proteins (Hsps) or S100/A8 and S100/A9 (calprotectin) (Chen and Nunez, 2010; Ehrchen et al., 2009; Park et al., 2006). Tissue injury liberates also other DAMPs, such as hyaluronan, biglycan, heparan sulphate or fragments of fibronectin (FN) from the extracellular matrix (ECM), that interact with TLR4 (Birdsall et al., 2005). Plasma FN (pFN) can also affect parenchymal innate immune cells upon vascular damage, suggesting that it may act as an omnipresent latent (yet invisible) pool also for microglia. However, many other molecules can potentially serve as DAMPs, and namely via TLR4, like fetuin A (as a link of free fatty acids to TLR4-driven sterile inflammation) (Pal et al., 2012) or parts of the amyloid plaques in AD (Fassbender et al., 2004; Liu et al., 2005; Reed-Geaghan et al., 2009)

Stroke, i.e. cerebral ischemia, may also serve as a good example for a DAMP-driven sterile inflammation in the CNS. Due to the arterial occlusion, the blood flow is halted, which results in a lack of oxygen (hypoxia) and nourishment as well as in a diminished clearance of toxic metabolites. Longer ischemia culminates in cell necrosis, thereby releasing intracellular DAMPs. Subsequent restoration of blood flow, re-oxygenation and reperfusion also by the immune cells, e.g. neutrophils and monocytes, further exacerbates the tissue damage.

Animals lacking TLR4 were shown to have better outcomes in terms of the stroke size (Wang et al., 2011), and it was especially the HMGB1 (Wang et al., 2011; Yu et al., 2006), which was considered to be the relevant candidate for a DAMP driving the sterile inflammation via TLR4 activation. However, with the vascular leakage accompanying the cerebral ischemia, cells of the CNS are getting into contact with soluble plasma proteins or parts of the degraded ECM. In the periphery, these factors can trigger an immune response, like in the case of fibrinogen (Hodgkinson et al., 2008; Smiley et al., 2001), but they are often largely ignored. In the CNS, on the other hand, cells are shielded by a blood-brain barrier (BBB) and they get into contact with plasma proteins only in the case of an injury or BBB leakage.

Also here, in response to DAMPs, the co-receptor CD14 plays an important role. Murine macrophages and human astrocytoma cells require CD14 for the induction of inflammatory cytokines in the presence of HMGB1 and Hsp70, respectively (Asea et al., 2000; Kim et al., 2013). In AD, CD14 directly interacts with $A\beta_{42}$ peptides (as a component of the amyloid plaques) (Liu et al., 2005) and regulates the sterile inflammation. On one hand, CD14 has beneficial actions, enabling the phagocytosis of these peptides, but on the other hand, it fuels the microglial response to fibrillar Aβ (Fassbender et al., 2004; Liu et al., 2005; Reed-Geaghan et al., 2009). As a TLR2 co-receptor, CD14 was also shown to enhance

immune responses by peritoneal cells to necrotic cells (Chun and Seong, 2010). Taking together, CD14 seems to be far more than a simple chaperon in LPS binding.

2. Aim of the Study

The TLR4 system was primarily understood to be a major sensor of bacterial infection. However, TLR4 has more recently also been considered for participation in immune responses to tissue damage and cell impairment. Recognition of both bacterial LPS and injury-related factors can lead to the activation of tissue-resident innate immune cells and the recruitment of peripheral immune cells, which essentially participate in the inflammatory processes. While acute inflammation predominantly contributes to anti-microbial defense, wound healing and tissue regeneration, excessive inflammation can rather lead to destructive cascades and even culminate in organ failure and death. Inflammatory processes must thus be kept under a tight control—especially in the CNS. This is reflected by the severe impairment and lethal outcomes as associating with CNS infections as well as non-infectious diseases, including stroke, trauma, autoimmune and neurodegenerative diseases. Based on the critical roles of the CNS-resident microglia and their TLR4 signaling system in immune responses to infection and damage, we addressed the following questions:

1. **What are the roles of the TLR4 co-receptor CD14 in the organization of CNS responses to infection?**
   - How does CD14 affect immune reactions of microglia to bacterial LPS, as the prototypical PAMP agonist, and how is this mirrored by consequences of CNS challenges with LPS and *E.coli*?
   - Are there differences in the employment of CD14 by microglia and extraneural macrophage populations for supporting efficient and preventing excessive responses?

2. **What are the roles of the TLR4 co-receptor CD14 in the organization of CNS responses to damage?**
   - How does CD14 influence microglial responses to plasma FN, as a representative DAMP, and how does CD14 participate in the immune reactions to CNS challenges with a DAMP, by mechanical injury and ischemic stroke?

3. **How is CD14 involved in managing distinct microglial responses to DAMPs and PAMPs?**

4. **How is CD14 itself regulated by TLR4, other TLR and non-TLR systems to govern TLR4 functions?**

- Is CD14 subject to a positive and/or negative (expression) control which could recruit, exclude or shape TLR4 functions in responses to infectious and non-infectious challenges?

- Could also other TLRs and non-TLR signaling systems thereby indirectly have access to a damage-sensing capacity of the TLR4 complex?

The project involved a series of experiments *in vitro* and *in vivo* as based on mouse strains with deficiencies in TLR-relevant components, on animal models of diseases and on cellular approaches in combination with cell-biological, biochemical as well as molecular-biological assays and bioinformatic analyses.

3. Material and Methods

3.1 Animals

C57BL/6J and NMRI wt as well as CD14- (B6.129S4-$Cd14^{tm1Frm}$/J), TLR4- ($tlr4^{-/-}$) and TRIF-deficient ($trif^{lps2}$) mice were bred and obtained from the Central Animal Facility of the University Medicine Göttingen (UMG) and housed under standard or pathogen-free (SPF) conditions. The $tlr4^{-/-}$ and $cd14^{-/-}$ mice were from The Jackson Laboratory. The $trif^{lps2}$ mice were kindly provided by Dr. Bruce Beutler, La Jolla, USA. These animals carry a frameshift error mutation in the C terminus of TRIF, resulting in an abrogation of TRIF-mediated functions (Hoebe et al., 2003). The homozygous mice ($trif^{lps2/lps2}$) were thus employed as a model of impaired TRIF activity. All animals were treated according to the guidelines for animal care of the University of Göttingen.

3.2 Neonatal microglial and astroglial cultures

Whole brains from newborn (p0, neonatal) mice were liberated from meninges and blood vessels, washed with Hank's balanced salt solution (HBSS, Biochrom, Berlin, Germany) and incubated with 2.5% trypsin (Biochrom) 2 x 5 min at 37°C, with gentle vortexing between incubations. The enzymatic reaction was stopped by addition of Dulbecco's modified Eagle's medium (DMEM, Invitrogen/Gibco, Karlsruhe, Germany), supplemented with 10% fetal calf serum (FCS, Invitrogen/Gibco), 100 U/ml penicillin and 100 µg/ml streptomycin (both Biochrom). This cell suspension was further incubated in the complete medium supplemented with 0.4 mg/ml DNAse (CellSystem, St.Katherine, Switzerland) at 37°C for 5 min. Remaining cell clusters were mechanically separated by pipettes with decreasing diameter and the suspension was centrifuged at 200g at 4 °C for 10 min. The supernatant was removed, cells were resuspended in fresh complete medium and seeded in 75 cm^2, poly-L-lysine (PLL)-coated culture flasks. (30 min prior to use, flasks were incubated with 100 µg/ml PLL (Invitrogen/Gibco) at RT, followed by three rinses with sterile ddH$_2$O. Subsequent cultures were carried out in a humidified atmosphere with 5% CO$_2$ at 37 °C. The following day, primary mixed-glial cultures were washed three times (PBS, Invitrogen/Gibco) and received fresh complete medium. Culture medium was then changed every other day. After 5 days, microglial proliferation was stimulated by adding complete medium supplemented with 30% of L929-conditioned cell culture supernatant (see below). After another 3–5 days, microglial cells were harvested by shaking them off the astrocytic layer. Cells were washed with complete medium

and counted. Cells were plated in 96-well plates at a density of 1.5×10^4 cells/well, in 12-well plates at a density of 2×10^5 /well or in 6-well plates at a density 10^6 cells/well.

In order to obtain pure astroglial cultures, mixed-glial cultures were incubated in the complete medium with 200 µg/ml dichloromethylenedisphosphonic acid disodium salt (Clodronate) (Sigma-Aldrich, Taufkirchen, Germany) for 48 h (5% CO_2 at 37°C). Microglia cells were removed by overnight shaking (250 rpm, 37°C). Pure astrocytic cultures remaining at the bottom of the flasks then received a fresh complete medium for 48 h. To plate the astrocytes for stimulation experiments, cells were incubated with 0.05%/0.02% trypsin/EDTA (Biochrom) for 5 min at 37°C. Reaction was stopped by addition of complete medium; cells were transferred into 50 ml conical tubes and centrifuged 200g for 10 min at 4°C. Afterward, cells were counted, resuspended in the complete medium and plated at the same densities as microglia. The astroglial cultures prepared this way from newborn microglia were also used for culturing of the adult microglia (refer to chapter 3.3).

3.3 Adult microglial cultures

The whole brains of adult (postnatal) mice were dissected into brain stem, cerebellum and cerebral hemispheres and liberated from blood vessels, meninges and choroid plexus components. Tissue was dissociated into small pieces ($\sim$1 mm^3), washed and enzymatically processed as described for preparation of newborn microglia (chapter 3.2). The single cell suspensions were seeded into 75-cm^2 tissue culture flasks containing a confluent monolayer of neonatal astrocytes. The astrocyte cell culture was prepared as described in 3.2 from newborn mixed-glial cultures from NMRI wt mice, as to be necessary for a proper growth supply of the cultured adult microglia. The postanatal microglia were harvested every 7 days.

3.4 Bone marrow-derived macrophages (BMDM)

Mice (8-12 weeks old) were sacrificed by cervical dislocation and placed on disposable pads abdomen up. Abdomen and hind legs were sterilized with 70% ethanol and after an incision in the middle of the abdomen, the hind legs were extracted by sterile scissors and forceps. The residual muscle tissue was removed by paper tissues soaked with 70 % ethanol and the femurs were flushed using syringe with 0.45 x 12 mm needle with the Pluznik medium (Dulbecco's modified Eagle's medium, DMEM with L-Glutamine (Invitrogen/Life Technologies) supplemented with 10 % FCS (Invitrogen/Gibco), 5% horse serum (Sigma-Aldrich), 1% sodium pyruvate (Sigma-Aldrich) , 1000x diluted β2-mercaptoethanol 100 U/ml penicillin and 100 µg/ml streptomycin (both Biochrom, Berlin, Germany). Bone marrow from one

femur was plated with 10 ml of Pluznik medium on one 10 cm-Petri dish (92x16 mm with cams, Sarstedt, Nürnbrecht, Germany) and subsequent cultures were carried out in a humidified atmosphere with 5% CO_2 at 37°C. The next day, cells in medium were collected into conical 50 ml tubes, centrifuged 10 min at 200g at 4°C and resuspended in 40 ml of Pluznik medium. Cell cultures were consequently plated (femur/4 plates) and the medium was changed on day 4. Differentiated BMDM were harvested on day 7 by addition of accutase (Biochrom) or 4 mM EDTA, followed by incubation for 10 min at 37°C. Cells were washed with complete medium, counted and plated in 96-, 12- or 6-well plates at densities of $1.5x10^4$, $2x10^5$ or 10^6 cells per well, respectively, in complete medium and used the following day for stimulation experiments.

3.5 Peritoneal macrophages

Mice (8-10 weeks old) were sacrificed by cervical dislocation and placed on disposable pads abdomen up. The skin was carefully cut by scissors above the peritoneum about midway the length of the abdomen. Through the exposed peritoneal membrane 10 ml of cool sterile PBS (Invitrogen/Gibco) were injected into the peritoneal cavity by a sterile syringe and 22-gauge needle. The peritoneal cavity was gently massaged to loosen the macrophages; the enriched fluid was collected by the same syringe into a 50 ml Falcon tube and centrifuged (10 min, 200g, 4°C). Cells were washed with complete medium and counted using hemocytometer. Cells were plated in 96-well plates at a density of $2.5x10^4$ cells/well in complete medium and used the following day for a stimulation. For a flow cytometry analysis, cells were washed with FACS buffer (PBS supplemented with 2% FCS, 0.01 M EDTA pH 8.0 and 0.1% NaN_3)and seeded into FACS tubes (BD Bioscience, Falcon™) at a density of $2x10^5$ cells/tube. Cells were stained with PE anti-mouse CD14 antibody (1:100, clone Sa14-2) and APC anti-mouse CD11b antibody (1:100, clone M1/70; eBioscience, Frankfurt, Germany) in FACS buffer for 20 min on ice in dark. Cells were then centrifuged at 800g for 10 min at 4°C and acquired on FACS Canto II (BD Bioscience). The data was analyzed using FlowJo (Tree Star, Ashland, OR, USA). CD11b positive cells with high SSC and FSC were considered as peritoneal macrophages.

3.6 Blood monocytes

Animals were injected with 5 U/g of heparin (Sigma), anesthetized with overdose of 14% chloralhydrate (Merck) and blood was collected from the retrobulbar venous plexus using glass capillary into heparin pre-coated microcentrifuge tubes kept on ice. All collected blood (approximately 600-1000 µl depending on the size of the animal) was mixed gently with ammonium chloride solution (StemCell Technologies,

Grenoble, France) in the ratio of 9:1 (NH_4Cl : blood) and the blood cells were allowed to lyse for 14 min on ice. Samples were centrifuged (300g, 10 min, 4°C) and the cells were washed with the same volume of PBS + 2%FCS+1mM EDTA used for the erythrocyte lysis. The washing step was repeated one more time. The cells were counted using hemacytometer and the monocytes were isolated using negative isolation based on magnetic beads (EasySep, Mouse Monocyte Enrichment Kit; StemCell Technologies) according to manufacturer's instructions. The negatively isolated monocytes were stained with the following antibodies: Pacific Blue anti-mouse Ly-6G (1:100, clone 1A8), PE anti-mouse CD14 (1:100, clone Sa14-2) (both Biolegend, London, Great Britain), APC anti-mouse CD11b (1:100, clone M1/70; eBioscience) in dark for 20 min on ice. As a control, a sample of blood was taken prior to monocyte enrichment; it was processed as described in the section 3.17 and stained also for CD14, CD11b and Ly-6G. Cells were acquired on FACS Canto II (BD Bioscience) and data was analyzed using FlowJo (Tree Star, Ashland, OR, USA).

3.7 L929 mouse fibroblast cultures

L929 fibroblasts were routinely cultured in complete medium and passaged (1:5) every 2 weeks. After 14 days of continuous cultivation (no medium change in between), supernatants were isolated and stored at -20 °C until used for the stimulation of microglial proliferation. After 30 passages, fresh L929 cultures were established from a stock stored in liquid nitrogen.

3.8 *In vitro* stimulation experiments

S-LPS (smooth chemotype lipopolysaccharide, *Escherichia coli*, serotype O55:B5), Ra-LPS (Ra chemotype LPS, E. coli, serotype EH100), Rc-LPS (Rc chemotype LPS, *E. coli*, serotype J5), Re-LPS (Re chemotype LPS, *E. coli*, serotype R515) and lipid A (*E. coli*, serotype R515) were purchased as ultra-pure (TLRgrade™) preparations from Enzo Life Sciences/Alexis; Lörrach, Germany). S.e.-LPS (presumably of Ra chemotype, *Salmonella enterica*, serotype *Minnesota*) and bovine plasma fibronectin were from Sigma. Mouse plasma fibronectin was from Molecular Innovations (Novi, MI, USA). In addition to TLR4 stimulation by LPS variants, microglia were also routinely stimulated with the following TLR agonists: Pam_3CSK_4 (TLR1/2), poly(I:C) (TLR3, TLRgrade™) and MALP-2 (TLR6/2) were from Enzo Life Sciences/Alexis, poly(A:U) (TLR3) from Sigma, poly(U) (TLR7/8) and CpG ODN (TLR9, TLRgrade™) from Enzo Life Sciences/Alexis. Monoclonal rat anti-mouse CD14 antibody (clone 4C1) was from BD Pharmingen (Heidelberg, Germany), mouse soluble recombinant CD14 (sCD14), BTK inhibitor terreic acid and dynasore from Enzo Life Sciences. PLC inhibitor U-73122 and Syk inhibitor Bay 61-3606 were purchased

from Sigma. Recombinant mouse interferon-γ (IFNγ), IL-4 (both carrier-free preparations) polyclonal goat IgG anti-mouse IFNα/β R1 and IFNα/β R2, cytochalasin D were purchased from R&D Systems (Wiesbaden, Germany). Mouse IFNβ was from PBL Biomedical Laboratories (Piscataway, NJ, USA). Jak inhibitor I was from Calbiochem/Merck Millipore (Nottingham, UK). Chlorpromazine, chloroquine, filipin III were from Sigma Aldrich. All working solutions were freshly prepared from frozen or refrigerated stocks by dilution in complete medium immediately prior to use. Medium, in which the cells were resting after seeding, was exchanged for complete medium containing the stimuli. Cells were further incubated for a time period depending on experiment in a humidified atmosphere at 37°C with 5% CO_2. In experiments, in which blocking antibodies or inhibitors were used, cells received the compound 30 min to 1 h prior the addition of other stimuli.

3.9 Determination of cell viability

All compounds used for stimulation of the cells were also tested for toxicity. Following supernatant removal, cells received fresh complete medium supplemented with 10% of WST-1 reagent (Roche Applied Science, Mannheim, Germany). After 3 h of incubation at 37°C, the amount of formazan was measured at 450 nm (with 655 nm as the reference wavelength) in a microplate reader (BioRad, Munich, Germany).

3.10 Quantification of soluble factors in cell culture supernatants

Release of cytokines and chemokines by cultured microglia and astrocytes, 1.5×10^4/well or by BMDM or peritoneal macrophages (2.5×10^4/well) was analyzed in supernatants by commercial enzyme-linked immunosorbent assay (ELISA) test systems in 96-well plates. Levels of IL-6, IL-10, CCL2 (monocyte chemoattractant protein, MCP-1), CCL3 (macrophage inflammatory protein, MIP-1a), CCL5 (regulated upon activation normal T-cell expressed and presumably secreted, RANTES), CXCL1 (KC, mouse equivalent of human GROα) and CXCL2 (macrophage Inflammatory protein 2, MIP-2) were determined using DuoSet ELISA Development Kits (R&D Systems). TNFα and IFNβ levels were measured using an ELISA kit from BioLegend (San Diego, CA, USA) and total IL-12p40 (including monomeric p40) levels were determined with an ELISA kit from eBioscience (San Diego, CA, USA). Absorbance was measured at 450 nm (with 540 nm as reference wavelength) using a microplate reader (Bio-Rad).

3.11 Quantification of chemokines in serum

Blood samples were collected from the rertrobulbar venous plexus using capillary into a microcentrifugation tube and left for another 30 min to 1 h at RT. Subsequently, samples were centrifuged for 10 min at 2,500xg at 4°C, the serum was removed and stored at -20°C until assayed. The levels of CXCL1 and CCL2 were determined in 1:10 diluted serum using DuoSet ELISA Development Kits (R&D Systems) following the manufacturer's instructions.

3.12 Quantitative Real-Time PCR (qRT-PCR) of CD14 in microglia

Microglia ($1x10^6$ /well in 6-well plate) were stimulated with TLR agonists in a humidified atmosphere at 37°C with 5% CO_2 for 3 h or time period depending on experiment. Subsequently, cells were washed with PBS, lysed, harvested and total RNA was isolated and purified using RNeasy Mini Kit (Qiagen, Hilden, Germany) according to the manufacturer's instructions. Isolated total RNA (500 ng) was used for synthesis of cDNA by QuantiTect Reverse Transcription Kit (Qiagen) and qRT-PCR was then further performed with resulting cDNA by QuantiTect SYBR Green PCR Kit on iQ5 BioRad (icycler) using the following primers: forward 5'-gcgtgtgcttggcttgttg-3' and reverse 5'-cagggctccgaatagaatccg-3'. Gene expression was assessed using GAPDH as an internal control.

3.13 Flow cytometry analysis of CD14 and MHC I expression by microglia and BMDM

Microglia or BMDM ($2x10^5$/well in 12 well plate) were incubated with stimuli for the indicated time period in complete medium. Thereafter, cells were washed with PBS and treated with 0.05%/0.02% trypsin/EDTA (Biochrom) for up to 5 min at 37°C. The enzymatic reaction was stopped by adding fresh complete medium, cells were carefully scraped and collected into microcentrifuge tubes. After centrifugation at 800g for 10 min at 4°C, cells were resuspended in FACS buffer (PBS supplemented with 2% FCS, 0.01 M EDTA pH 8.0 and 0.1% NaN_3) and the washing step was repeated one more time. Subsequently, the Fc receptors were blocked by anti-mouse antibody against CD16/CD32 (1:100, Fc Block™, clone 2.4G2, BD Biosciences) for 10 min on ice. Cells were further stained with Pacific Blue anti-mouse CD11b antibody (1:200, clone M1/70, BioLegend) and PE anti-mouse CD14 antibody (1:200, clone Sa14-2, BioLegend) or Alexa Fluor 647 anti-mouse H-2K^d/H-2D^d antibody (MHCI, 1:200, clone 34-1-25, Biolegend) in FACS buffer for 20 min on ice. In parallel, corresponding isotype controls were used (1:200, PE rat IgG2aκ, Alexa Fluor 647 mouse IgG2κ). After the staining period, cells were centrifuged (800g for 10 min at 4°C), washed and after resuspension in FACS buffer acquired on FACS Canto II. Only CD11b$^+$

events were used for analysis of CD14 or MHC I protein expression. Data were analyzed using FlowJo (Tree Star).

For intra- and extracellular staining of CD14 receptors, microglia were firstly stained extracellularly with Pacific Blue anti-mouse CD11b antibody (1:200, clone M1/70, BioLegend) for 20 min on ice. Subsequently, cells were washed with PBS and resuspended in BD Cytofix/Cytoperm™ solution (BD Biosciences) and incubated for 20 min at 4°C in the dark. After washing step with FACS buffer, intracellular Fc receptors were blocked by adding Fc Block™ (1:200) in Perm/Wash buffer (2% FCS and 0.1 % saponin in PBS) for 15 min at RT. Then, cells were stained intracellularly with APC anti-mouse CD14 antibody (1:200, clone rmC5-3, BD Biosciences) for 30 min at room temperature. Cells were then washed with FACS buffer and acquired on FACS Canto II.

3.14 Flow cytometry analysis of CD14 protein expression on astrocytes

The plated astrocytes ($2x10^5$/well in 12 well plate) were not all completely attached to the bottom of the wells, in comparison to microglia. To ensure the stimulation of all seeded cells, the supernatants were transferred into micro-centrifuge tubes. The residual cells at the well bottoms received a fresh medium. The supernatants were centrifuged for 10 min at 800g at RT and resuspended in the complete medium containing the stimuli. After an aspiration of medium from the wells, the cell suspensions were added to the rest of seeded cells. After 18 h, cells were washed with PBS and treated with 0.05%/0.02% trypsin/EDTA (Biochrom) for up to 5 min at 37°C. The enzymatic reaction was stopped by adding fresh complete medium, cells were carefully scraped and collected into microcentrifuge tubes. After centrifugation at 800g for 10 min at 4°C, cells were resuspended in FACS buffer (PBS supplemented with 2% FCS, 0.01 M EDTA pH 8.0 and 0.1% NaN_3) and the washing step was repeated one more time. Astrocytes were firstly stained extracellularly with anti-mouse CD14 antibody (1:200, clone Sa14-2, BioLegend) or incubated with isotype control PE rat IgG2a κ isotype antibody (1:200, e-Bioscience) for 20 min on ice. Subsequently, cells were washed with PBS and resuspended in BD Cytofix/Cytoperm™ solution (BD Biosciences) and incubated for 20 min at 4°C in the dark. After washing step with FACS buffer, intracellular Fc receptors were blocked by adding Fc Block™ (1:200) in Perm/Wash buffer (2% FCS and 0.1 % saponin in PBS) for 15 min at RT. Astrocytes were then stained intracellularly with Alexa Fluor 647 anti-mouse GFAP antibody (2μl/sample, clone 1B4, BD Pharmingen) for 20 min at RT. Cells were then washed with FACS buffer and acquired on FACS Canto II.

3.15 Analysis of *E.coli* phagocytosis by flow cytometry

Cells ($2x10^5$ /well in 12 well plate) were incubated with 2×10^6 cfu/ml *E.coli*-DsRed (apathogenic strain DH5α; a generous gift of S. Hammerschmidt, Ernst Moritz Arndt University Greiswald, Germany) (Sörensen et al., 2003) in complete medium with ampicillin (Sigma-Aldrich) 100 µg/ml and without penicillin/streptavidin for 2 h in a humidified atmosphere at 37°C with 5% CO_2. After the incubation period, cells received for 1 h 100 µg/ml gentamicin (Sigma) to eliminate the *E.coli*, which was not engulfed. Cells were then harvested and stained with APC anti-mouse CD11b antibody (1:200, clone M1/70, eBioscience) as described in the chapter 3.12. Cells were acquired on FACS Canto II and only CD11b positive cells were used for analysis of DsRed fluorescent *E.coli* phagocytosis by microglia. Data were analyzed using FlowJo (Tree Star, Ashland, OR, USA).

3.16 Analysis of blood samples by flow cytometry

Blood samples were collected from the rertrobulbar venous plexus using capillary into conical 5 ml tube (FACS tube) containing FACS buffer (PBS supplemented with 2% FCS, 0.01 M EDTA pH 8.0 and 0.1% NaN_3) and after centrifugation for 7 min at 200g at 4°C, cells were incubated in FACS buffer with anti-mouse CD16/CD32 antibody (1:50, Fc Block™, clone 2.4G2, BD Biosciences) for 10 min on ice. Subsequently, cells were stained with antibodies conjugated with fluorescent dies. For the blood analysis after intracerebral infection with *E.coli* K1 were used the following monoclonal antibodies: Pacific Blue anti-mouse Ly-6G (1:200, clone 1A8, Biolegend), PerCP anti-mouse CD45R/B220 (1:200, clone RA3-6B2, BD Bioscience), APC anti-mouse anti-Ly-6C (1:200, clone AL-21, R&D Systems), FITC anti-mouse/human CD11b (1:200, clone M1/70, eBioscience). For the analysis of CXCR2 expression on neutrophils the following antibodies were used PerCP anti-mouse CD45R/B220 (1:200, clone RA3-6B2, BD Bioscience), Alexa Fluor 647 anti-mouse CXCR2 (1:150, clone TG11, BioLegend), FITC anti-mouse/human CD11b (1:200, clone M1/70, eBioscience), Pacific Blue anti-mouse Ly-6G (1:200, clone 1A8, Biolegend). For the analysis of CCR2 on monocytes, the following antibodies were used: PE anti-mouse CCR2 (5 µl/sample, clone 475301, R&D Systems), FITC anti-mouse/human CD11b (1:200, clone M1/70, eBioscience), APC anti-mouseLy-6C (1:100, clone HK1.4, BioLegend), PerCP anti-mouse CD45R/B220 (1:200, clone RA3-6B2, BD Bioscience). Cells were stained for 20 min at 4°C in dark. Afterwards, erythrocytes were lysed with BD FACS Lysing Solution (BD Bioscience) (diluted 1:10 in ddH_2O at least 15 min prior to use) for 5 min at RT in dark. To stop the reaction, FACS buffer was added and cells were twice washed and centrifuged (7 min, 200g, 4°C). Resuspended cells in FACS buffer were acquired by FACS Canto II (BD Biosciences). Data were analyzed using FlowJo (Tree Star, Ashland, OR, USA).

3.17 Brain infection by *E.coli* K1

The *Escherichia coli* strain K1 (serotype O18:K1:H7), which was originally isolated from the cerebrospinal fluid (CSF) of a child with neonatal meningitis (gift of Gregor Zysk, Institute of Medical Microbiology, Düsseldorf, Germany), was grown on agar plates overnight. Bacteria was harvested by using 0.9% NaCl and stored at -80°C. The frozen aliquots were diluted in saline and injected into the right frontal neocortex (1.25 x 10^4 CFU/mouse) of ketamine (60 mg/kg bodyweight) (Medistar, Hanover, Germany) / xylazin (8 mg/kg bodyweight)(Riemster Arzneimittel AG, Greifswald Hansestadt, Germany) anesthetized animals (8-12 weeks old). After 24 h, animals were sacrificed with i.p. injection of lethal dose of 14% chloralhydrat (Merck), perfused with PBS, brains were dissected and further analyzed as described in the chapter 3.20.

3.18 Microinjections, long-term delivery and generation of stab wounds

Mice were anesthetized i.p. by a mixture of ketamine /xylazin. The fur on head was shaved, thoroughly washed with 70% ethanol and the animals were placed on stereotactic frame (model 900 with mouse head holder and cup ear bars, David Kopf Instruments). A rostro-caudal cut was performed to give access to the skull and a hole was drilled using a 0.5 mm round-headed drill (Hager & Meisinger GmbH) at position 0.5 mm rostral to bregma (AP 0.5), on right hemisphere (ML 1.5) for the following injections (based on coordinates in Paxinos & Franklin, The mouse brain in stereotaxic coordinates, Elsevier Academic Press, Amsterdam, 2004). (Allen Brain Atlas, available on http://mouse.brain-map.org/static/atlas, coronal sections, atlas version 1 (2008) – picture 49). For injections, a NeuroSyringe 7001 KH SYR with 33 gauge cannula (Hamilton) was mounted in a stereotactic manipulator and lowered into the tissue with the cannula tip position at 3.0 mm beneath the skull surface. LPS chemotypes, mouse pFN or recombinant mouse CXCL1 (carrier free preparations, R&D Systems) dissolved in 1 µl of vehicle at the indicated concentrations were delivered over 3 min. The cannula was slowly removed and the skin incision was subsequently closed by a suture. The compounds were delivered over 3 min. For a generation of stab wounds, animals were injected in the same manner and position of the brain with only adequate solvent (ddH$_2$O or PBS) of LPS or FN. To induce CNS injury, cannulas of distinct diameter were inserted for vehicle injections over 3 min to create a defined volume entry in the tissue.

For a long-term delivery, 1 mg/ml S-LPS (*Escherichia coli*, serotype O55:B5) or 600 µg/ml mouse plasma fibronectin (Molecular Innovations) was infused by micro-osmotic pumps (model 1007D, 0.5 µl/h) connected to cannulas of the Brain Infusion Kit 3 (both Alzet) for 24, 48 or 72 h. Cannula were

installed under stereotactic control as described and fixed to the skull bone with Loctite 454 Adhesive Gel (Alzet).

As an analgesic, animals received i.p. injection with rimadyl (5µg/10 g bodyweight) (Pfizer, Berlin, Germany) after the surgery. In the case of a delivery lasting longer than 24 h, 2 days prior and 2 days after a surgery animals were treated with Novaminsulfon (Metamizol) (Ratiopharm, Ulm, Germany) in a drinking water.

For CXCR2 blocking studies, mice received a striatal injection of 1 µg S-LPS followed by i.v. injection of 40 µg/animal of anti-mouse CXCR2/IL-8 RB antibody (clone 242216) or isotype control rat IgG2A (clone 54447) (both R&D Systems).

3.19 Preparation of single cell suspensions and flow cytometry analysis of brains

Mice were anesthetized by i.p. injection of a lethal dose of 14% chloral hydrate (Merck) and perfused via left cardial ventricle by PBS. Brains were dissected and single cell suspensions were generated using Neuronal Tissue Dissociation Kit (T) (Miltenyi Biotec, Bergisch Gladbach, Germany) and gentleMACS™ Dissociator following the manufacturer's instructions. Obtained single cell suspension was resuspended in 37% Percoll™ (GE Healthcare Life Sciences, Freiburg, Germany) in DMEM supplemented with 10% FCS and this solution was carefully layered over 70% Percoll™ in DMEM + 10% FCS in 15 ml centrifuge tube. After uninterrupted (with a minimal acceleration and without brakes) centrifugation for 25 min, 500g at 4°C, upper layers of myelin and 37% Percoll™ were removed. The cells at the interphase were carefully transferred into a 10 ml centrifugation tube and washed with FACS buffer and centrifuged for 10 min, 300g at 4°C. Fc receptors were further blocked by anti-mouse CD16/CD32 antibody (1:50, Fc Block™, clone 2.4G2, BD Biosciences) for 10 min at 4°C. Cells were stained for 25 min at 4°C with following antibodies: Pacific Blue anti-mouse Ly-6G (1:100, clone 1A8); PerCP anti-mouse CD45 (1:100, clone 30-F11), APC anti-mouse Ly-6C (1:100, clone HK1.4), PE anti-mouse CD14 (1:100, clone Sa14-2) all purchased from BioLegend, FITC anti-mouse/human CD11b (1:100, clone M1/70, eBioscience). After washing, samples were acquired on FACS CantoII (BD Bioscience). Data were analyzed by FlowJo (Tree Star, Ashland, OR, USA).

3.20 Immunocytochemistry of microglia

Microglia (5×10^4 per well) were plated in complete medium on poly-L-lysin (PLL, Invitrogen/Gibco) pre-coated cover slips. The following day, microglia were stimulated with 10 ng/ml S-LPS (*E. coli* serotype O55:B5) or left untreated for 30 min at 37°C with 5% CO_2. The stimulation was stopped by addition of

ice-cold complete medium and the cells were subsequently washed with PBS, fixed with pre-cooled methanol (Merck) for 5 min at -20°C, rinsed with PBS-0.05% Triton X-100 and blocked with PBS-0.1%Triton X-100 + 5% rabbit serum for 1 h at RT. After washing with PBS-0.05%Triton, cells were incubated overnight at 4 °C with rat anti-mouse CD14 (1:100, clone rmC5, BD Pharmingen) in PBS-0.05% Triton X-100 + 2.5% rabbit serum. Afterwards, cells were washed with PBS-0.05% Triton X-100 and stained with secondary rabbit anti-rat TRITC (1:100, Sigma-Aldrich) and antibody against tomato lectin conjugated with FITC (1:100, Vector Laboratories, Burlingame, CA, USA) for 1 h at RT. Cells were then twice washed with PBS-0.05% Triton X-100, rinsed with PBS and nuclei were stained with DAPI in PBS (1:1000, Roche) for 3 min at RT. Afterwards, the coverslips with cells were rinsed with PBS, briefly dipped into ddH_2O and placed with a fluorescent mounting medium (Dako, Hamburg, Germany) on object slide (Leica SM 2000 R, Superfrost Plus microscope slides, Thermo Scientific). Cells were imaged using confocal microscopy. Pictures were taken at 60 x magnification using a laser-scanner (Olympus Fluoview FV1000) and the software Olympus Flouview FV10-ASW 3.1. Images were collected at 1 µm intervals with the 405 nm, 488 nm and 561 nm laser to create a stack in z axis. Images from z axis were subsequently used to create a 3-dimensional reconstruction with Imaris 7.4.0.

3.21 Histology of brains infused with mouse pFN

Anesthetized (14% chloral hydrate, Merck) mice were perfused with PBS (with Phenol Red as a color indicator) via left cardial ventricle followed by 4% PFA in PBS (4% PFA, Merck, 1.0 µM sodium hydroxide, 1 x PBS in ddH_2O, pH 7.3) and they were subsequently decapitated. The whole heads were transferred into a 50 ml centrifugation tube with 4% PFA and post-fixed for 2 days at 4°C. Brains were then carefully removed and put for 24 h into fresh PBS. Afterwards, tissue was dehydrated through a series of graded alcohol/xylene/paraffin using an automated tissue processor overnight. The tissues were then embedded in paraffin blocks in the Leica TP 1020 Tissue Processor according to standard procedure.

Brains were sliced by microtome to 1 µm in the coronal plane, around bregma 1.7 mm up to 1.4 mm, transferred to ice-cooled water and subsequently unfolded in a 40°C water bath. Sections were then coated onto object slides (Leica SM 2000 R, Superfrost Plus microscope slides, Thermo Scientific) and dried overnight at 37°C. Prior to the staining procedure, tissue was deparaffinizied and hydrated by performing the graded xylene and isopropyl alcohol steps. Sections were immersed 4 times in xylene (5min), once in isoxylene (1min), twice in 100% isopropyl alcohol (4min), once in 90%, 70% and 50% isopropyl alcohol (3min) and washed with distilled water. Stained sections were dehydrated after the

staining procedures by performing the above described series in reversed order and mounted in DePex medium.

3.22 Iba-1 and Mac3 staining

Deparaffinized and rehydrated tissue sections were subjected to citrate buffer (10 mM citric acid, adjusted to pH 6.0 with NaOH, both Merck) 3x 3 min by turns with 2x ddH$_2$O in a steamer. Cooled off sections were washed in PBS and endogenous peroxidase was blocked by 3% H$_2$O$_2$ in PBS for 20 min at 4°C. Sections were further rinsed in PBS and blocked by 10% FCS in PBS for 1 h at RT. Subsequently, tissue sections were overnight incubated with primary antibody against Mac3 (1:200, anti-mouse monoclonal rat, BD Phamingen) and Iba-1 (1:1000, anti-human polyclonal rabbit, Wako). Primary antibodies were diluted in blocking solution and sections were incubated in 100 µL antibody solution overnight at 4°C. The following day, tissue sections were 3x washed with PBS and incubated with a biotin-conjugated secondary antibody (1:500) diluted in 10% FCS in PBS for 1 h at RT. Avidin-peroxidates and 3,3′-diaminobenzidine were used to visualize antibody binding. After washing with PBS, staining was developed with diaminobenzidin (DAB, Sigma) and rinsed in dH$_2$0. Then, sections were incubated 30 s with Mayer's hemalum solution (Merck) and thoroughly washed in tap water for 10 min. After rinsing the sections in dH$_2$0, tissue was dehydrated and embedded in synthetic mounting medium DePeX (Serva).

3.23 Haematoxylin-Eosin (H&E) staining

Haematoxylin-Eosin (H&E) staining was performed on deparaffinized and rehydrated sections, to obtain a general overview of the tissue morphology. Sections were incubated in Mayer's solution (Merck) for 5 min, washed with dH$_2$0 and differentiated by 1 % HCl-alcohol (1% HCl in 90% isopropyl alcohol). After thorough washing for 10 min in tap water, tissue was incubated in 1% eosin solution (1% eosin G, Merck, in 70% isopropyl alcohol, stirred and filtered, 10 drops of glacial acetic acid was added prior to use) for 5 min. Sections were rinsed in dH$_2$0 and dehydrated and embedded in synthetic mounting medium (DePeX, Serva).

3.24 Luxol Fast Blue/ Periodic Acid Schiff (LFB/PAS) staining

Demyelinized areas were detected by LFB/PAS staining. Deparaffinized sections were rehydrated to 90% alcohol and incubated in LFB solution (0.1% w/v LFB in 96% ethanol, 0.05% acetic acid) overnight at 60°C. Subsequently, sections were washed shortly in 90% isopropyl alcohol and differentiated by dipping into

0.05% lithium carbonate (diluted in dH_2O, Roth) followed by 70% alcohol. The deep blue colour of myelin was developed in distilled water. Sections were incubated for 5 in 1% periodic acid (Merck) in order to obtain PAS staining. Then they were washed thoroughly 5 min under tap water and rinsed with dH_2O. After 20 min incubation in Schiff´s reagent (Sigma), tissue sections were thoroughly washed for 5 min under tap water, rinsed with dH_2O and differentiated in 1% HCl-alcohol. Sections were properly washed by tap water, dehydrated in increasing alcohol series and embedded in synthetic mounting medium DePeX (Serva).

3.25 Bielchowsky silver staining

Bielschowski silver impregnation was used in order to evaluate the axonal loss and integrity. Insoluble silver nitrate binds with higher affinity to axons and in the following step it is reduced to metallic silver particles leading to a black impregnation. The background tissue is stained yellow to brown. Sections were incubated in dark with 20% silver nitrate ($AgNO_3$) + dH_2O solution for 20 min and then washed with dH_2O. The solution of 32% ammonium hydroxide in dH_2O was added to the $AgNO_3$ + dH_2O solution drop by drop while shaking until the precipitations cleared up. The sections were transferred in this solution for 15 min in the dark and then washed with dH_2O containing few drops of ammonium hydroxide. Approximately 10 drops of developer solutions were added to the silver nitrate/ammonium hydroxide solution. This solution was used for the development (5-6 min) of the black staining of the axons. The tissue was subsequently washed with dH_2O, fixed for 2 min with 2% sodium thiosulfate, dehydrated and mounted with DePex medium.

3.26 Morphometry

Two brain sections of Bregma 1.4 and 1.7 (according to the pictures from Allen Brain Atlas, available on http://mouse.brain-map.org/static/atlas, coronal sections, atlas version 1 (2008), coronal level 37 and 39) stained for Mac3 and Iba-1 were pictured at 20 x magnifications. The images were automatically scanned using the .slide-system of Olympus including the software dotSlide 2.1. For quantification of Mac3- or Iba-1-positive areas, whole hemispheres (with exclusion of the injection site) were analyzed using ImageJ software plug-in (available online at http://www1.em.mpg.de/acmac3). The results were presented as ratio of positive stained area to total area. Sections stained by LFB-PAS and H&E were scanned with the .slide-system at 10x magnification. Bielschowsky-staining was pictured at 10x magnification using Olympus cam-era DP71 and the software Cell Sens Dimension 1.7.1. Images were

digitally processed to improve visual appearance according to the Guide-lines for Good Scientific Practice of the University of Göttingen.

3.27 Deep sequencing - Illumina

The deep sequencing gene analysis was done in collaboration with Microarray and Deep-Sequencing Facility (Transkriptomeanalyselabor, TAL, Göttingen; Dr. Gabriela Salinas-Riester, Dr. Claudia Pommerenke). For the preparation of RNA samples, microglial cells (10^6 per well in 6-well plate) were stimulated for 3 h with 0.1 or 10 ng/ml Re-LPS (Re chemotype LPS, E. coli, serotype R515) or with 100 µg/ml mouse plasma fibronectin (Molecular Innovations). Cells were subsequently washed with complete medium and PBS, and homogenized in TRIzol® Reagent (Life Technologies) according to manufacturer instructions. RNA quality was assessed by measuring the RIN (RNA Integrity Number) using an Agilent 2100 Bioanalyzer (Agilent Technologies, Palo Alto, CA). Library preparation for RNA-Seq was performed using the TruSeq RNA Sample Preparation Kit (Illumina, Cat. N°RS-122-2002) starting from 500 ng of total RNA. Accurate quantization of cDNA libraries was performed by using the QuantiFluor™ dsDNA System (Promega). The size range of final cDNA libraries was determined applying the DNA 1000 chip on the Bioanalyzer 2100 from Agilent (280 BP). cDNA libraries were amplified and sequenced by using the cBot and HiSeq2000 from Illumina (SR; 1x50 bp;5- 6 GB ca. 30-35 million reads per sample). Sequence images were transformed with Illumina software BaseCaller to bcl files, which were demultiplexed to fastq files with CASAVA v1.8.2. Quality check was done via fastqc (v. 0.10.0, Babraham Bioinformatics). The Alignment was performed using Bowtie2 v2.1.0 to murine UCSC genome reference, gene annotation was done via UCSC gtf file. Data were conversed and sorted by samtools 0.1.19 and reads per gene were counted via htseq version 0.5.4.p3. Data analysis was performed using R/Bioconductor (3.0.2/2.13). Differential gene expression analysis was done with R-package EdgeR (Robinson et al., 2010).

3.28 Weighted Gene Co-expression Network Analysis (WGCNA)

R-package Weighted Gene Co-expression Network Analysis (WGCNA) was applied to the expression dataset (Langfelder and Horvath, 2008). First, lowly expressed or stably expressed genes were filtered using two criteria. Genes that were expressed in more than 1 sample by 2 Counts per Million (CPM) and that varied more than the first Standard Deviation-quantile were included, leaving 9608 genes in the analysis. Second, by using EdgeR-package (Robinson et al., 2010), predictive log fold change values were

calculated and used as normalized expression values for WGCNA. Based upon the scale free criteria, a co-expression network was generated with a SoftPower value of 6.

Modules were cut at a height of 0.8, with minimal module size of 200 genes, and a deep-split of 3. Of each module, the Module EigenGene (ME) was calculated, which is the first principal component and represents the average expression profile of that particular module. Expression of the ME across conditions was visualized using boxplots. Statistical significance testing of the ME expression values was done using SPSS Version 20 and a multivariate general Linear Model was applied to all ME-values simultaneously, testing for two main effects: Genotype (G) and Stimulation (S), and an interaction (G*S) effect, cell isolation was used as a batch effect. Genes clustered within each significantly affected module were used as input for Ingenuity Pathway Analysis (IPA) (Ingenuity® Systems, www.ingenuity.com) and a core analysis was performed to test for the enrichment of canonical pathways and biological functions.

3.29 Experimental stroke (Middle Cerebral Artery Occlusion, MCAO)

Male mice aged 8 to 12 weeks were exposed to a 60-minute filamentous MCAO as described (Katchanov et al., 2001). Briefly, mice were anesthetized for induction with 1.5% halothane and maintained in 1.0% halothane in 70% N_2O and 30% O_2 using a vaporizer. Cerebral ischemia was induced with an 8.0 nylon monofilament coated with a silicone resin/hardener mixture (Xantopren M Mucosa and Activator NF Optosil Xantopren; Haereus Kulzer). The filament was introduced into the left internal carotid artery up to the anterior cerebral artery. Thereby the middle cerebral artery and anterior choroidal arteries were occluded. Filaments were withdrawn after 60 min of ischemia to allow reperfusion. Core temperature during the experiment was maintained at 36.5°C ± 0.5°C with a feedback temperature control unit.

3.30 Infarct volumetry

Histological determination of infarct lesion volume was performed at 24 h or 3 days after MCAO surgery. Briefly, the animals were deeply anesthetized by isoflurane anesthesia (4%) and decapitated. Brains were frozen in methylbutane on dry ice and stored at -80°C until further use. The brains were cut into 20 μm-thick sections on a cryostat and stained with hematoxylin and eosin. Cerebral infarct sizes were determined with an image analysis system (SigmaScan Pro 4.0; Jandel Scientific, Corte Madera, CA) and calculated by summing the volumes of each section directly or indirectly using the following formula: contralateral hemisphere (mm^3) - undamaged ipsilateral hemisphere (mm^3). Differences between "direct" and "indirect" infarct size are likely to be accounted for by brain swelling.

3.31 Bacteriological analysis

Three days after MCAO, mice were anesthetized and washed with 70% ethanol under sterile conditions. The lungs were removed after thoracotomy and homogenized. For determination of CFU, tissue homogenates were plated at three different dilutions (1:1, 1:10, and 1:100) onto LB plates, incubated at 37°C for 18 h, and bacterial colonies were then counted.

4. Results

4.1 CD14 deficiency causes excessive CNS infiltration by neutrophils upon *E.coli* infection

Bacterial infection is recognized by tissue-resident immune cells, which in reaction produce cyto- and chemokines to attract peripheral immune cells. Monocytes and neutrophils represent the first cell populations infiltrating the affected tissue, and they use their microbicidal functions to eliminate the spreading pathogens. Gram-negative bacteria are essentially sensed via TLR4, as it accepts the cell wall component LPS as an agonistic ligand. LPS binding is thereby assisted by CD14. Accordingly, CD14 deficiency would impair such a response.
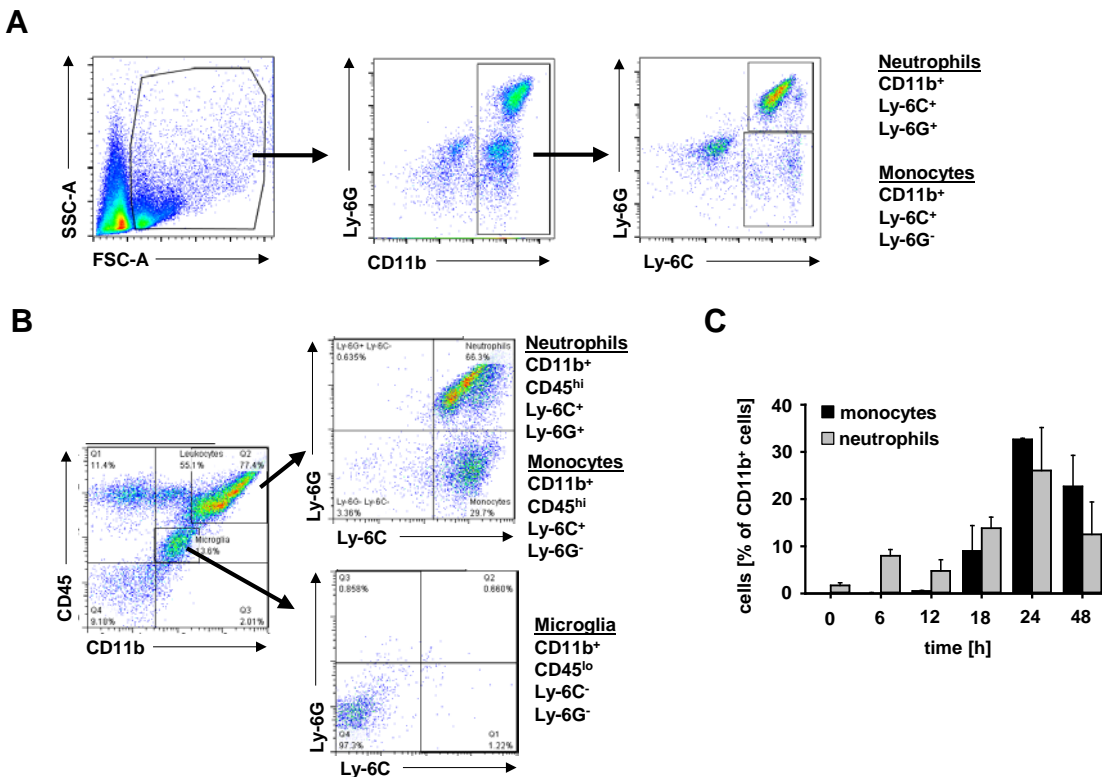
Figure 4.1: Neutrophils and monocytes infiltrate the CNS upon intracerebral *E.coli* infection.
Wildtype (wt, C57BL/6J) mice received an intracerebral injection of *E.coli* K1 (1.25 x 10⁴ CFU/mouse) or the vehicle only (controls, CTL). At the indicated time points, animals were perfused with PBS. Single cell suspensions were prepared from whole brains and analyzed by flow cytometry. 10,000 CD11b⁺ cells were collected. **(A)** Representative flow cytometry plots showing the sequence of gating used for evaluation of cell infiltration as studied in (C). **(B)** Representative flow cytometry plots showing cell types in the brains of infected mice expressing CD11b, CD45, Ly-6G and Ly-6C. **(C)** Quantification of monocyte (CD11b⁺Ly-6C⁺Ly-6G⁻) and neutrophil (CD11b⁺Ly-6C⁺Ly-6G⁺) infiltration. Data represent the mean ± SEM with n=2-4 per group.

In order to select an optimal timing frame for the assessment of a CD14 role in *E.coli* infection, wt mice were intracerebrally inoculated with *E.coli K1,* a strain also known as a causative agent of CNS meningitis (Glode et al., 1977). Leukocyte infiltrates were analyzed at various time points by flow cytometry. The use of the markers CD11b, Ly-6C and Ly-6G enabled us to distinguish the infiltrated immune cell populations in the infected brains. Neutrophils were considered as CD11b$^+$Ly-6C$^+$Ly-6G$^+$ cells and monocytes were identified by a CD11b$^+$Ly-6C$^+$Ly-6G$^-$ immunophenotype (Fig. 4.1A). To make sure that the Ly-6C expression in our system is specific for the infiltrating monocytes and that we are not including microglia in the counting (due to unexpected expression of this protein), we stained the brain infiltrates in addition for CD45. Based on the expression level of CD45, we could distinguish between microglia (CD11b$^+$CD45^{lo}) and infiltrated cells (CD11b$^+$CD45^{hi}) (Fig. 4.1B). The gating on the microglial population further showed that these cells do not express Ly-6C or Ly-6G (Fig. 4.1B, right panel). In agreement with the literature, the first infiltrating cells found in the brain were neutrophils, appearing already at 6 h after infection, while first monocytes were detected after 18 h. Both monocytes and neutrophils had a peak of recruitment at 24 h (Fig. 4.1C).

For a more complex overview, blood samples were collected and stained for monocyte/neutrophil-specific markers. Flow cytometry analysis revealed that 12 h after infection neutrophil counts doubled, with a further increase (up to 50% of blood cells) at 24 h. The number of monocytes slightly increased at 12 and 24 h (Fig. 4.2A, B). Since the ratios of immune cells in the blood would probably reflect the levels of respective chemokines, the concentrations of monocyte and neutrophil chemoattractants, i.e. CCL2 and CXCL1, were quantified in blood samples. The highest concentrations of CXCL1 and CCL2 were detected at 12 h, correlating well with the observed high counts of the respective cells at 24 h (Fig. 4.2C).
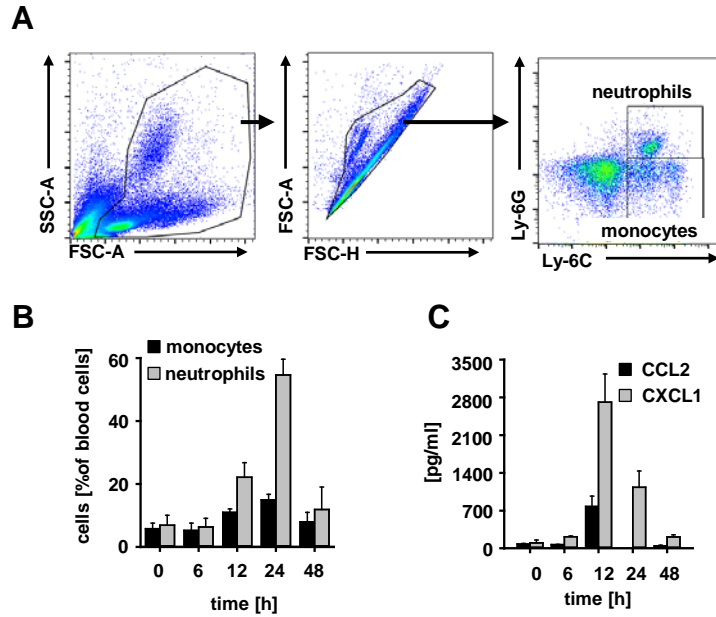
Figure 4.2: *E.coli* **infection of the CNS leads to increased levels of the chemokines CCL2/CXCL1 and counts of monocytes/neutrophils in the circulation.**
(A, B) Monocytes (Ly-6C$^+$ Ly-6G$^-$) and neutrophils (Ly-6C$^+$ Ly-6G$^+$) were determined in the blood of wt mice (C57BL/6J, 8 to 12 weeks old) that had received an injection of *E.coli K1* (1.25 x 10^4 CFU/mouse) into the right neocortex. Blood samples were collected from the retrobulbar venous plexus at indicated time periods after infection. Samples were subsequently stained for Ly-6G and Ly-6C and analyzed by flow cytometry. **(A)** Representative flow cytometry plots showing the sequence of gating used for the evaluation of cell infiltration as studied in (B). **(B)** The graph shows the frequency (%) of monocytes and neutrophils in the whole blood of infected animals. Data are mean ± SEM with n=2-4 per time point. **(C)** Serum levels of the monocyte- and neutrophil-attracting chemokines CCL2 and CXCL1 were determined by ELISA at the indicated time points after infection. Data are mean ± SEM with n=2-5 per group. (CCL2 levels at 24 h could not be determined).

To determine the role of the TLR4 co-receptor CD14 in monocyte and neutrophil recruitment upon Gram-negative bacterial infection of the CNS, wt and *cd14*$^{-/-}$ mice were intracerebrally inoculated with *E.coli* K1. Amounts of infiltrated leukocytes in the brain were assessed by flow cytometry 24 h after the injection. Thus, it was possible to track monocytes and neutrophils simultaneously. The comparison of wt controls and *cd14*$^{-/-}$ mice showed the same number of infiltrating monocytes in both groups, but a significantly higher amount of neutrophils in *cd14*$^{-/-}$ (Fig. 4.3A). Furthermore, 9 of 10 *cd14*$^{-/-}$ mice infected with *E.coli* had *E.coli*-positive blood cultures, while there was no bacterial load detectable in the blood of wt animals (data not shown). In addition to this observation, a higher number of neutrophils was detected in the blood of *cd14*$^{-/-}$ animals (Fig. 4.3B).
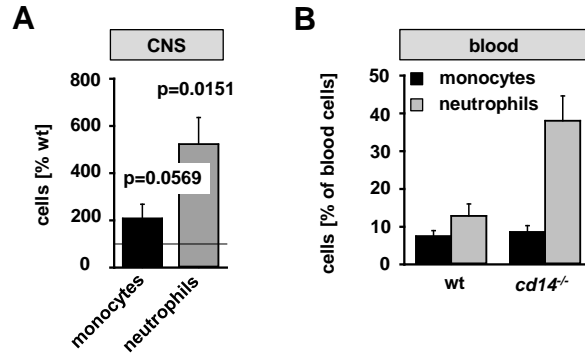
Figure 4.3: CD14 deficiency results in higher neutrophil counts in the CNS and blood circulation of the mice intracerebrally infected with *E.coli* K1.

Mice (wt or *cd14*^{-/-}) received an intracerebral injection of *E.coli* K1 (1.25 x 10^{4} CFU/mouse) or the vehicle only (controls, CTL). **(A)** After 24 h, mice were perfused with PBS and brains were dissected. Single cell suspensions were prepared from whole brains and monocyte and neutrophil subpopulations among 10,000 CD11b^{+} cells were analyzed by flow cytometry. Values for *cd14*^{-/-} mice were expressed as percent of those obtained in wt controls. CD11b^{+} Ly-6C^{+} Ly-6G^{-} were considered as monocytes, CD11b^{+} Ly-6C^{+} Ly-6G^{+} cells as neutrophils. Data are mean ± SEM with n=11-12 per group. Injection of PBS in wt and *cd14*^{-/-} mice resulted in 12.32 and 6.96 % of monocytes as well as 24.98 and 13.48 % of neutrophils, as compared to the respective *E. coli*-infected groups. The Mann-Whitney U test was used for statistical analysis. **(B)** Monocytes (Ly-6C^{+} Ly-6G^{-}) and neutrophils (Ly-6C^{-} Ly-6G^{+}) were determined in the blood of *cd14*^{-/-} and wt mice (C57BL/6J, 8 to 12 weeks old) that had received an injection of *E.coli K1* (1.25 x 10^{4} CFU/mouse) into the right neocortex. Blood was collected from the retrobulbar venous plexus 24 h after infection. Samples were subsequently stained for Ly-6G and Ly-6C and analyzed by flow cytometry. The graph shows the frequency (%) of monocytes and neutrophils in the whole blood of infected animals. Data are mean ± SEM with n=11 and 12 for *cd14*^{-/-} and wt mice, respectively. Cell counts in the infected animals did not differ from controls (PBS injections), except for neutrophils.

4.2 Wt and *cd14*^{-/-} mice reveal comparable expression of CCR2 and CXCR2

During the pathogenic infection, local cells produce various cytokines and chemokines, which attract peripheral monocytes and neutrophils to eradicate the pathogens. The previously shown altered leukocyte infiltration in brains of infected *cd14*^{-/-} mice could be due to different expression levels of their respective chemokine receptors, thereby affecting the chemoattraction. To exclude this possibility, blood samples of *cd14*^{-/-} and wt mice were analyzed by flow cytometry to assess expression levels of CXCR2 (the receptor for CXCL1 and CXCL2) on neutrophils and CCR2 (as the receptor for CCL2) on monocytes. Blood neutrophils (CD11b^{+}Ly-6G^{+} cells) of both *cd14*^{-/-} as well as wt mice, had the same levels of CXCR2 (Fig. 4.4A, B). Murine blood monocytes consist of two major sub-populations, based on their Ly-6C expression levels (Geissmann et al., 2003). Since the results (Fig. 4.1B) showed that preferentially Ly-6C^{hi} monocytes were recruited into the infected brains, CCL2 expression was measured in these cells (Fig. 4.4A). Also in this case, there was no significant difference in the expression between *cd14*^{-/-} and wt mice

(Fig. 4.4B). The recruitment of innate immune cells into the brains of *cd14⁻/⁻* was thus not due to altered expression levels of the chemokine receptors.
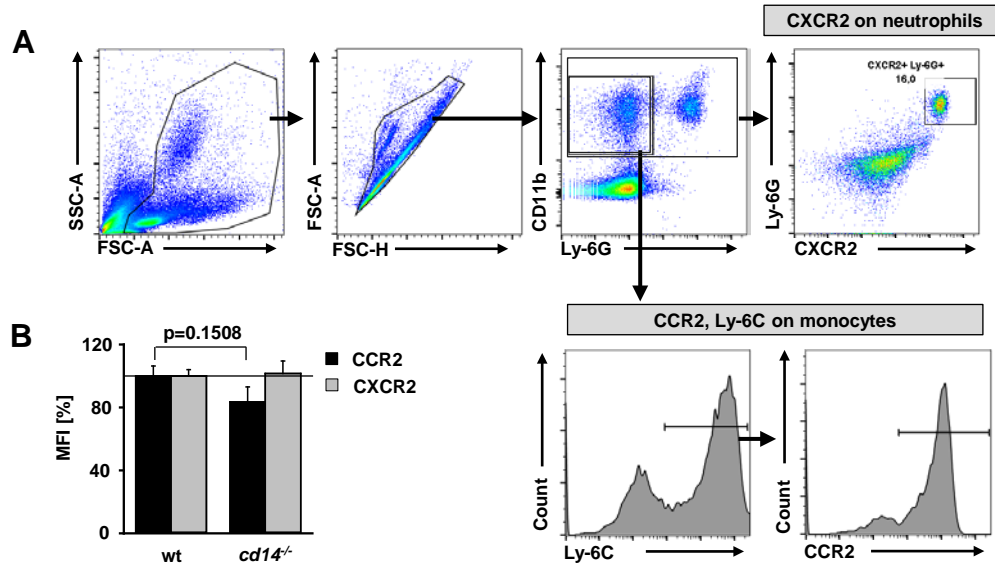
Figure 4.4: Monocytes and neutrophils from both wt and *cd14⁻/⁻* mice express comparable levels of CCR2 and CXCR2.

Blood samples were obtained as in (Fig. 4.2) and stained in addition for CD11b. (A) Representative flow cytometry plots showing the gating used for evaluation of blood samples. (B) Absolute levels of CCR2 and CXCR2 mean fluorescence intensity (MFI) on *cd14⁻/⁻* cells were normalized to MFI values measured in wt cells. Data are mean ± SEM with n=5. The Mann-Whitney U test was used for statistical analysis.

4.3 CD14 is expressed on microglia, monocytes and peripheral macrophages, but not on astrocytes

Since we aimed at studying the regulatory role of the co-receptor CD14, it was important to characterize CD14 expression levels on various cells types from wt mice. CD14 has been reported to be expressed especially on cells of myeloid origin, like macrophages or monocytes. To confirm these observations, negatively isolated blood monocytes, peritoneal macrophages and bone-marrow derived macrophages (BMDM) were stained for CD14 and analyzed by flow cytometry. As shown in Figure 4.5A, CD14 was strongly expressed especially by BMDM and peritoneal macrophages, whereas the levels of CD14 were much lower on blood monocytes. CD14 expression was also determined on microglia and astrocytes as they are the potentially affected cells in the challenged brains of *cd14⁻/⁻* mice. CD14 was highly expressed on cultured microglia from both newborn and adult mice (Fig. 4.5B). However, no CD14 was detected in

astroglial cultures. Thus, microglia seem to be the prominent cells in the CNS as being affected by the absence (or functional block) of CD14.
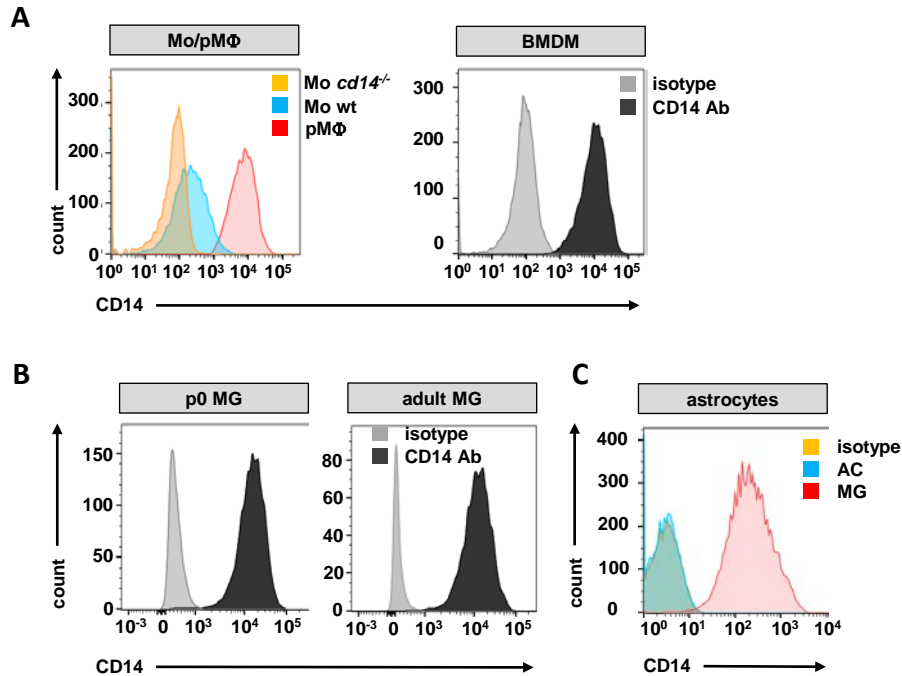
Figure 4.5: CD14 is expressed by microglia, monocytes/macrophages, but not by astrocytes.
(A) Negatively isolated monocytes (Mo) from the blood of wt or *cd14*[-] mice (8-12 weeks) or wt peritoneal macrophages (pMΦ) were stained with PE-anti-CD14 and Pacific Blue-anti-Ly-6G or Pacific Blue-anti-CD11b, respectively, and analyzed by flow cytometry. pMΦ were identified based on high SSC/FSC and CD11b positivity. Histograms are representative for up to 4 preparations and analyses. **(B)** Cultures of microglia (from P0 and 17 weeks old wt mice) were harvested, washed and stained with PE-anti-CD14 and Pacific Blue-anti-CD11b for acquisition by flow cytometry. Only CD11b^{+} events were included. For a staining control, cells were processed with a matching isotype control. **(C)** Cultures of microglia and astrocytes were permeabilized, FcγRII/III-blocked and stained intra- and extracellular with Pacific Blue-anti-CD11b, APC-anti-GFAP and PE-anti-CD14 for acquisition by flow cytometry. CD14 expression was assessed on microglia (CD11b^{+}GFAP^{-}) or on astrocytes (CD11b^{-}GFAP^{+}).

4.4 Microglia lacking CD14 exert impaired *E.coli* phagocytosis

Local macrophages, like microglia, contribute to the eradication of invading pathogens by several ways. As professional phagocytes, microglia engulf the invading microorganism and degrade them to prevent a spread of infection. This feature occurs immediately after microglial recognition of PAMPs and precedes the subsequent recruitment of peripheral immune cells (Sierra et al., 2013). Impaired phagocytosis could lead to a more severe inflammation, since the load of bacteria would also not stay stable, but even

rather increase due to their multiplication. Since $cd14^{-/-}$ mice suffered from a more severe CNS inflammation (Fig. 4.3), it was necessary to clarify whether microglial phagocytosis was altered in these mice. To test this, cultured microglia were incubated with *E.coli* expressing *Discosoma* red fluorescent protein (DsRed) for 2 h. After killing of non-internalized bacteria by antibiotic treatment, microglia were stained for CD11b, a pan-population marker of microglia, and analyzed by flow cytometry. In a wt situation, half of the CD11b-positive cells were also positive for DsRed (Fig. 4.6). The deficiency in CD14 led to a significant decrease, with only 30% of cells being capable of *E.coli* phagocytosis. This result shows that CD14 is important for microglial *E.coli* phagocytosis and that a deficiency in this function may contribute to the inefficient bacterial clearance in the CNS of $cd14^{-/-}$ mice.
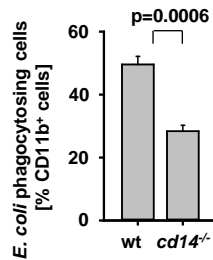
Figure 4.6: Microglia deficient in CD14 display impaired phagocytosis of *E.coli*.
Cultures of microglia from C57BL/6J wt or $cd14^{-/-}$ mice were challenged with $2x10^{6}$ *E.coli*-DsRed for 2 h. Subsequently, they were FcγRII/III-blocked (with mAb against CD16/CD32), stained with PE-anti-CD14 and Pacific Blue-anti-CD11b for acquisition by flow cytometry. For data analysis, only CD11b^{+} events were included. The graph shows the percentage of CD11b^{+} cells that phagocytosed *E.coli*. Data are mean ± SEM with n=7 from 4 independent experiments. The Mann-Whitney U test was used for statistical analysis.

4.5   CD14 confers high sensitivity to LPS especially in microglia

LPS is a major component of the Gram-negative bacterial cell wall and accounts for most of the infection-related consequences, such as fever and organ failure. It is recognized by the TLR4 complex on the surface of innate immune cells. Therefore, LPS was used as a surrogate to characterize the immune responses of macrophages in an infectious setting in detail. As a biochemically better defined compound it also allows for a more convenient experimental handling, regarding concentrations and doses. We had already shown earlier that microglial responses to various LPS chemotypes in terms of cytokine and chemokine production were very effective. This, however, held true only if CD14 was present and functional (Regen et al., 2011); Fig. 4.7 right panel in the red box, data obtained from Dr. Tommy Regen). In the absence of CD14, microglia lost their sensitivity, meaning that a higher dose was needed for

stimulation to elicit a detectable response. This effect was most striking in the case of stimulation with S-LPS, where *cd14*^{-/-} microglia needed a 100 times higher dose in comparison to wt controls.

Microglia differ by origin and location in the body from BMDM and peritoneal macrophages. This could imply a cell-specific response to infection as an adaptation to the environment in which they operate. Thus, we tested if peripheral macrophages and microglia vary in their responses to infectious stimuli and whether CD14 is important for that. To do so, BMDM and peritoneal macrophages of wt and *cd14*^{-/-} mice were stimulated with increasing doses of S- and Re-LPS. Using ELISA, cyto- and chemokine release was measured in the supernatants after 18 h. The decreased responsiveness of BMDM and peritoneal macrophages stimulated with LPS revealed the *a priori* higher sensitivity of microglia, especially to the S-LPS (Fig. 4.7). While microglia responded to S-LPS at concentration of 10^{-9} g/ml, BMDMs and peritoneal macrophages needed 10 times (10^{-8} g/ml) and 100 times higher (10^{-7} g/ml) concentrations, respectively. This cell-specific sensitivity was due to the functional presence of CD14, as *cd14*^{-/-} microglia had the same (low) sensitivity as the other macrophages (Fig. 4.7). (Data from experiments using peritoneal macrophages were kindly provided by Dr. Tommy Regen.) In other words, all three cell types would reveal a comparable response via their TLR4 complexes in the absence of CD14, suggesting a similar organization. Importantly, functional availability of CD14 then makes the difference. Simply by CD14 assistance, cells gain sensitivity—but they do so by a dramatically distinct scale.
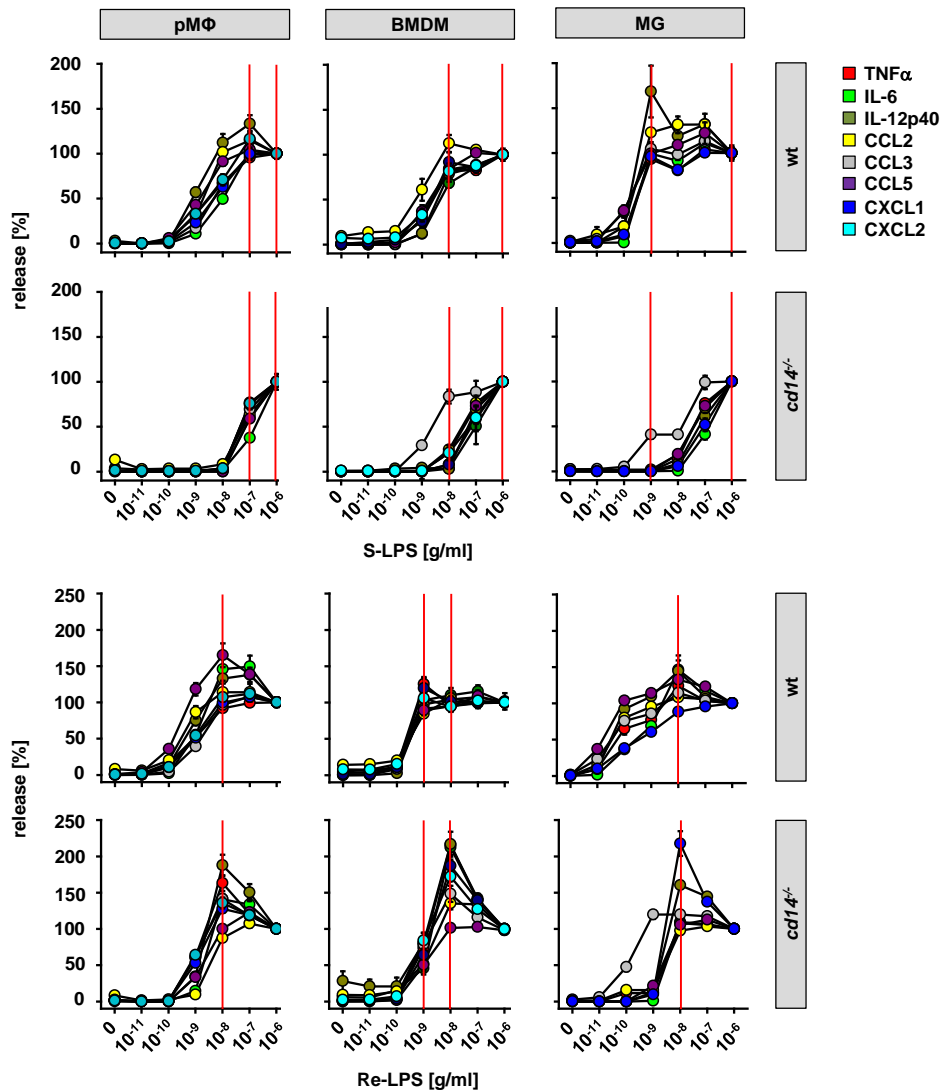
Figure 4.7: CD14 controls cellular response sensitivity in LPS-induced cytokine and chemokine production by microglia and macrophages.

Cultures of peritoneal macrophages (pMΦ), bone marrow-derived macrophages (BMDM) and microglia (MG) from C57BL/6J wt and $cd14^{-/-}$ mice were stimulated with S-LPS or Re-LPS at the indicated concentrations for 18 h. Cyto- and chemokine release was determined in the culture supernatants by ELISA. Absolute values were normalized to the amounts as released by stimulation at maximal agonist concentration (10^{-6} g/ml, taken as 100%). The presentation by percentage was chosen to facilitate comparison of potencies. Red lines indicate agonist concentrations at which maximal responses are elicited in wt and $cd14^{-/-}$. Data are mean ± SEM with n=12 from 2-3 individual experiments. (Data of cyto- and chemokine release by pMΦ and by BMDM were kindly provided by Dr. Tommy Regen.)

4.6   CD14 controls responses to TLR4 challenges of microglia and macrophages individually

The comparison of absolute releases by wt and *cd14^{-/-}* microglia revealed a more complex control by CD14. As described above, the lack of CD14 led to a silencing of the microglial responses to a low concentration of Re-LPS (e.g. 0.1 ng/ml). Nevertheless, a high concentration of Re-LPS (10 ng/ml) had a variable outcome in cytokine and chemokine production. In the absence of CD14, TNFα, IL-6, IL-12p40, and CXCL1 were overproduced by microglia, whereas the production of CCL2, CCL3 and CCL5 was not affected (Fig. 4.8A).
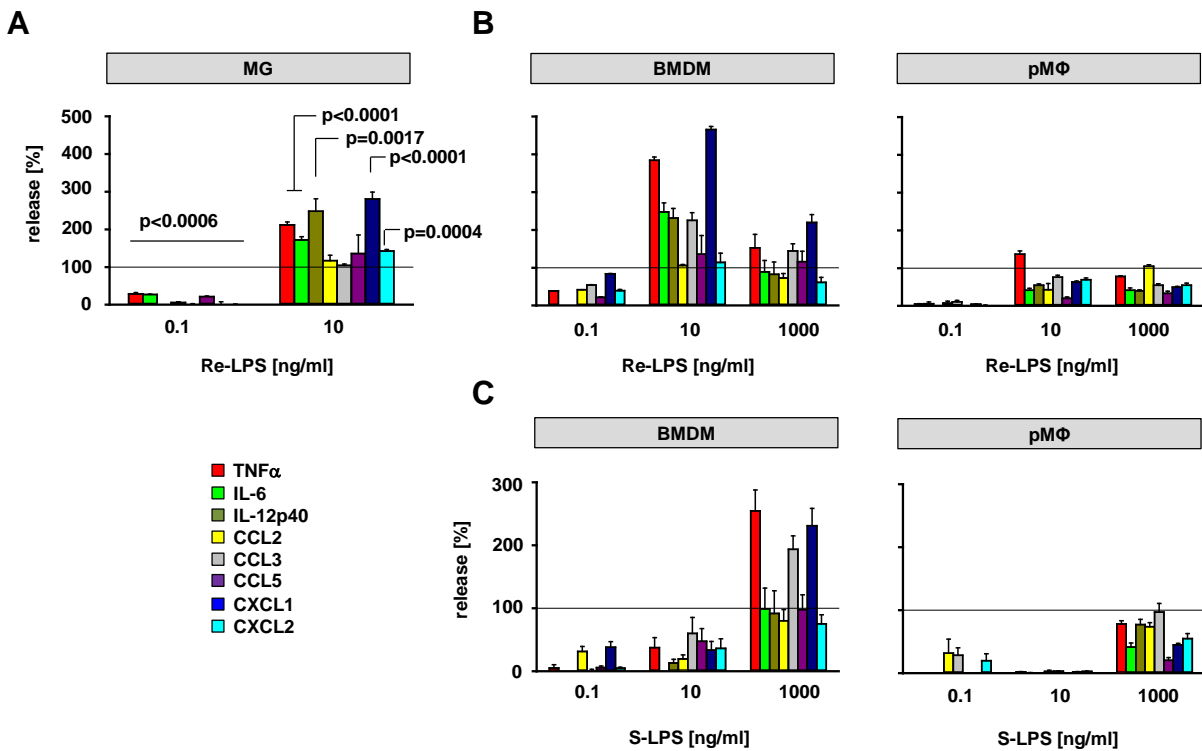
Figure 4.8: CD14 controls TLR4 S- and Re-LPS triggered cytokine and chemokine production efficacy in macrophages.
(A) Cultures of microglia (MG) from C57BL/6J wt and *cd14^{-/-}* mice were stimulated with Re-LPS at the indicated concentrations for 18 h. Cyto- and chemokine release was determined in the culture supernatants by ELISA. Absolute values as induced in *cd14^{-/-}* cells were normalized to amounts obtained from equivalent stimulations of the respective wt cells (horizontal lines indicating 100%). Data are mean ± SEM with n=12 from 2-3 individual experiments. **(B)** Bone marrow-derived macrophages (BMDM) or peritoneal macrophages (pMΦ) from C57BL/6J wt and *cd14^{-/-}* mice were stimulated with Re-LPS and analyzed as in (A). Data are mean ± SEM with n=12 from 2-3 individual experiments. **(C)** BMDM or pMΦ were stimulated with S-LPS and analyzed as in (A) Data are mean ± SEM with n=12 from 2-3 individual experiments. The Mann-Whitney U test was used for statistical analysis.

CXCL2 also showed some enhancement in the *cd14*$^{-/-}$ situation. Like CXCL1, it serves in the recruitment of neutrophils, acting through the joint receptor CXCR2. Yet the impact of CD14 absence differed for the two chemokines, and we thus focused in our further work on CXCL1 as the more affected neutrophil attractant.

BMDM and peritoneal macrophages treated with low concentrations of Re- and S-LPS showed a decreased or completely diminished cyto- and chemokine production in the absence of CD14 (Fig. 4.8B, C). BMDM from *cd14*$^{-/-}$ mice stimulated with high concentrations of LPS showed a quite similar induction pattern as determined for *cd14*$^{-/-}$ microglia, with only few exceptions. The excessive production of CXCL1 and TNFα by BMDM was even higher than by microglia, and CCL3 was overproduced in their case. Since the BMDM and peritoneal macrophages needed higher doses of LPS than microglia, we also used a third concentration of LPS (1000 ng/ml). At this concentration of Re-LPS, only CXCL1, CCL3 and TNFα were more produced in *cd14*$^{-/-}$ BMDM, while others were not changed or even less produced (CXCL2), when compared to the wt condition. However, this pattern was completely different for peritoneal macrophages stimulated with Re-LPS. Peritoneal macrophages lacking CD14 did not produce excessive amounts of cyto- and chemokines, independent of the Re-LPS concentrations (Fig. 4.8B). As shown in Figure 4.7, especially S-LPS needed CD14 to trigger a response, which probably contributed to the shifted overshoot by BMDM, when 1000 ng/ml instead of 10 ng/ml were needed. Also, the only factors being produced with increased amounts were TNFα, CCL3 and CXCL1. Other factors were independent of CD14 presence. Furthermore, there was no overshoot by peritoneal macrophages triggered by any of the used concentrations of S-LPS, and even at the highest dose, CD14 was necessary for a release.

Taken together, CD14 on microglia and BMDM does not only support the response to low concentrations of LPS, but it prevents an overshooting reaction to high concentrations, especially for the neutrophil chemoattractant CXCL1. Furthermore, peritoneal macrophages lacking CD14 do not produce excessive levels of cyto- and chemokines, suggesting cell-type specific regulatory functions of CD14. The fact that BMDM and microglia resembled each other in terms of an overshoot control agrees with other findings that demonstrate similar organization in these two populations. They may both have to respond to already tiny amounts of LPS as a sign of infection in their sensitive compartments. In contrast, traces of LPS may spill occasionally from the intestinal microbiota to reach peritoneal macrophages, which may have to tolerate these events.

4.7 CD14 is partially involved in immune responses triggered by other TLR agonists

Association of CD14 in responses to other than TLR4 agonists has been reported already previously. However, it has not been shown, whether also microglial responses to other TLR agonists depend on CD14 and if yes, to which extend. Furthermore, it was interesting to find out whether BMDM react in the same way like microglia, since they manifested some variations in their response (Figs. 4.7 and 4.8). To address these aspects, microglia and BMDM from wt and *cd14*^{-/-} mice were stimulated *in vitro* with Pam$_3$CSK$_4$, MALP-2, poly(I:C), poly(A:U) or CpG ODN as agonists for TLR1/2, TLR6/2, TLR3 and TLR9. After 18 h, the supernatants were analyzed for a release of TNFα and CXCL1, as factors being induced via the MyD88 pathway, and levels of CCL3 and CCL5, which require both MyD88 and TRIF adaptor proteins for induction (Regen et al., 2011). Figure 4.9A shows that wt microglia were very potent and produced multiple times higher levels of the tested cyto- and chemokines than BMDM. Neither microglia nor BMDM released CXCL1 in response to the TLR3 ligand poly(I:C). Stimulation of BMDM with poly(I:C) also did not lead to a production of CCL3, which occurs in microglia. CD14 in BMDM served in general more as a suppressor, as seen by an overshoot of cyto- and chemokines upon stimulation with Pam$_3$CSK$_4$, MALP-2, CpG and (partially) poly(I:C) in the absence of CD14 (Fig. 4.9B). In *cd14*^{-/-} microglia, overshoot was observed only upon stimulation with CpG. The responses to poly(I:C) and MALP-2 were not affected, and the release triggered by Pam$_3$CSK$_4$ was even lower in the absence of CD14. Interesting results were obtained for the other putative TLR3 agonist, poly(A:U), which in wt microglia as well as BMDM triggered far stronger response than poly(I:C) (Fig. 4.9A). However, while CD14 absence did not have dramatic effect on poly(I:C)-triggered responses, it abolished the production of all selected cyto- and chemokines induced by poly(A:U) (Fig. 4.9B). The response to poly(A:U) was also completely abolished in *cd14*^{-/-} BMDM. These results show that microglial and BMDM responses to TLR1/2, TLR6/2, TLR3 and TLR9 agonists differ in terms of potency and magnitude of cyto- and chemokine release, which is further differently shaped by CD14. It should be added that neither poly(I:C) nor poly(A:U) may serve as selective agonists of TLR3. Poly(I:C) also activates melanoma differentiation-associated protein 5MDA5, a retinoic acid-inducible protein (RIG)-like protein (Kato et al., 2006). The use of poly(A:U) could run the risk of driving confounding activation of other TLRs (Hanisch, unpublished observation).
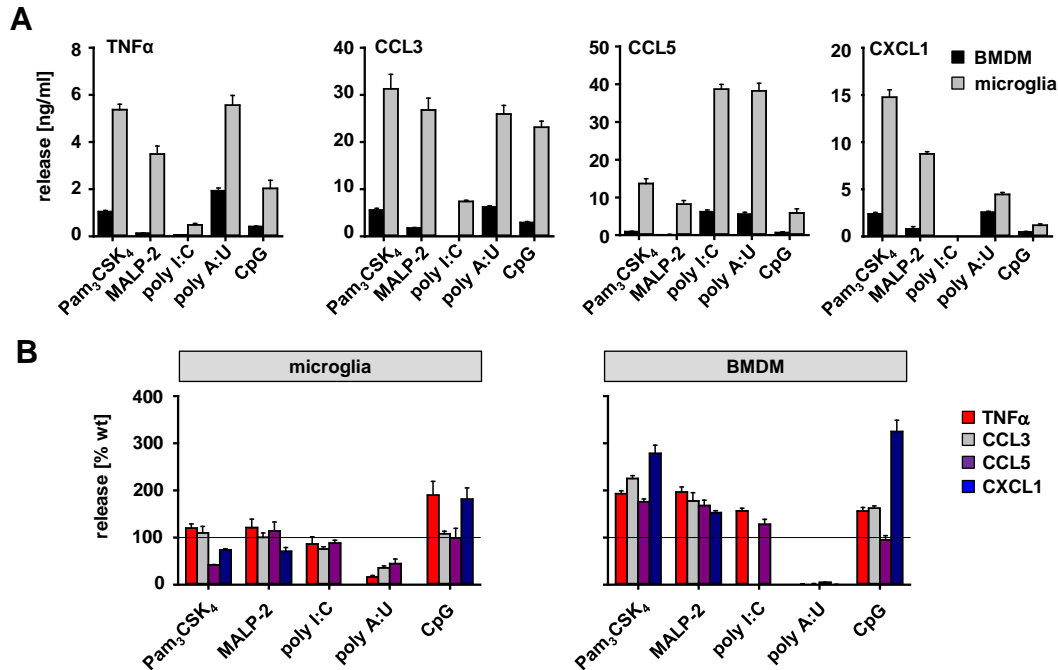
Figure 4.9: CD14 partially controls cytokine and chemokine release by BMDM and microglia triggered by other TLR agonists than TLR4.
BMDM and microglia cultures of wt and *cd14*^{-/-} mice were stimulated with Pam_3CSK_4, MALP-2 (both at 10 ng/ml), poly(I:C), poly(A:U) (both at 50 µg/ml) or CpG ODN (5 µg/ml) as agonists for TLR1/2, TLR6/2, TLR3 and TLR9 for 18 h. Cytokine and chemokine release was determined in the culture supernatants by ELISA. **(A)** Total amounts produced by wt microglia and BMDM. **(B)** Absolute values as induced in *cd14*^{-/-} cells were normalized to amounts obtained from equivalent stimulations of the respective wt cells (horizontal lines indicating 100%). Data are mean ± SEM with n=12 from 2 individual experiments.

4.8 Striatal injections of S-LPS and Re-LPS result in comparable monocyte and neutrophil infiltration into CNS

More neutrophils but the same amounts of monocytes were found in the brains of *cd14*^{-/-} animals inoculated intracerebrally with *E.coli* as compared to control mice (Fig. 4.3). These results go in line with the overshooting production of CXCL1 (as a critical neutrophil chemoattractant) and the unaltered levels of CCL2 (as the monocyte chemoattractant) by *cd14*^{-/-} microglia stimulated with high concentrations of LPS (Fig. 4.8; (Regen et al., 2011). For further studies, and to focus on the outcome of infectious challenges of different intensities, LPS was chosen because of the simplicity in carrying out controlled applications. While it is more difficult to titer the *E.coli*, LPS can be easily injected to the defined location at a precise concentration and within a given volume. For preliminary experiments, an amount of LPS of

1 µg in 1 µl of vehicle was chosen, according to previous studies (Rivest, 2009) and tested firstly for the effect of different LPS chemotypes, namely Re- and S-LPS, on the cell influx into CNS. Wt mice were, therefore, injected with Re- or S-LPS preparations into the striatum. The cell infiltrates in the brains were analyzed by flow cytometry after 24 h, as this time was identified as the most suitable to track both monocytes and neutrophils (Fig. 4.10A and Fig. 4.1C). Figure 4.10B shows that both, S-LPS and Re-LPS, resulted in the same number of neutrophils and monocytes in the CNS. Since the used *E.coli* K1 is predominantly bearing S-type of LPS (Cross et al., 1984), and this chemotype is the most complex and can thus well mimic infectious scenarios, further experiments were conducted with this LPS variant. The use of TLR4-deficient (*tlr4$^{-/-}$*) mice confirmed that the response, in terms of neutrophil and monocyte influx, was TLR4-dependent. Almost no cell infiltrates were observed in *tlr4$^{-/-}$* animals (Fig. 4.10C).
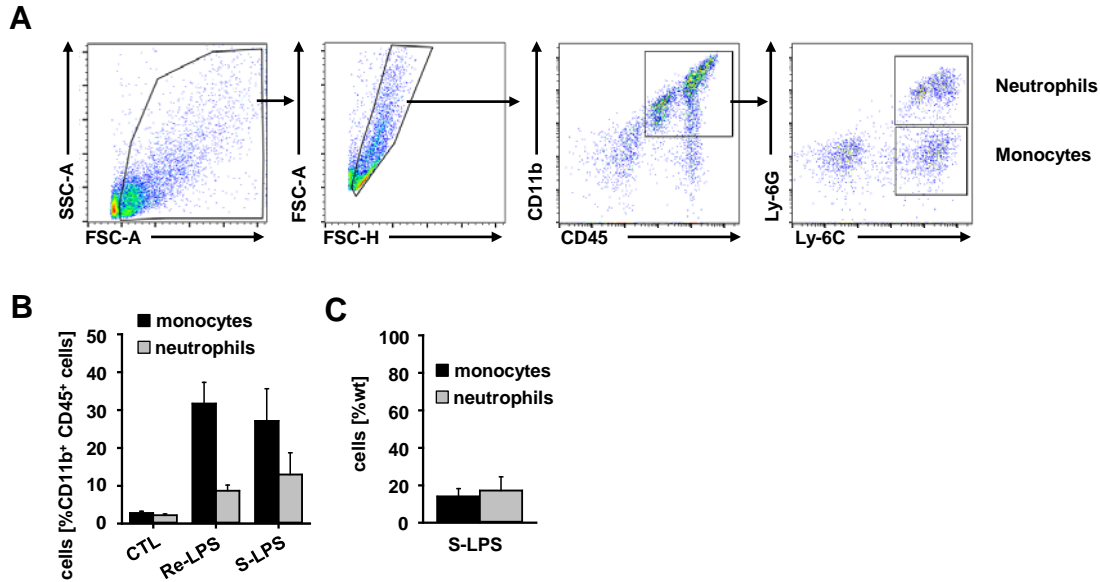
Figure 4.10: Intrastriatal injections of both S- and Re-LPS result in the same number of monocytes and neutrophils in the CNS and the LPS-triggered cell infiltration requires TLR4 signaling.
(**A**) Representative flow cytometry analysis of CNS infiltrates in a brain injected with S-LPS, as quantified in (B). **(B)** Mice (C57BL/6J wt) received a striatal injection of S-LPS or Re-LPS (both 1 µg). Controls (CTL) received vehicle only (H$_2$O). 24 h later, animals were perfused with PBS and brain infiltration of CD45$^+$ CD11b$^+$ Ly-6C$^+$ Ly-6G$^-$ monocytes and CD45$^+$ CD11b$^+$ Ly-6C$^+$ Ly-6G$^+$ neutrophils was analyzed by flow cytometry as in Fig. 4.3. Monocyte and neutrophil populations were expressed as percentage of CD45$^+$ CD11b$^+$ cells in the brain. **(C)** Mice (wt and *tlr4$^{-/-}$*) received S-LPS (1 µg) and their brains were processed as in (B). Monocyte and neutrophil infiltration in *tlr4$^{-/-}$* mice was expressed as percentage of respective cell infiltration in wt controls. Data are mean ± SEM with n=3-5 per group.

4.9   CD14 control over monocyte and neutrophil recruitment into the CNS depends on the LPS dose

Striatal injection of 1 µg of LPS triggered in the wt animals a response that was strong and roughly comparable to an *E.coli* challenge (Fig. 4.1C and Fig. 4.10B). Such a response, in terms of leukocyte influx intensity, gave the possibility to decrease and increase the applied LPS amounts. This enabled for a sophisticated study of a dose-dependent reaction in the presence and absence of CD14.
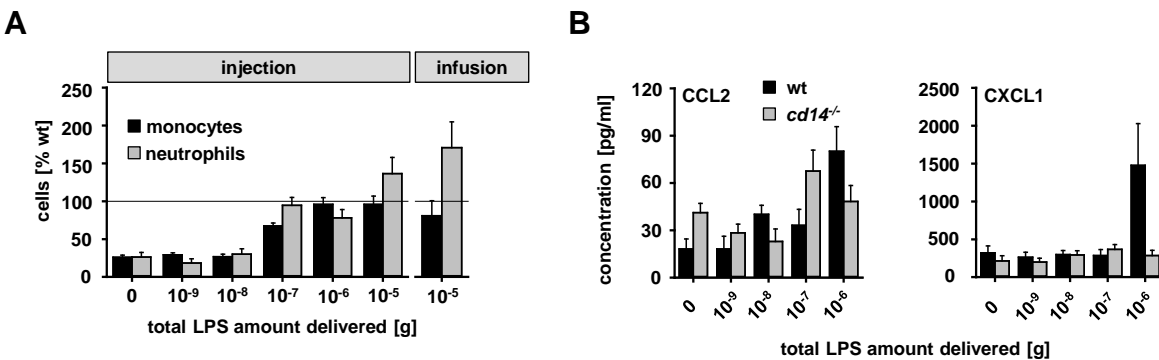
Figure 4.11: CD14 controls the recruitment of monocytes and neutrophils into the CNS upon striatal LPS administration.
(A) Mice (wt and $cd14^{-/-}$) received a striatal injection or a continuous infusion of S-LPS with the indicated total amounts. 24 h later, animals were perfused with PBS and brain infiltration of $CD45^+$ $CD11b^+$ $Ly-6C^+$ $Ly-6G^-$ monocytes and $CD45^+$ $CD11b^+$ $Ly-6C^-$ $Ly-6G^+$ neutrophils was analyzed by flow cytometry as in Fig. 4.3. Monocyte and neutrophil populations were expressed as percentage of $CD45^+$ $CD11b^+$ cells in the brain. Monocyte and neutrophil infiltrates in $cd14^{-/-}$ animals were normalized to the infiltrates obtained in wt animals. Data are mean ± SEM with n=3-5 per group in injected and n=7-8 per group in infused animals. **(B)** CCL2 and CXCL1 concentrations were determined by ELISA in the serum of wt and $cd14^{-/-}$ mice 24 h after they had received an injection of S-LPS as indicated. Data are mean ± SEM with n=6-10 per group from 3-5 independent injections. (Analysis of blood samples was performed by Christin Fritsche during her laboratory rotation period.)

To elucidate the effect of different doses of LPS on the brain infiltration in the absence of CD14, $cd14^{-/-}$ and wt animals were either once injected with an increasing dose of LPS into striatum or infused via ALZET pumps. The delivery via ALZET pumps mimicked a long-term presence of bacterial infection, while the total amount of LPS was equal to the highest dose used for the single injections. Flow cytometry of the brains after 24 h revealed less monocytes and neutrophils in the brains of $cd14^{-/-}$ mice injected with low doses of LPS (10^{-9} up to 10^{-8} g) than in the control animals (Fig. 4.11A). Infiltrates of monocytes in the $cd14^{-/-}$ brains achieved 70% of the wt at 10^{-7} g/ml LPS, and the higher doses of LPS attracted the same number of monocytes independently of CD14 presence. In contrast, LPS application of already 10^{-7} g/ml led to the same counts of recruited neutrophils into both genotypes. The highest injected dose (10^{-5} g/ml) resulted in more neutrophils in the mice lacking CD14. Analysis of the brains infused continuously with LPS for 24 h showed an even more pronounced and excessive infiltration of neutrophils in $cd14^{-/-}$

animals, while the monocyte number was the same in *cd14*^{-/-} as well as wt mice. Furthermore, blood analysis showed that only the highest doses of LPS led to an increase in circulating levels of chemokines CXCL1 and CCL2 (Fig. 4.11B), which occurred in a CD14-dependent manner. This was most likely the result of a spilling of the CNS-delivered LPS to the periphery, where it triggered a response in CD14 dependency. The comparison of the dose-response curves for central and peripheral effects made this the most likely explanation.

Taken together, the experiments on a defined and titrated delivery of LPS to the brain demonstrated the strictly dose-dependent impact of CD14, with a support of low-dose challenges and a containment of responses to high-dose exposure. Thus, LPS could be considered the essential PAMP agent driving the infiltration via chemokine induction—and CD14 was confirmed as the co-receptor deciding on the consequences in a LPS dose-dependent fashion.

4.10 Neutrophil recruitment into LPS-challenged brains is CXCR2-dependent

Cd14^{-/-} microglia reacted to LPS by either enhanced or diminished production of CXCL1 (Fig. 4.8A), which correlated with the effective rates of neutrophil infiltration to the brains of *cd14*^{-/-} animals. To find out, whether the neutrophil infiltration into the challenged brains was due to the CXCL1 chemoattraction, a recombinant CXCL1 was injected into the striatum and the brains were analyzed by flow cytometry. A single application of CXCL1 did not result in neutrophil recruitment (Fig. 4.12).
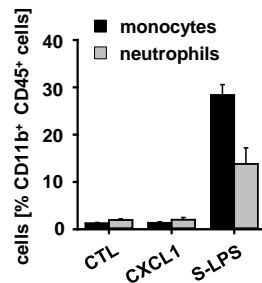
Figure 4.12: Single injection of CXCL1 into the CNS does not lead to recruitment of neutrophils.
Mice (wt) received an intracerebral injection of S-LPS (1 µg) or CXCL1 (100 ng). Controls (CTL) were treated with vehicle only. 24 h later, animals were perfused with PBS and brain infiltration of CD45^{+} CD11b^{+} Ly-6C^{+} Ly-6G^{-} monocytes and CD45^{+} CD11b^{+} Ly-6C^{+} Ly-6G^{+} neutrophils was analyzed by flow cytometry as in Fig. 4.3. Monocyte and neutrophil populations were expressed as percentage of CD45^{+} CD11b^{+} cells in the brain. Data are mean ± SEM with n=3-5.

However, the importance of the neutrophil chemoattractants CXCL1 and CXCL2, as those leading the neutrophils into the LPS-injected brains, was confirmed by blockade of the respective receptor CXCR2 (Fig. 4.13A). The mice that received an intravenous injection of a CXCR2-neutralizing antibody in addition to the striatal LPS showed a decreased number of neutrophils, while they revealed more monocytes in the brains, as compared to animals with intravenous injection of the matching isotype control. Less neutrophils were also observed in the blood of antibody-treated animals (Fig. 4.13B), which—in addition—showed also the role of the CXCR2 axis for the neutrophil egress from bone marrow reservoirs. In conclusion, CXCL1 alone may not be sufficient to organize the entire process of a neutrophil call to the CNS, but it is essential.
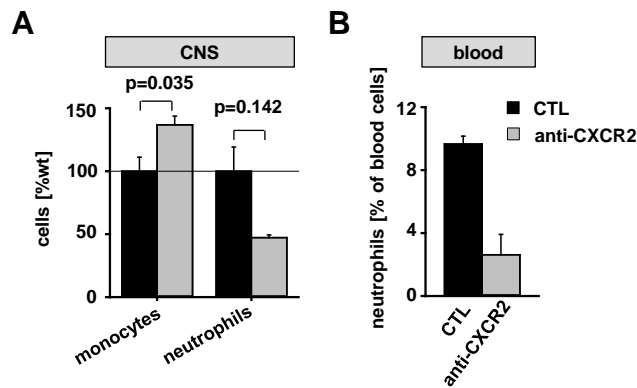
Figure 4.13: Neutrophils require functional CXCR2 to infiltrate CNS challenged with LPS.
(A) Mice (wt) received an intracerebral injection of S-LPS (1 µg) and an intravenous injection of anti-CXCR2 antibody (or an isotype control, CTL). Brain infiltration by monocytes and neutrophils was analyzed as in Fig. 4.3. Values were expressed as percent of those obtained in control animals. Data are mean ± SEM with n=3-5 per group. The Mann-Whitney U test was used for statistical analysis. **(B)** Mice (wt) were treated as in (A). Blood samples were analyzed for frequency of neutrophils as described in Fig.4.2.

4.11 LPS treatment does not affect CCR2 and CXCR2 expression in $cd14^{-/-}$ and wt mice

The expression levels of CCR2 and CXCR2 on monocytes and neutrophils, respectively, did not vary in the steady state situation (Fig. 4.4B). Since the results from the previous experiment showed the importance of these receptors for the CNS penetration, it was necessary to exclude that $cd14^{-/-}$ blood cells had altered expression levels upon a brain challenge. For that purpose, mice of both genotypes were either injected intrastriatally with LPS or left untreated, and blood samples were analyzed after 24 h. Figure 4.14A shows that levels of CCR2 on monocytes and CXCR2 on neutrophils from LPS-treated $cd14^{-/-}$ mice were not significantly different from the wt controls. All animals had also the same frequency of

inflammatory Ly-6C^{hi} monocytes, which did not change upon LPS injection (Fig. 4.14B). Furthermore, wt and *cd14$^{-/-}$* mice had the same number of circulating monocytes expressing both Ly-6C and CCR2, independently of the LPS treatment.
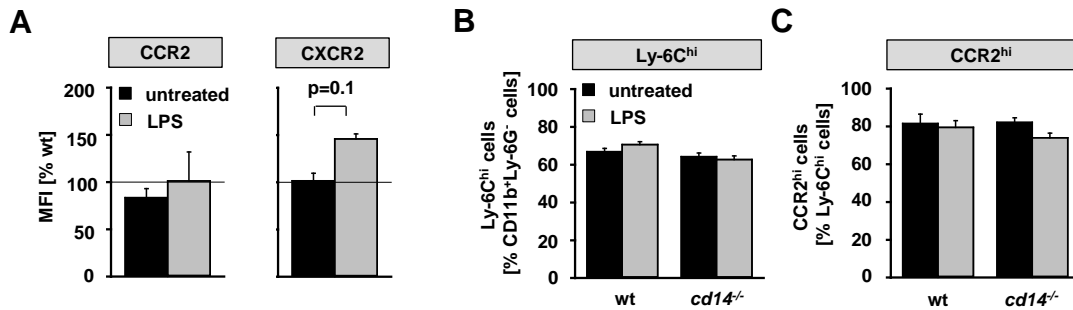
Figure 4.14: Intrastriatal LPS injection does not alter the expression levels of CCR2, CXCR2 and Ly-6C on blood cells of *cd14$^{-/-}$* and wt mice.

Mice (wt and *cd14$^{-/-}$*) received an intrastriatal injection of S-LPS (1 µg) or were not treated at all. Blood samples were analyzed 24 h later by flow cytometry as described in Fig. 4.2. **(A)** CCR2 and CXCR2 expression on monocytes (CD11b$^-$Ly-6G$^-$Ly-6C$_{hi}$) and neutrophils (CD11b$^+$Ly-6G$^+$). **(B)** The percentage of Ly-6C^{hi} monocytes. **(C)** The percentage of CCR2$^+$ cells among Ly-6C$_{hi}$ cells. The Mann-Whitney U test was used for statistical analysis.

4.12 CD14 is required for an injury-triggered CNS infiltration by immune cells

CNS tissue trauma can lead to a monocyte/neutrophil infiltration itself, i.e. also in the absence of obvious infection. This sterile inflammation is triggered by recognition of endogenous factors (DAMPs), which are released from necrotic cells or damaged tissue. Especially TLR4 showed the capacity to bind various DAMPs and to fuel a sterile inflammation. However, also other co-receptors appeared to be necessary to enable a full response (Chen and Nunez, 2010; Ehrchen et al., 2009; Pal et al., 2012; Park et al., 2006). To investigate the role of CD14 in triggering a sterile inflammation within the CNS, a stab wound model affecting the striatum upon transcortical and transcallosal penetration was used. A damage volume of 0.05 µl resulted in a very weak leukocytes influx, which was not further affected by CD14 absence. However, already a damage volume of 1 µl was sufficient for a monocyte and neutrophil infiltration of the brain in wt mice (Fig. 4.15). This response was absent in *cd14$^{-/-}$* animals, showing thereby the CD14 importance in the immune reaction to damage.
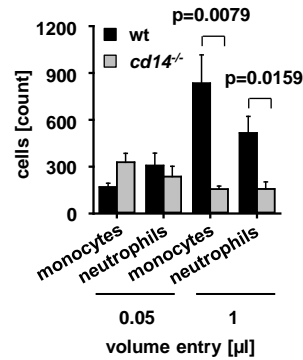
Figure 4.15: Cell recruitment in response to tissue damage depends on CD14.
Mice (wt and *cd14*^{-/-}) received an intracerebral stab wound in combination with an injection of a defined vehicle (H$_2$O) volume over 3 min to produce tissue injury of varying extent. 24 h later, animals were perfused and brains were processed to determine the infiltration by monocytes and neutrophils as in Fig. 4.3 (expressed as counts per 10,000 CD11b^{+} cells). Data are mean ± SEM with n=4 per group. The Mann-Whitney U test was used for statistical analysis.

4.13 Microglial responses to fibronectin, as a representative DAMP, are entirely dependent on CD14

The CNS trauma is associated with a tissue damage causing release of a plethora of DAMPs that can be sensed by microglial TLR4, including, for instance, fibronectin (FN). FN is found in the plasma and in the ECM. Under homeostatic conditions, it plays important roles in the coagulation cascade, in cell adhesion, migration and development (Pankov and Yamada, 2002). Both plasma- and ECM-derived FN could drive a microglial response through TLR4, its abnormal presence or presentation in the CNS assigning a DAMP character (Goos et al., 2007; Regen et al., 2011). As a plasma factor, which is usually invisible to parenchymal microglia, FN may enter the CNS upon BBB leakage or vascular disruption. Moreover, tissue injury will also cause some disintegration of the ECM, liberating soluble FN. Proteolysis accompanying the tissue damage can liberate functional domains of FN, revealing thereby its cryptic activities (Pagano and Reboud-Ravaux, 2011). We had observed that immobilized FN did not trigger microglial responses, whereas it did so when it was offered in soluble form (unpublished). We consider conformational flexibility as a key issue, suggesting that ECM-embedded FN stays inert to TLR4 unless it is released from the network. Lastly, resident CNS cells can produce FN in association with inflammatory lesions (Stoffels et al., 2013), which could similarly and further affect microglial reactions. All these observations pointed out that FN could be a very relevant DAMP in the context of CNS injury.
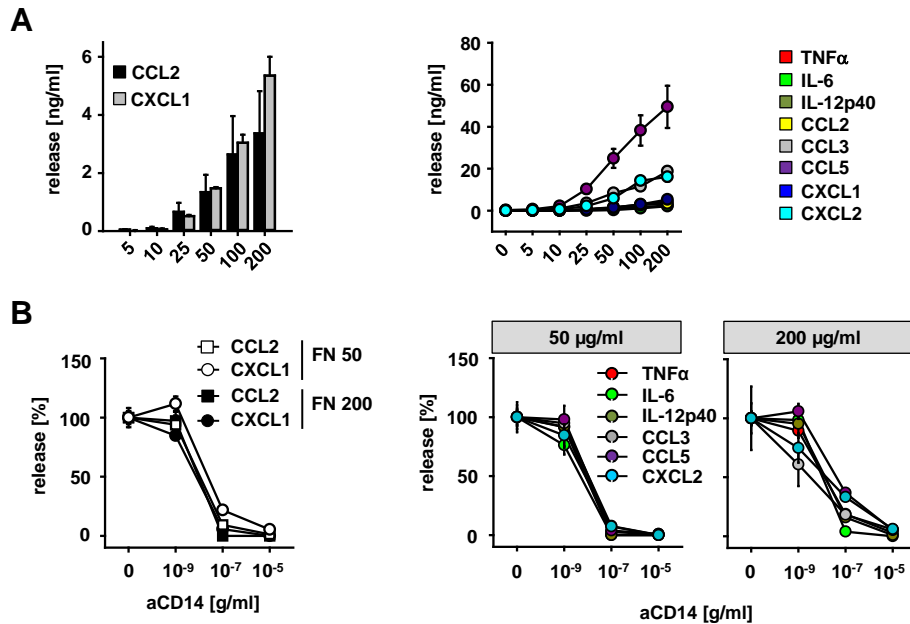
Figure 4.16: Microglial responses to pFN require functional presence of CD14.
(A) Microglia were treated with mouse pFN at indicated concentrations for 18 h. Cyto- and chemokine release was determined in the supernatants by ELISA. **(B)** Microglia were stimulated with mouse pFN at 50 or 200 µg/ml in the absence or presence of anti-CD14 antibody (clone 4C1) at different concentrations for 18 h. Cells also received a 30 min pre-incubation with the antibody at the respective concentration. Cyto- and chemokine release was determined in the supernatants. Absolute amounts were expressed as a percentage of the release obtained in the absence of CD14 blocking antibody. Data are mean ± SEM with n=4.

To evaluate the role of CD14 in microglial response to FN, as the representative of the DAMPs, microglial cultures were stimulated with plasma fibronectin (pFN) in the presence and absence of CD14 blocking antibody. Microglia responded dose-dependently to increasing doses of pFN with a production of all tested cyto- and chemokines (Fig. 4.16A). However, the blockade of CD14 completely halted this response, independently of the pFN concentration (Fig. 4.16B). Of note, blockade of CD14 did not cause excessive production of CXCL1 or any other cyto- and chemokine upon stimulation with high concentrations of pFN, as observed in cells treated with high concentrations of LPS. These results show the mandatory role of CD14 in the response to pFN and further indicate a potential role of CD14 in a differential regulation of reactions to damage *versus* infection.

4.14 CD14 is required for a DAMP-triggered CNS infiltration by immune cells

The efficacy of pFN to induce cyto- and chemokines by microglial treatment was comparable to that of a LPS stimulation, although the pattern differed by the quantity of individual factors—suggesting distinct

signatures despite the shared use of TLR4 (Regen et al., 2011). Since LPS injections into the brains of wt mice led to leukocyte infiltration, the question was whether an application of pFN would do the same. Therefore, mice received a single injection of pFN into the striatum, to mimic a vascular leakage. After 24 h, the brain infiltrates were analyzed for neutrophils and monocytes. The highest concentrations of pFN caused only a moderate cell recruitment, in comparison to LPS, and these cells were identified only as monocytes (Fig. 4.17A). During a CNS injury, transmigration of plasma factors due to vascular leakage is probably not a short-lasting event, but may rather last longer. For that reason, the single injection approach was exchanged for a continuous delivery by ALZET pumps over 24 and 48 h and the concentration of 600 µg/ml was chosen to match the actual plasma levels of pFN in mice. In order to verify that the cell recruitment depended on CD14, $cd14^{-/-}$ mice received pFN, in addition to wt mice. The infusion of wt mice for a period of 24 and 48 h resulted in response of the same magnitude as in the case of a single injection. Importantly, CD14 deficiency led to ablation of cell recruitment (Fig. 4.17B). These results show that LPS and pFN cause a similar activation profile of microglia *ex vivo*, i.e. in terms of a production of cyto- and chemokines, while both agonists differ by the strength of response *in vivo*.
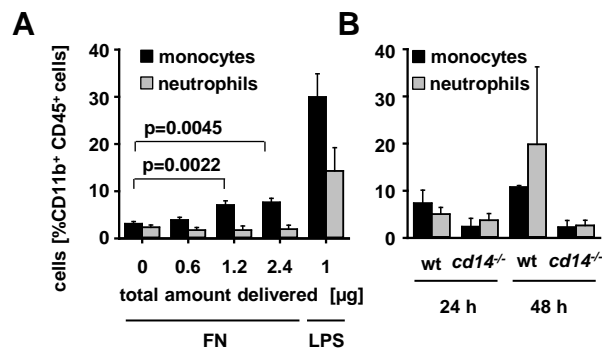
Figure 4.17: CD14 deficiency halts the leukocyte infiltration into the brains challenged with pFN.
(A) Mice (wt) received an intracerebral injection of mouse pFN or S-LPS (amounts as indicated). Controls (CTL) were treated with vehicle (PBS) only. 24 h later, animals were perfused with PBS and brain infiltration by monocytes and neutrophils was determined as in Fig. 4.3. Data are shown as mean SEM with n=4 per group. For statistic significance Mann-Whitney U test was used. **(B)** Mice (wt and $cd14^{-/-}$) received an intracerebral infusion of mouse pFN (600 µg/ml; 0.5 µl/ml) for 24 or 48 h, the animals were subsequently perfused with PBS and brain infiltration by monocytes and neutrophils was determined as in Fig. 4.3. Data are shown as mean SEM with n=2-3 per group.

4.15 Delivery of fibronectin into CNS activates local microglia but does not cause further damage

The continuous delivery of pFN resulted in a moderate response, in terms of immune cell infiltrations (Fig. 4.17B). These results, however, did not reflect the pFN effects on tissue outcomes and how they would further depend on CD14. For that, pFN or PBS was continuously delivered into wt and $cd14^{-/-}$ mice

for 72 h. The brains were consequently embedded into paraffin and stained. Figure 4.18A-D shows the pFN-triggered activation of microglia/macrophages (visualized by immunostaining for Mac3 and Iba-1) in wt animals, while this response was absent in the *cd14*^{-/-} mice. On the other hand, pFN infusion caused neither demyelination nor axonal loss, as visualized by LFB-PAS and Bielchowsky stainings, respectively (Fig. 4.19A, B). In summary, pFN activates microglia in the functional presence of CD14 but does not lead to overt tissue impairment, in addition to the cannula-associated damage. (A more detailed study involving histology was a part of the Master Thesis of Anne-Sophie Ernst, who performed the analysis.)
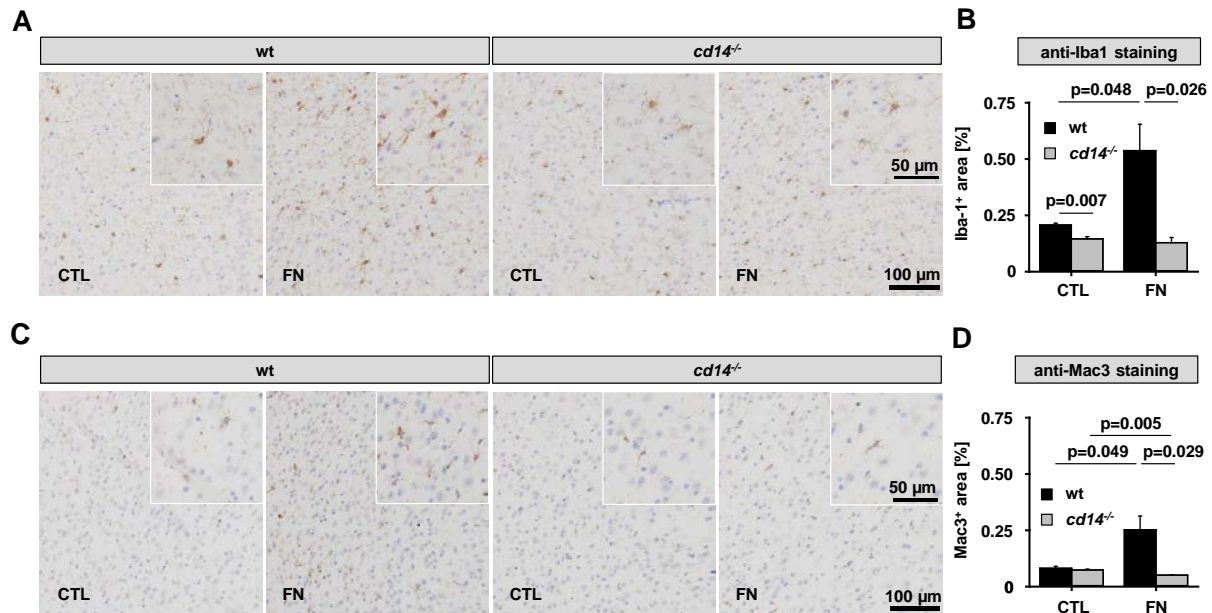
Figure 4.18: The up-regulation of Mac3 and Iba-1 on microglia/macrophages in the brains infused with pFN requires CD14.
(Images were adopted from Master's Thesis of Anne-Sophie Ernst.) Mice (wt and *cd14*^{-/-}) received an intracerebral infusion of mouse pFN (600 µg/ml; 0.5 µl/h) or vehicle for 72 h, followed by histological characterization in brain tissue sections. **(A)** Representative light microscopy images of anti-Iba1 staining. **(B)** Quantitative analyses of the anti-Iba1 staining. Values refer to the relative size of positive areas in an ipsilateral hemisphere. **(C)** Representative light microscopy images of anti-Mac3 staining. **(D)** Quantitative analyses of the anti-Mac3 staining. Values refer to the relative size of positive areas in an ipsilateral hemisphere. Data are mean ± SEM with n=3 per group. Two-sided Student´s t-test was used for statistical analysis.
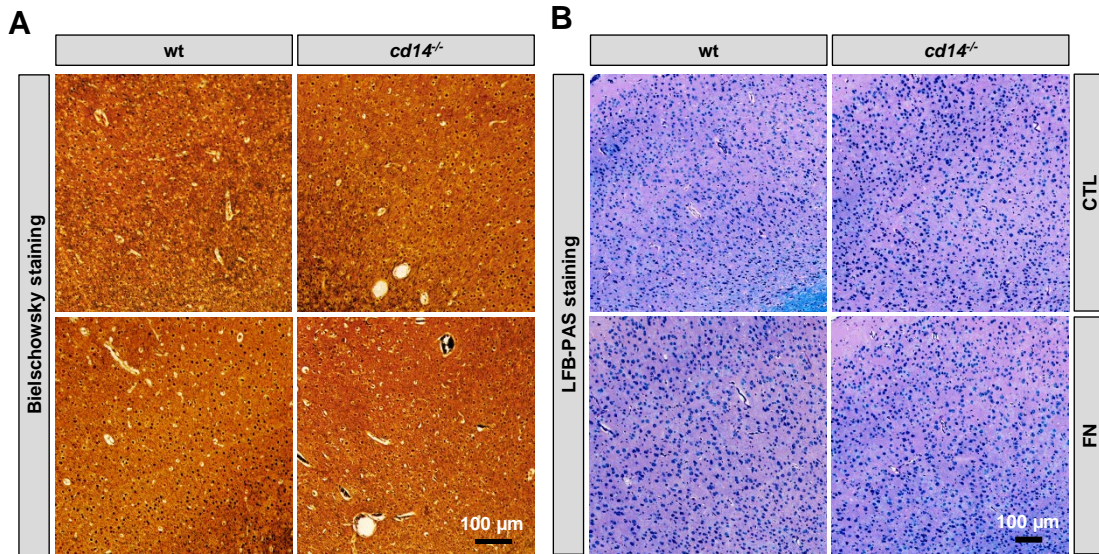
Figure 4.19: Intracerebral pFN infusion causes neither demyelination nor axonal loss.
(Images were adopted from Master's Thesis of Anne-Sophie Ernst.) Mice (wt and *cd14*$^{-/-}$) were treated as in Fig. 4.18. **(A)** Representative light microscopy images of Bielschowsky staining of axonal structures. **(B)** Representative light microscopy images of LFB/PAS staining of myelin structures.

4.16 CD14 deficiency impairs monocyte influx in a stroke model

Stroke is one of the leading causes of death worldwide. A sterile inflammation process as triggered by DAMPs plays an important role (Iadecola and Anrather, 2011). For that reason we decided to elucidate the role of CD14 in transient middle cerebral occlusion (MCAO), a mouse model of ischemic stroke. In the previous experiments (infectious setting), the emphasis was always on the response within the first 24 h, because neutrophils and monocytes were detectable at the same time (Fig. 4.1). For the MCAO approach, brains were analyzed 24 h after surgery as well. However, due to the particular kinetics of cell recruitment upon MCAO, a second time point of analysis was chosen at 72 h. While neutrophils are already terminally differentiated cells and thus can be easily detected at any time point using the same markers, monocytes entering the tissue differentiate further into macrophages. Therefore, analysis after 24 h considered the presence of monocytes, whereas after 72 h, cells were rather considered as monocytes/macrophages. Accordingly, they were further analyzed for Ly-6C expression (Fig. 4.20A, B).
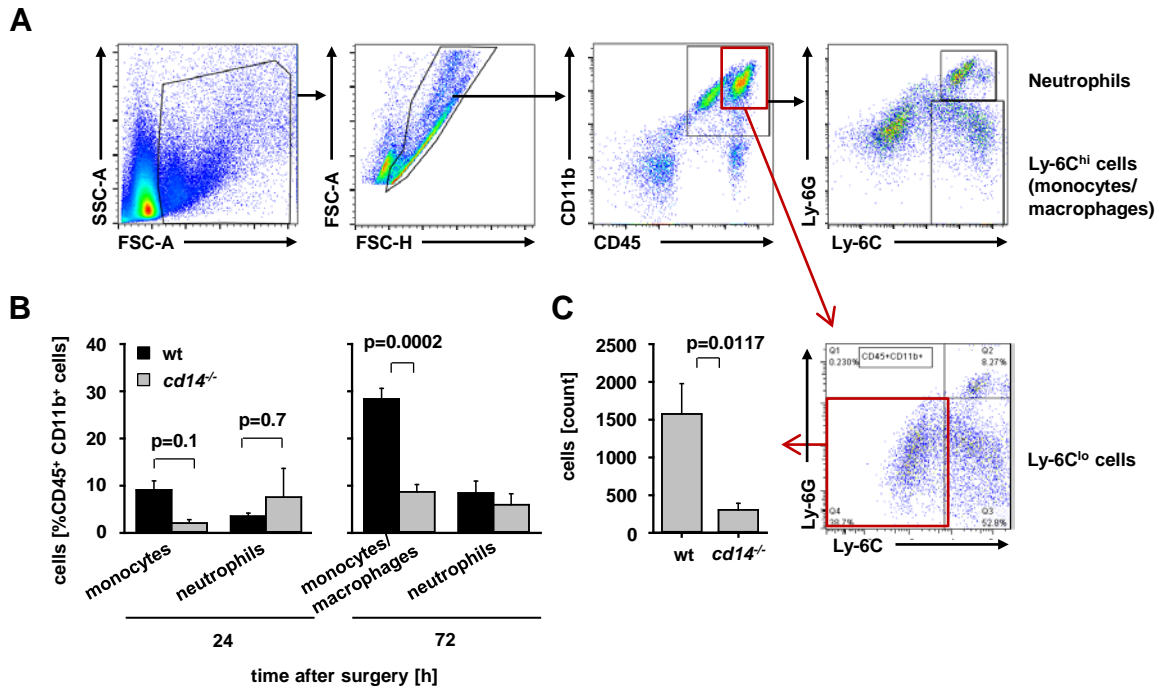
Figure 4.20: CD14 deficiency leads to impaired monocyte recruitment into CNS upon MCAO induction.
Mice (wt and $cd14^{-/-}$) underwent MCAO for 60 min with a subsequent reperfusion. After 24 h or 72 h, animals were perfused with PBS and single cell suspensions were prepared from ipsilateral brain hemispheres and analyzed by flow cytometry, as described in Fig. 4.3. 10,000 CD45$^+$ cells were collected and processed to determine the cell infiltration. **(A)** Representative of flow cytometry analysis. **(B)** Quantification of CD45$^+$CD11b$^+$Ly-6G$^-$Ly-6C^{hi} cells and neutrophils by flow cytometry. Data are mean ± SEM with n_{24h}=3 and n_{72h}=7-10. **(C)** Quantification of CD45^{hi}CD11b$^+$Ly-6G$^-$Ly-6C^{lo} cells after 72 h expressed as cell counts per 10,000 CD45$^+$ cells. Data are mean ± SEM with n=7-10. The Mann-Whitney U test was used for statistical analysis.

The controlled transient obstruction of the blood flow in $cd14^{-/-}$ and wt mice was performed by Peggy Mex (as part of a collaboration with the laboratory of Prof. Josef Priller, Charité Berlin). Flow cytometry analysis of the brains showed a reduced number of monocytes in the $cd14^{-/-}$ mice after 24 h (Fig. 4.20B). CD14 deficiency had an even more striking effect after 72 h. Then, the frequency of cells identified as monocytes/macrophages (by the expression profile CD45$^+$CD11b$^+$Ly-6G$^-$Ly-6C^{hi}) decreased from 30% to 10% (Fig. 20B). Furthermore, the CD14 absence also resulted in significantly less CD45^{hi}CD11b$^+$Ly-6G$^-$Ly-6C^{lo} cells in the brain 72 h after surgery, in comparison to the wt mice (Fig. 4.20C). On the other hand, neutrophil infiltrations after 24 as well as 72 h were not affected.

4.17 CD14 deficiency enhances the infarct size and bacterial load in the lungs

Blood flow occlusion and subsequent reperfusion of the brain result in large-scale damages, which are responsible for the devastating consequences of stroke, even causing death. For an evaluation of CD14 involvement in the general outcome for the animals upon stroke, *cd14*[^-/-] and wt mice underwent MCAO and after 72 h, the infarct volume was assessed by staining of brain sections. The *cd14*[^-/-] mice were less vital and had a higher death incidence (Table 4.1). In line with this observation, *cd14*[^-/-] mice had an infarct volume mounting to the double of the size as obtained in the wt counterparts (Fig. 4.21A). As it is known that ischemic brain injury can also lead to a systemic immunosuppression with a higher risk of pulmonary infection (Prass et al., 2003), suspensions of the lungs were checked for bacterial load. Figure 4.21B shows that the *cd14*[^-/-] mice had a significantly higher bacterial load in the lungs than the wt animals.

Table 4.1: Death incidence of wt *versus cd14*[^-/-] mice after 60 min of MCAO.
The table summarizes a number of wt *versus cd14*[^-/-] mice per a total number of used animals that did not survive 72 h after MCAO.

genotype	N deaths/N used mice
wt	10/10
***cd14*[^-/-]**	6/10
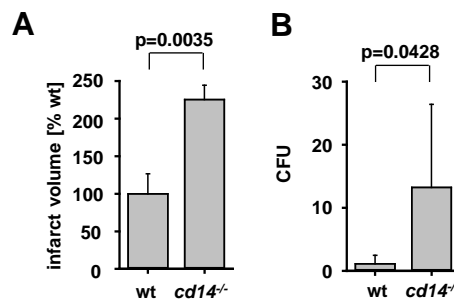
Figure 4.21: CD14 deficiency enhances the infarct volume in the CNS and the bacterial load in the lungs upon MCAO induction.
(A) The infarct volume was determined in mice 72 h after MCAO treatment as in Fig. 4.20 by quantitative histology. Data are mean ± SEM with n=6-7. **(B)** The bacterial load was determined in the lungs of mice 72 h following MCAO and expressed as total colony forming units (CFU). Data are mean ± SEM with $n_{cd14-/-}$=4; n_{wt}=7. The Mann-Whitney U test was used for statistical analysis.

4.18 CD14 expression is highly regulated by TLR agonists and cytokines

In comparison to peripheral macrophages, microglia express only very low levels of CD14 under normal conditions (Gautier et al., 2012). However, this can change in pathological situations (Glezer et al., 2003a; Lacroix et al., 1998; Landmann et al., 2000). To see whether CD14 levels can be regulated in our system, microglia were stimulated for different time periods with selected TLR and non-TLR agonists. CD14 transcripts and protein expression were measured by real time quantitative PCR (qRT-PCR) and flow cytometry, respectively. TLR4 agonists, i.e. pFN and LPS, induced both a rapid increase in CD14 mRNA, with subsequent increases of the surface-expressed as well as total protein (Fig. 4.22A-C). Also Pam$_3$CSK$_4$, poly(A:U) and CpG as TLR1/2, TLR3 and TLR9 agonists, respectively, up-regulated CD14 expression in a time-dependent manner. Other factors (IL-4, IFNβ and IFNγ), on the other hand, dramatically reduced the CD14 expression within 48 h (Fig. 4.22B). Furthermore, CD14 transcription was similarly up- and down-regulated, independently of the mouse strains (Fig. 4.22D). LPS stimulation led also to an equal enhancement in CD14 expression on adult microglia, confirming that the observed phenomenon is age-independent (Fig. 4.22E). In addition, on astrocytes, where no basal CD14 was detectable, LPS treatment did also not change the situation (Fig. 4.22F), pointing thus to microglia as the only cells in the CNS parenchyma that can take a benefit of having CD14.

The opposing regulatory roles of various factors on the regulation of CD14 expression are shown in Figure 4.23A. Here, cells were pretreated ("primed") with IFNγ and subsequently challenged with LPS (at different concentrations) and pFN in the absence or presence of IFNγ. The TLR4 stimuli-increased CD14 levels were not affected by IFNγ pre-treatment. However, while high doses of LPS abolished the reduction effect of IFNγ, pFN and low concentrations of LPS did not raise the CD14 levels above those measured for untreated cells (100%). These results imply that CD14, as a strong regulator of TLR-triggered responses, is—in turn—itself highly regulated. TLR4 agonists can thereby increase CD14 levels to organize for their own signaling support and regulation. Low doses of LPS would require CD14 for their efficient action, and pFN as a DAMP would even mandatorily depend on the co-receptor for any response. High doses of LPS would thereby arrange for the containment of microglial reactions as CD14 exerts a negative influence on certain gene inductions.
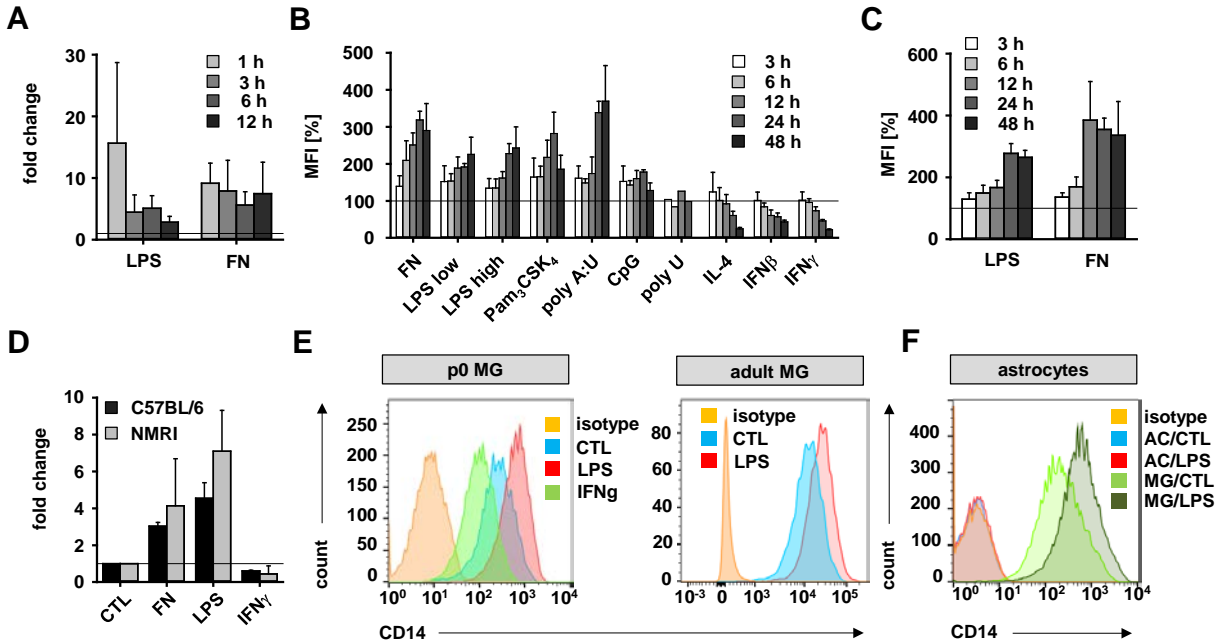
Figure 4.22: TLR agonists and cytokines regulate expression of CD14 by microglia.
(A) Microglia (p0, wt) were stimulated with Re-LPS (10 ng/ml) or bovine pFN (100 µg/ml) for the indicated time periods and CD14 transcripts were quantified by qRT-PCR, using GAPDH as an internal control. The CD14/GAPDH ratio for untreated samples was set as a baseline value to which all transcript levels were normalized as x-fold change. Data are mean ± SEM with n=3 from 3 experiments. **(B)** Cells were stimulated with Pam_3CSK_4, LPS ('high'), MALP-2, IFNγ, IFNβ, (all 10 ng/ml), LPS ('low', 0.1 ng/ml), poly(I:C), poly(A:U) (both 50 µg/ml), poly(U), CpG ODN (both 5 µg/ml) or bovine pFN (100 µg/ml) for the indicated time points. Subsequently, cells were FcγRII/III-blocked (with anti-CD16/CD32 mAb), stained with PE-anti-CD14 and Pacific Blue-anti-CD11b for acquisition by flow cytometry. By this procedure, surface-expressed CD14 protein is determined. For data analysis, only CD11b^{+} events were included. Median fluorescence intensity (MFI) was normalized to values obtained with unstimulated cells (set to 100%). Data are mean ± SEM with n=3 from 3 experiments. **(C)** Cells were stimulated as in (A), subsequently permeabilized, blocked and processed for flow cytometry with MFI calculation as in (B). This procedure determines intra- and extracellular CD14. Data are mean ± SEM of n=3 from 3 experiments. **(D)** Microglia from wt NMRI or C57BL/6J were stimulated as in (A) in addition with IFNγ (10 ng/ml) for 3 h and CD14 transcripts were quantified by qRT-PCR as in (A). Data are mean ± SEM with n=2-3 from 2-3 experiments. **(E)** Cultures of p0 and adult (17 weeks) microglia were stimulated with LPS and IFNγ (both 10 ng/ml) for 24 h. Microglia were stained as in (B) and analyzed by flow cytometry. Untreated cells served as an experimental control (CTL) and cells processed with a matching isotype were used as staining control. **(F)** Cultures of microglia and astrocytes (from wt mice) were treated with LPS (10 ng/ml). Subsequently, cells were permeabilized, FcγRII/III-blocked and stained intra- and extracellular with Pacific Blue-anti-CD11b, APC-anti-GFAP and PE-anti-CD14 for acquisition by flow cytometry. CD14 expression was assessed on microglia (CD11b^{+} GFAP^{-}) or on astrocytes (CD11b^{-} GFAP^{+}). Histograms are representative for up to 4 preparations and analyses.
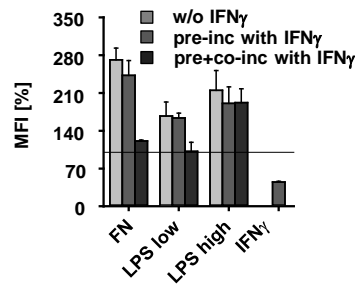
Figure 4.23: High LPS challenges overwrite the down-regulation of CD14 expression by IFNγ.
Cells were treated with IFNγ (10 ng/ml) for 48 h and then stimulated with Re-LPS (0.1 ng/ml as 'low', 10 ng/ml as 'high') or bovine pFN (100 µg) for additional 18 h either in the absence or further presence of IFNγ. Another group only received IFNγ for 48 h. CD14 surface expression was determined as in Fig. 4.22. Data are mean ± SEM with n=2 from 2 experiments.

Since CD14 serves as a link of TLR4 to TRIF signaling, we wanted to determine whether CD14 expression itself depends on TRIF. For that, we quantified the surface CD14 expression in wt and TRIF-deficient ($trif^{lps2}$) microglia, as stimulated with TLR agonists. As revealed in Figure 4.24, CD14 levels were induced in both strains similarly, showing that CD14 does not need the TRIF pathway activity to induce its own expression.
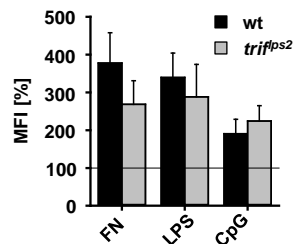
Figure 4.24: Induction of CD14 expression does not occur via TRIF-dependent pathway.
Microglia (from wt and $trif^{lps2}$ mice) were stimulated with bovine pFN (100 µg/ml), Re-LPS (10 ng/ml) or CpG ODN (5 µg/ml) for 18 h and CD14 surface expression was determined as in Fig. 4.22. Data are mean ± SEM with n=2 from 2 experiments.

4.19 Membrane-anchored CD14 is required to establish regulation of TLR4 activities

CD14 is attached to the cell surface only by a GPI anchor. Some cells (endothelial, epithelial cells) do not express membrane-anchored CD14, but can recruit the soluble form (sCD14) and use it subsequently for TLR4-triggered responses (Pugin et al., 1993). Under normal situations, sCD14 is not present in the CNS,

but it can be found in the CSF during infections or CNS pathologies (Cauwels et al., 1999; Yin et al., 2009). It was thus interesting to test whether sCD14 could substitute for a CD14 absence in microglia to restore responses. Therefore, wt and *cd14*^{-/-} microglia were stimulated with LPS of high and low concentrations and with pFN in either the absence or presence of recombinant sCD14. Measurements of released CXCL1 and CCL2 were considered to demonstrate whether sCD14 would (i) rescue the insufficient production by *cd14*^{-/-} cells as triggered by low doses of LPS, (ii) establish release responses to pFN and (iii) suppress the excessive CXCL1 production upon exposure to a high dose of LPS. However, addition of recombinant sCD14 to *cd14*^{-/-} cells treated with TLR4 agonists did not recover their responses to a wt situation (Fig. 4.25A). sCD14 did neither restore the reduced or missing chemokine production in low-dose LPS and pFN challenges nor decrease the exaggerated levels of CXCL1 upon high-dose LPS treatment. On the other hand, wt cells were affected by the presence of sCD14 as they showed some dose-dependent increase in chemokine induction.

To address this phenomenon further, flow cytometry analysis of surface CD14 was employed. Increased CD14 levels, to the extent measured upon TLR4 agonist treatments, were detected on cells incubated alone with a high concentration of sCD14 (Fig. 4.25B). This probably occurred due to the agonist-independent attachment to a TLR complex, as presence of sCD14 together with LPS or pFN treatment did not further increase the measured amounts of CD14.

Taken together, microglia need the membrane-anchored version of CD14 to control responses to TLR4 challenges, and soluble version of CD14 cannot substitute for the absence of the cell-attached form.
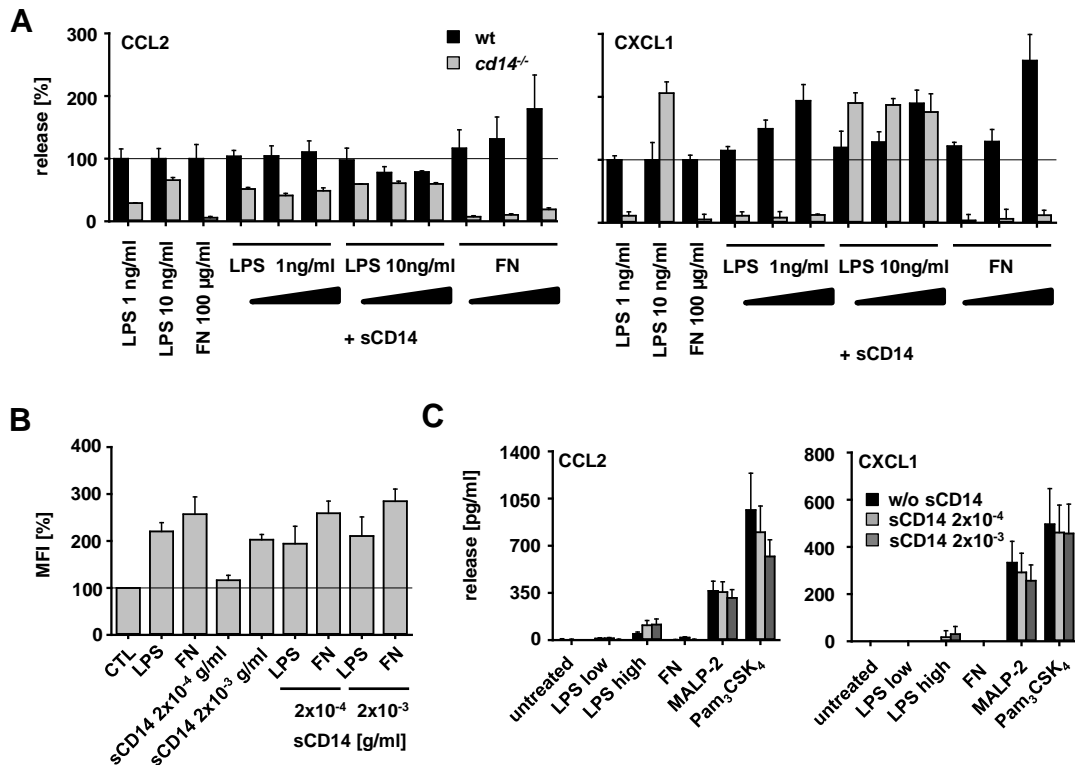
Figure 4.25: Soluble CD14 does not substitute for the membrane anchored CD14-mediated control of the TLR4-triggered responses by microglia and does not affect release by astrocytes.
(A) Microglia (from wt and *cd14*^{-/-} mice) were stimulated with Re-LPS (1 or 10 ng/ml) or with bovine pFN (100 µg/ml) in the absence or presence of recombinant sCD14 at different concentrations ($2x10^{-8}$, $2x10^{-7}$ or $2x10^{-6}$ g/ml) for 18 h. Chemokine release was determined in the supernatants by ELISA. Absolute values were expressed as a percentage of the release by cells stimulated with the respective agonist and concentration in the absence of sCD14. Data are mean ± SEM with n=12 from 2-3 experiments. **(B)** Microglia (wt) were stimulated with Re-LPS (10 ng/ml) or bovine pFN (100 µg/ml) in the absence or presence of sCD14 ($2x10^{-4}$ or $2x10^{-3}$ g/ml) for 18 h. Subsequently, they were FcγRII/III-blocked (with Ab against CD16/CD32) and stained with PE-anti-CD14 and Pacific Blue-anti-CD11b for acquisition by flow cytometry. Only CD11b^{+} events were included. MFI was normalized for unstimulated cells (CTL). Data are mean ± SEM with n=3 from 3 independent experiments. **(C)** Astrocytes (AC) from wt mice were stimulated and CCL2 and CXCL1 release was determined as described in (A). Bovine pFN, MALP-2 and Pam$_3$CSK$_4$ were used for stimulation at concentrations of 100 µg/ml, 10 ng/ml and 10 ng/ml, respectively. Data are mean ± SEM with n=12 from 3 independent experiments. (Experiments on release by AC were performed by Michelle Dworschak during her laboratory rotation period.)

Surface CD14 was not detected on astrocytes, and its expression was not induced upon stimulation with TLR agonists (Figs. 4.5 and 4.22). In our laboratory, we measured moderate levels of TLR4 mRNA. However, there was no induction triggered by TLR4 agonists, such as LPS and pFN (Master Thesis of Anna-Lisa Roser, 2012). On the other hand, astrocytes were shown to respond to challenges by the TLR1/2 and TLR6/2 agonists Pam$_3$CSK$_4$ and MALP-2, as to the production of selected cytokines and

chemokines—which is in agreement with the detected expression of these TLRs on astrocytes (Bowman et al., 2003; Carpentier et al., 2005; Esen et al., 2004). To test whether astrocytes could recruit sCD14 and use it for a response to TLR4 agonists, wt astrocytic cultures were stimulated with LPS or pFN in the presence and absence of sCD14. Furthermore, cells were also stimulated with MALP-2 and Pam_3CSK_4 to test whether a triggered production could be affected by sCD14, since mCD14 was demonstrated to interact also with these TLRs. No CXCL1 or CCL2 was measured in the supernatants of cells stimulated with TLR4 agonists, and this did not change upon addition of sCD14 (Fig. 4.25C). There was also no significant effect of sCD14 on the release as triggered by MALP-2 and Pam_3CSK_4. To summarize this part, sCD14 does not enable the response to TLR4 agonists and it also does not change the production profile of astrocytes treated with TLR1/2/6 agonists. (These experiments on astrocytes were performed by Michelle Dworschak during her laboratory rotation period.)

4.20 CD14 regulation of microglial responses to DAMPs and PAMPs needs different timing

The results thus far showed that responses to DAMPs and PAMPs are differentially dependent on CD14. While microglia can react to strong LPS challenge without a CD14 help, pFN, as a representative of the DAMPs, can trigger a response only in CD14 presence. These observations could suggest an employment of different signaling events and elements as linked to CD14 upon DAMP *versus* PAMP stimulations. As a first approach to dissect the distinct requirement of CD14, we considered the time period needed by CD14 to establish its influences. We therefore enabled a functional CD14 presence for limited time periods. Microglia were stimulated with LPS at high and low doses or treated with pFN. The situation of a globally impaired CD14 "signaling" was mimicked by using $cd14^{-/-}$ as well as by putting wt microglia under the condition of a constant CD14 block, performed by adding a neutralizing CD14 antibody for the entire stimulation period (48 h). Narrower time windows of CD14 functionality were then imposed by timed addition of the anti-CD14 antibody. Thus, the system was allowed to use CD14 only for the first 6 or 24 h, as the CD14-blocking antibody was given to the cells at these time points (counted from the beginning of the stimulation with the respective TLR4 agonist) and left in the culture medium till the end of the stimulation (Fig. 4.26A).
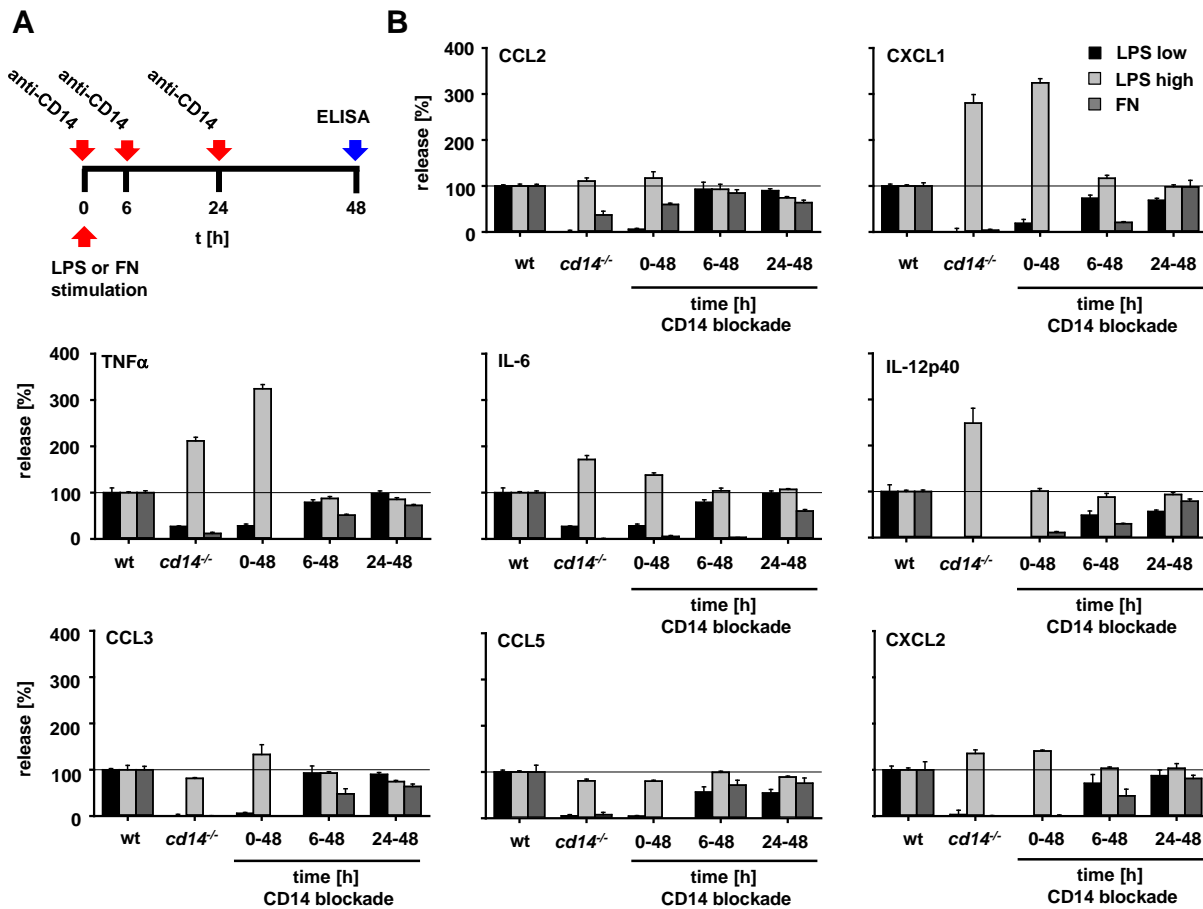
Figure 4.26: pFN-triggered responses need CD14 functional presence for longer time periods than those triggered by LPS.
(A) The scheme illustrates stimulation, incubation, time points of addition of anti-CD14 Ab and supernatant collection for ELISA analysis of cyto- and chemokines as quantified in (B). **(B)** Microglia (from wt and *cd14*$^{-/-}$ mice) were stimulated with Re-LPS (0.1 ng/ml as 'low', 10 ng/ml as 'high') or bovine pFN (100 µg/ml) for cyto- and chemokine induction. Wt microglia were stimulated in the absence or timed presence of anti-CD14 (10^{-5} g/ml) as indicated in (A). Absolute values were expressed as a percentage of the release by cells (wt) stimulated with the respective agonist and concentration in the absence of anti-CD14. Data are mean ± SEM with n=12 from 3 experiments.

Both the biological absence (*cd14*$^{-/-}$) as well as the physical blockade of CD14 over the entire time showed the previously described pattern of cyto- and chemokine production (Fig. 4.26B). The only exception regarded IL-12p40, which was over-produced by *cd14*$^{-/-}$ cells stimulated with high LPS concentrations, but not by wt cells in the presence of the CD14-blocking antibody. Interestingly, functional presence of CD14 for the first 6 h prevented the over-production of selected cyto- and chemokines (e.g. CXCL1, TNFα) in response to high LPS doses and restored the diminished production upon treatment with low LPS doses. This indicates that CD14 control over LPS-triggered reactions is

established within the first 6 h. In contrast, microglia needed CD14 assistance to react to pFN for a longer period. The anti-CD14 antibody led to decreased production of cyto- and chemokines when administered at 6 h of the ongoing stimulation. The release improved to nearly normal levels (obtained with unblocked cells over the total 48 h period), when CD14 function was allowed for 24 h.

One could speculate that the insufficient release upon stimulation with pFN was caused by a postponed reaction, in comparison to LPS. To see whether the production of cyto- and chemokines, as a response to DAMPs and PAMPs, has the same or a different time course *per se*, microglial cells were stimulated with pFN and LPS, respectively, for 1 to 48 h. Measurement of the produced factors in the culture supernatants showed, however, that the effective release was in general not slower upon pFN stimulation, as compared to LPS (Fig. 4.27). Furthermore, the onset of TNFα and CXCL1 production by cells treated with pFN was even earlier. Only CCL2 production was relatively faster by stimulation with LPS, in comparison to pFN. Thus, the decreased or diminished response to pFN by cells without a functional CD14 for the first 6 h cannot be due to a later induction of release, which would result in less cyto- and chemokines in the supernatant.
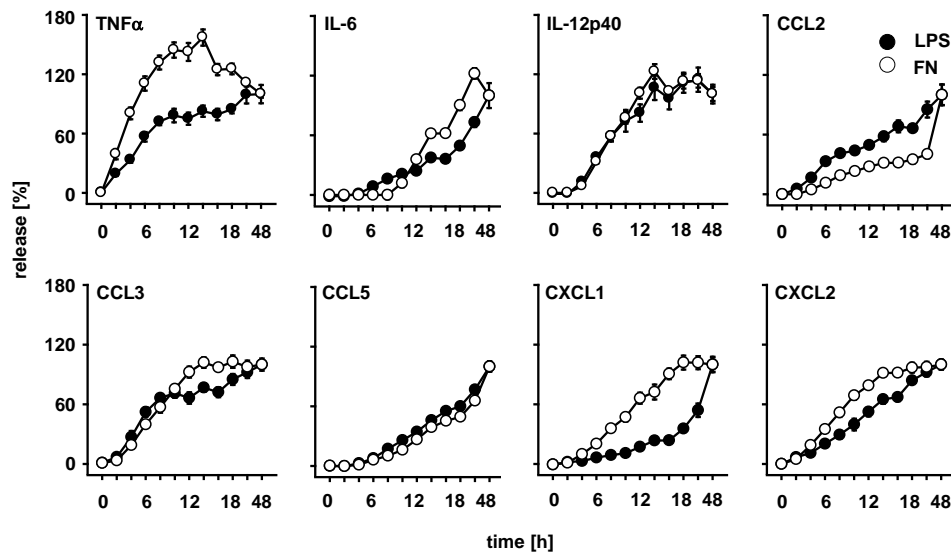
Figure 4.27: LPS and pFN stimulations reveal differences in the induction efficacy of individual factors.
Microglia were stimulated with Re-LPS (10 ng/ml) or bovine pFN (100 µg/ml) for the indicated time periods and cyto- and chemokine release was determined in the supernatants by ELISA. Absolute amounts were normalized to the release obtained with control cells stimulated for 72 h (endpoint set to 100 %). Data are mean ± SEM with n=8 from 2 independent experiments.

4.21 Inhibition of Syk, PLC or BTK cannot phenocopy the CD14 deficiency in microglia

CD14, as a GPI-anchored protein, was not considered to have links to any TLR4-independent signaling. However, recent studies by Zanoni and co-workers showed that CD14 has some unexpected roles in the signaling of DCs. Syk and PLC were characterized as the main candidates in this context (Zanoni et al., 2009, 2011). Thus it was essential to investigate whether CD14 control over microglial responses, as to the prevention of overshooting and support of insufficient release, is downstream regulated by Syk and PLC. Bruton's Tyrosine kinase (BTK) was chosen as another candidate, because of the demonstrated link to PLCγ signaling and associations with both the B cell receptor as well as TLRs (Brunner et al., 2005). Therefore, wt and $cd14^{-/-}$ microglia were stimulated with pFN and LPS in the presence or absence of PLC, Syk and BTK inhibitors. CXCL1 levels were measured as to obtain its excessive production upon LPS high treatment in the absence of CD14 and because it is predominantly induced via the adaptor protein MyD88 (Regen et al., 2011). Next to it, CCL5 levels were determined to describe effects on a release, which uses both MyD88- as well as TRIF-dependent signaling pathways. Figure 4.28A shows that the inhibition of neither of the chosen enzymes led to the same pattern of release as seen in the absence of CD14. None of the inhibitors caused an excessive release of CXCL1. Inhibition of Syk and BTK either slightly decreased the microglial CXCL1 and CCL5 production or had no effect at all. The PLC inhibitor, on the other hand, prevented the release upon low-dose application of LPS and for pFN treatment in general. However, it also completely abolished the induction of CCL5 as well as of CXCL1 in the cells stimulated with high doses of LPS. The induction of neither CCL5 nor CXCL1 strictly requires TRIF. However, CD14 was shown to be especially necessary for TLR4 endocytosis, which allows the TRIF-dependent signaling to be initiated, a pathway characteristically culminating in IFN type I production (Zanoni et al., 2011). Next to IFNα/β, induction of MHC class I molecule (MHC I) by TLR4 agonists in microglia was recently shown to be strictly dependent on the TRIF pathway (Regen et al., 2011). Furthermore, the induction of MHC I expression is also partially under control of CD14. For that reason, we compared the impact of Syk and PLC inhibition also on the induction of MHC I in wt and $cd14^{-/-}$ cells. As expected, MHC I surface levels on $cd14^{-/-}$ microglia stimulated with LPS or pFN reached only half or even less of the levels as measured for wt cells (Fig. 4.28B). Also in this case, the inhibition of Syk did not have a significant effect on the MHC I induction. PLC inhibition resulted in a complete abolishment of induction, which could imply that PLC was involved in signaling leading to MHC I induction. However, considering the total loss of responses measured by the chemokine release (Fig. 4.28A), this PLC inhibitor had rather a global inhibiting effect, which was not directly linked to CD14 signaling. In summary, Syk, PLC and BTK are not likely to contribute to the CD14 downstream effects that, at the same time, prevent

the over-production of factors, like CXCL1, under high LPS and as well provide higher sensitivity to pFN and low doses of LPS. In other words, these candidates of signaling elements could be ruled out to underlie the CD14-organized control mechanisms.
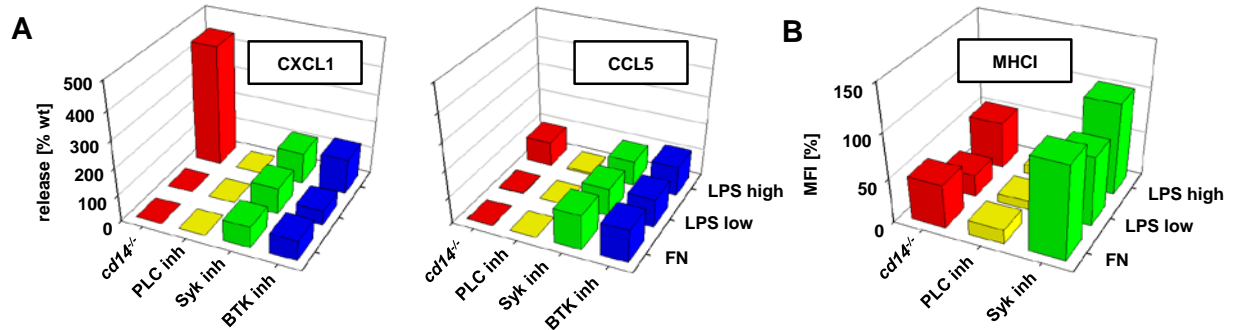
Figure 4.28: PLC, Syk or BTK have no contributions in CD14 control over TLR4-mediated MyD88- and/or TRIF-dependent responses.
(A) Microglia (from wt and *cd14*^{-/-} mice) were stimulated with Re-LPS (0.1 ng/ml as 'low' and 10 ng/ml as 'high') or with bovine pFN (100 µg/ml) in the absence or presence of U-73122 (10 µM), Bay61-3606 (75 nM) or terreic acid (10 µM) as inhibitors of PLC, Syk and BTK, respectively, for 18 h (with a pre-incubation of the cells with the inhibitors for 1 h). Amounts of CXCL1 as a MyD88-dependent and of CCL5 as a MyD88- as well as TRIF-dependent factor were determined in the supernatants and expressed as percentage of the release obtained with respective stimulations of wt cells in the absence of the inhibitor. Data are mean ± SEM of n=12 from 3 experiments. **(B)** Microglia were treated as in (A) and subsequently analyzed for the expression of MHC I as a solely TRIF-dependent response. To do so, cells were FcγRII/III-blocked, stained with Alexa Fluor 647-anti-MHC I and Pacific Blue-anti-CD11b for acquisition by flow cytometry. Only CD11b^{+} events were included. MFI was normalized to values obtained with stimulated cells in the absence of the inhibitors. Data are mean of n=3 from 3 experiments.

4.22 Only small amounts of CD14 are internalized by microglia during the TLR4-triggered response

CD14 was shown to be especially important for LPS-triggered responses that are dependent on TRIF. Here, CD14 regulates the internalization of the TLR4-LPS complex, thereby enabling for the second wave of signaling from endosomes. However, the CD14 internalization has been so far documented only in DCs and peripheral macrophages (Ling et al., 2014; Zanoni et al., 2011). It was thus interesting to investigate whether (i) the endocytosis of a TLR4-LPS complex could be shown also in microglia, (ii) whether it requires CD14 assistance and (iii) whether this happens to the same extent as in BMDM. Microglia, and as a control BMDM, were stimulated with S- as well as Re-LPS chemotypes. The rationale behind using both was that even though S-LPS was shown to have a direct link to TRIF-dependent signaling in peritoneal macrophages (Jiang et al., 2005) and thus its use would appear better for these studies, in microglia the situation differs. Microglia did not differentiate between S-LPS and Re-LPS for induced secretion of the respective cyto- and chemokines. Both used MyD88 and TRIF adaptor proteins, even in

nearly the same way (Regen et al., 2011). After 20 min of incubation with Re- and S-LPS at two different concentrations, surface CD14 was measured by flow cytometry in order to detect a loss due to the internalization of the complex with LPS-TLR4. Figure 4.29A shows that CD14 levels on the surface of microglia did not significantly change upon stimulation with either of the LPS chemotypes. Less CD14 was detected on BMDM as stimulated with higher concentrations of both LPS variants. However, the decrease was not as dramatic as described in previous reports. In order to rule out that a failure in detecting a CD14 loss was due to inappropriate timing, microglia were stimulated with LPS for 10, 30 and 90 min. As recapitulated by the histograms in Figure 4.29B, LPS did not lead to any changes in CD14 expression on microglia at any time point after stimulation.
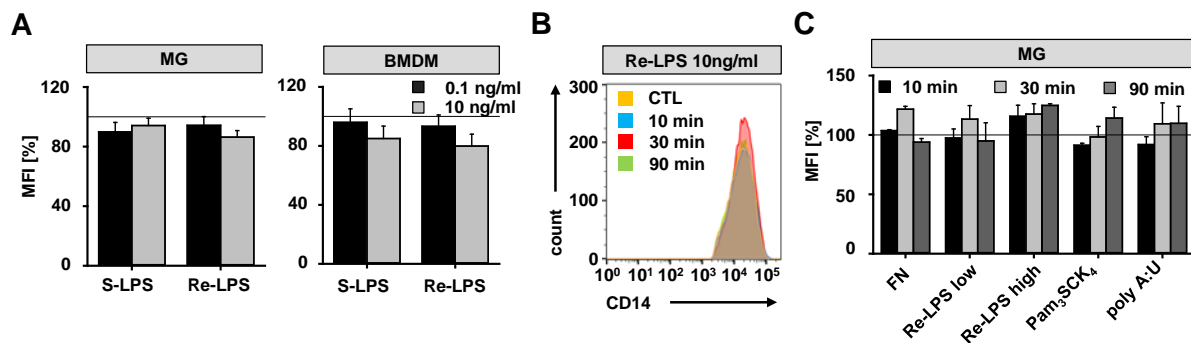
Figure 4.29: Flow cytometry analysis cannot show a significant loss of CD14 surface expression upon TLR stimulation.
(A) Microglia or BMDM were stimulated for 20 min with S-LPS or Re-LPS at the indicated concentrations. Subsequently, cells were FcγRII/III-blocked, stained with PE-anti-CD14 and Pacific Blue-anti-CD11b Abs for acquisition by flow cytometry. For data analysis, only CD11b$^+$ events were included. MFI was normalized to values obtained with unstimulated cells (set to 100%). Data are mean ± SEM with n=3-4. **(B)** Microglia were stimulated with Re-LPS (10 ng/ml) for the indicated time points. Loss of CD14 surface expression was assessed as in (A). **(C)** Cells were stimulated with Pam$_3$CSK$_4$, Re-LPS ('high') (both 10 ng/ml), Re-LPS ('low', 0.1 ng/ml), poly(A:U) (50 µg/ml) or bovine pFN (100 µg/ml)) for the indicated time points. Loss of CD14 surface expression was assessed as in (A). Data is mean ± SEM with n=2 from 2 experiments. (Flow cytometry analysis of surface CD14 on BMDM was performed by Anne-Sophie Ernst during her Master Thesis period.)

The previous results showed that the microglial TRIF-dependent production of CCL5 in the response to pFN but also to other TLR agonists was reduced in a CD14-dependent manner (Figs. 4.9B and 4.16B). To see, whether it is the CD14 assistance that is needed for the full response by these agonists and whether this could differ as compared to a LPS stimulation, microglia were stimulated with pFN, with Pam$_3$CSK$_4$ (as a TLR2/6 agonist) and poly(A:U) (as a TLR3 agonist). However, as seen upon stimulation with LPS, CD14 surface levels were not changed upon stimulation with any of the ligands, no matter how long the cells were incubated (Fig. 4.29C).

In a second approach, internalized CD14 was detected by confocal microscopy. For that, microglia were stimulated with LPS for 30 min or left untreated. After fixation, the cells were stained to detect intracellular CD14. Prior to stimulation, CD14 was located at a high density at the surface of microglia (white arrows) (Fig. 4.30A-D), but some pool of CD14 was also located inside the cells, i.e. in proximity to the nucleus (Fig. 4.30M). 30 minutes after LPS stimulation, the layer of membrane CD14 was rearranged (Fig. 4.30E-L, indicated by white star), and CD14 was found to be concentrated inside the cell (Fig. 4.30N). However, the amount of internalized CD14 was low and most of the CD14 remained at the cell surface. (A more detailed study involving confocal imaging is a part of the Master Thesis of Anne-Sophie Ernst, who performed all these evaluations.)

Due to the difficulty to track a loss of CD14 from the surface membrane by flow cytometry, it was not clear whether there were differences between microglia and BMDM and to which extent CD14 truly facilitated endocytosis. Apparently, microglia internalize only a small amount of the total surface-expressed CD14. This is probably sufficient to support a cellular incorporation of the LPS-TLR4-complex. Indeed, the amount of TLR4 could be relatively small (unpublished observations), and as a consequence, not much reduction of the surface CD14 can be noticed. Yet our functional data on TRIF-dependent inductions (e.g. MHC I) clearly indicated that TLR4 did have an intracellular action.
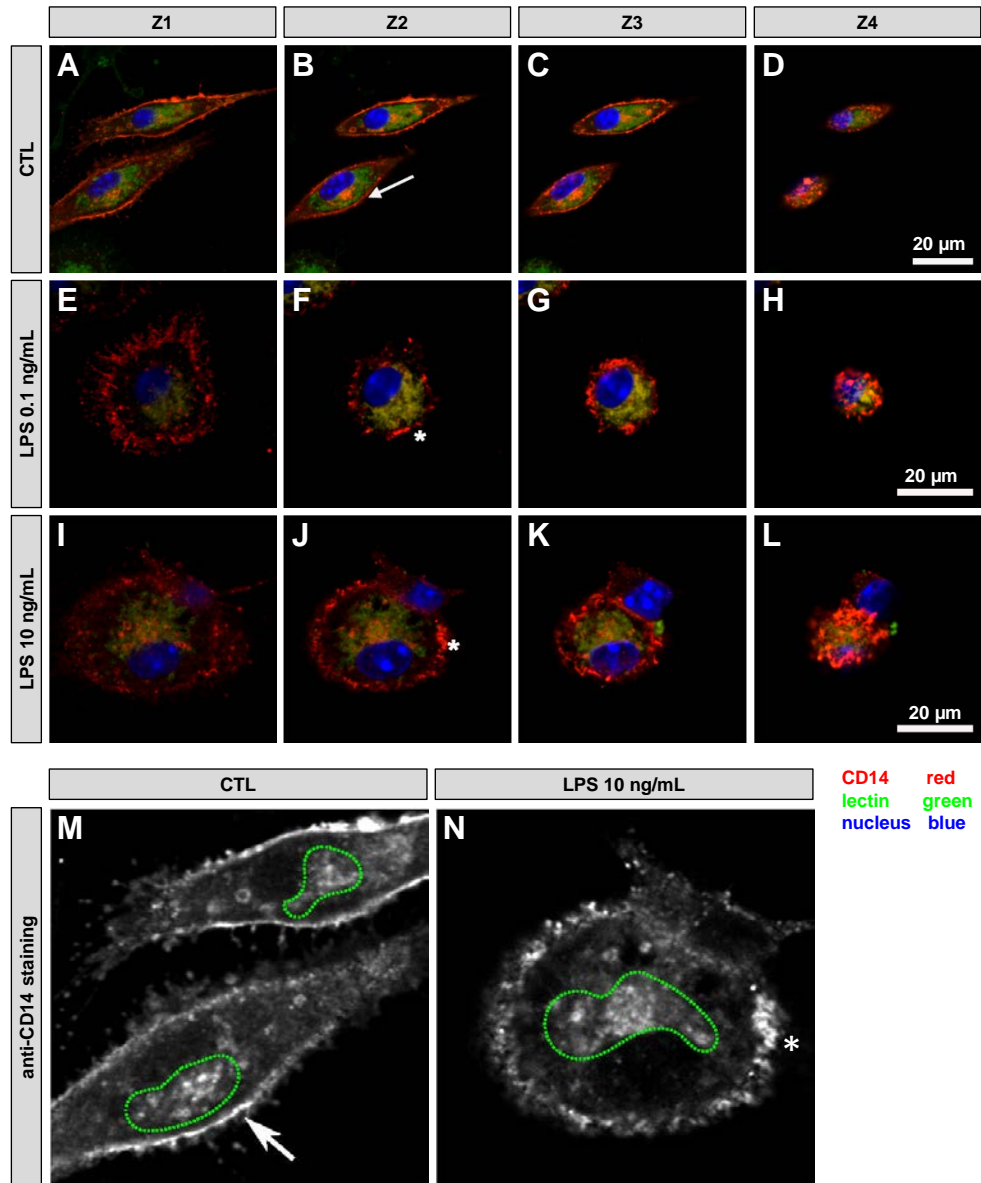
Figure 4.30: Microglia internalize only small amount of CD14 upon LPS stimulation.
(A) Microglia (wt) were stimulated for 30 min with S-LPS at indicated concentrations or left untreated. Subsequently, cells were stained with fluorescently labeled antibody against CD14 (red), lectin (green) and the nucleus (blue). Images were obtained by scanning confocal laser microscopy and collected at 1 μm intervals to create a stack in the z axis (Z). (A-L) Representative images show (A-D) unstimulated microglia, (E-H) microglia stimulated with LPS 0.1 ng/ml, (I-L) microglia stimulated with LPS 10 ng/ml. (M) Higher magnification of (B), red channel only. (N) Higher magnification of (J), red channel only. Dotted line indicates accumulation of CD14 close to the nucleus. Arrow heads indicate evenly distribution of CD14 on cell surface, stars indicate accumulation of CD14 on the surface. (Imaging was performed by Anne-Sophie Ernst during her Master Thesis period.)

4.23 CD14 presence allows for similar responses to DAMPs and PAMPs on the global level

The data obtained thus far in this work have been pointing to differences in the CD14-dependent control over microglial responses to DAMPs and PAMPs. Distinct reactions to LPS (as a PAMP and prototypical TLR4 agonist) and to pFN (as a TLR4-agonistic DAMP) were already studied in our group. Jörg Scheffel showed that the induction pattern of wt microglia stimulated with pFN varies from that with LPS and that microglia respond to LPS or pFN with individual gene expression patterns (Doctoral Thesis, Jörg Scheffel). However, these studies addressed microglial reactions to only one LPS concentration in a comparison to bovine pFN (instead of the mouse protein) in the presence of CD14. To see the microglial reactions to infectious *versus* damage scenarios at a more global scale and to determine the role of CD14 therein, a more complex approach was needed. Deep sequencing analysis served thus as a method to pinpoint and quantify differences in mRNA expression as a function of stimulation with LPS (at different concentrations) and pFN in association with CD14 deficiency. For that, microglia from either wt or *cd14$^{-/-}$* mice were left only in medium or were treated for 3 h with mouse pFN, LPS at a high concentration (LPS 'high') and LPS at a low concentration (LPS 'low'), followed by an analysis of the whole genome as performed in collaboration with Dr. Gabriela Salinas-Riester (Transcriptome Analysis Laboratory, TAL, University Göttingen) using an Illumina approach.

For the first bioinformatic analysis of a total up- or down-regulation in the gene expression by different comparisons between genotypes and treatments, a cut-off for candidate genes was set to a log$_2$FC (relating to a 4-fold change) and FDR corrected *p* value < 0.01. The results are summarized in Table 4.2 showing that at the steady state, when the cells were not stimulated, wt and *cd14$^{-/-}$* microglia varied only in the expression of CD14 (one gene 'down-regulated' in *cd14$^{-/-}$* cells) (Table 4.2 I). While this difference was expected and had to be found in the data, the fact that no further distinctions could be made indicated an otherwise comparable situation in the two genotypes. Treatment of wt microglia with LPS 'high' or pFN led to the same number of up-regulated (around 900) as well as down-regulated (about 600) genes (Table 4.2 IIa). The LPS 'low' stimulation was less efficient in activating wt cells and up-regulated three times fewer genes, when compared to the other treatments. Furthermore, only a very small amount of genes was down-regulated (30 genes) upon LPS 'low', indicating that pFN and LPS 'high' may have even more negative regulations. The comparison of the treatments with pFN and LPS 'high' did not reveal candidate genes that would be significantly different (FDR<0.01) at the log$_2$FC scale (Table 4.2 IIb).

Table 4.2: CD14 deficiency affects up- and downregulation of genes upon stimulation.
Microglia p0 cultures from $cd14^{-/-}$ and wt mice were stimulated with LPS 'high' (10 ng/ml), LPS 'low' (0.1 ng/ml), mouse pFN (100 µg/ml) or were left untreated (CTL) for 3 h. Cells were subsequently washed and lysed with Triazol. The cDNA libraries prepared from mRNA were amplified and sequenced by cBot and HiSeq2000 from Illumina. Differential gene expression analysis was done with R-package Edge-R upon library preparation by Illumina sequencing. Candidate genes were filtered to a minimum of a 4-fold change and a FDR-corrected p value < 0.01. Table shows the total numbers of genes that were up- or downregulated upon stimulation in wt and $cd14^{-/-}$ microglia.

Comparison	Genes up-regulated	Genes down-regulated
I. Effect of genotype without stimulation		
Wt CTL *vs.* $cd14^{-/-}$ CTL	0	1
II. Effect of stimulation on gene expression in wt cells		
a. Unstimulated vs. stimulated		
CTL *vs.* LPS 'low'	364	30
CTL *vs.* LPS 'high'	905	633
CTL *vs.* FN	911	641
b. Comparison of different stimulations		
LPS 'high' *vs.* FN	0	0
III. Effect of CD14 deficiency on gene expression of stimulated cells		
LPS 'low' wt *vs.* $cd14^{-/-}$	6	235
LPS 'high' wt *vs.* $cd14^{-/-}$	19	109
FN wt *vs.* $cd14^{-/-}$	173	575

The situation changed once CD14 was not present (Table 4.2 III). The CD14 deficiency affected gene expression as triggered by each treatment. However, the effect intensity varied in dependence on the stimulation. The expression of genes in the cells stimulated with pFN was affected by CD14 absence the most, as seen by the biggest difference in numbers of up- or down-regulated genes. In contrary, the gene expression upon stimulation by LPS 'high' showed to be the least affected. In other words, CD14 absence affected dramatically the stimulation consequences of a LPS challenge at low concentration as well as the DAMP-driven reaction.
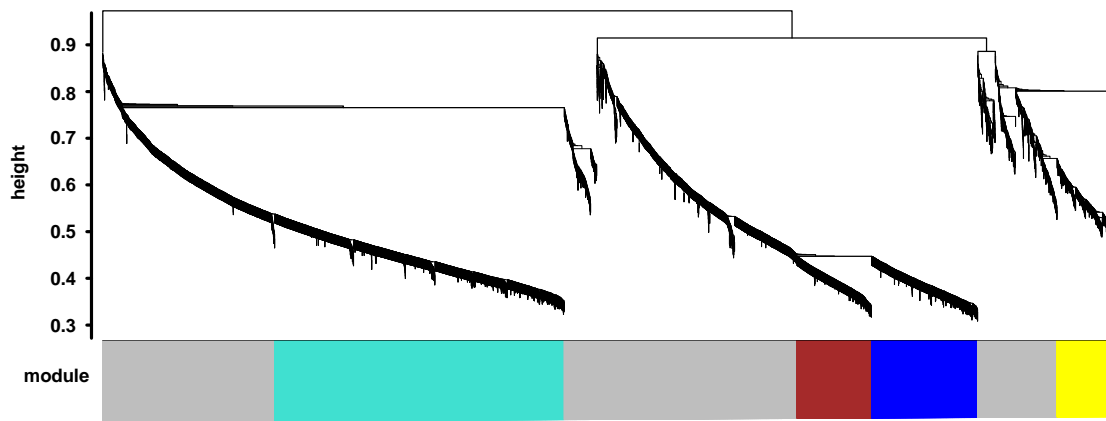
Figure 4.31: Network analysis of gene expression upon stimulation with pFN and LPS reveals several gene co-expression modules.
Wt or *cd14*^{-/-} microglia were stimulated with Re-LPS (0.1 ng/ml as 'low', 10 ng/ml as 'high'), mouse pFN (100 µg/ml) or left untreated for 3 h. The cells were processed and the analysis was further performed as described in Table 4.2. Average linkage hierarchical clustering with the topological overlap dissimilarity measure was used to identify gene co-expression modules, each of which was assigned a unique color. For further analysis, modules were cut at a height of 0.8 with a minimal size of 200 genes.

In order to obtain more information in terms of biological relevance and affected functional domains, a Weighted Gene Co-expression Network Analysis (WGCNA) was performed in co-operation with Inge R. Holtman (Laboratory of Dr. Bart J. L. Eggen and Prof. Hendrikus Boddeke, University of Groningen). The WGCNA analysis is used to generate gene networks based on co-expression, noting that genes that share biological functions are often co-regulated and hence co-expressed. For all genes in the network, pair-wise correlations were calculated and transformed into a topological overlap matrix by raising the correlations to a soft-power value. This is determined by the scale free criteria and by taking the strenght of the relationship of each other neighbor into account (Langfelder and Horvath, 2008). Next, by using average linkage hierarchical clustering, branches of genes that highly co-express were formed, and a dynamic but arbitrary tree cut algorithm was applied to form the modules. Modules were randomly assigned unique colors. The remaining lowly connected genes were assigned a gray color (Fig. 4.31). To study the expression pattern of each module, the Module EigenGene (ME) of each module was calculated, which is the first principal component and the main representative of the gene expression profile. To test whether the expression patterns of the modules were significantly affected between conditions, a multivariate general linear model was applied to the ME values. The turquoise, brown and blue modules were identified as being significantly affected ($p<0.005$) by the main effects of the genotype (G), the stimulation (S) and by the interaction effect (G*S). Moreover, a yellow module was

found, that was not significantly related to any variable. It was therefore left out from the subsequent analyses.

Table 4.3: Ingenuity pathway analysis (IPA) identified canonical pathways and biological functions in the modules of highly correlated genes.
Table summarizes the examples of relevant pathways or functions within the modules. Size=number of genes per module.

Module	Size	Annotation category or pathway	Ingenuity Class	*p* value
Blue	1008	TNFR2 signaling	Pathway	3.98E-16
		TNFR1 signaling	Pathway	2.40E-10
		iNOS signaling	Pathway	7.94E-11
		NF-κB signaling	Pathway	3.24E-09
Brown	708	interferon signaling	Pathway	1.58E-11
		antigen presentation pathway	Pathway	1.66E-07
Turquoise	2748	replication and repair of DNA	Function	4.33E-12

Turquoise, brown and blue modules were functionally annotated in the Ingenuity pathway analysis (IPA) to thereby determine whether they are enriched for particular canonical pathways, networks or biological functions. Importantly, use of IPA allowed us to identify significant changes in canonical or biological pathways associated with differentially expressed genes within a group. The analysis showed that the blue module was enriched for several pro-inflammatory signaling/canonical pathways, including TNF-related pathways such as TNF-R1/2, iNOS signaling and NF-κB signaling (Table 4.3). Pathways for interferon signaling and antigen presentation were significantly enriched in the brown module. The turquoise module, as the largest module, was significantly enriched for regulation of transcription, repair of DNA as well as DNA and RNA metabolic processes, thus also relating to proliferation.

Figure 4.32 depicts the average expression profile (ME) across conditions. In the brown, blue and turquoise modules, we did not observe any differences in the expression profiles between unstimulated wt and *cd14*$^{-/-}$ cells. In the presence of CD14, LPS 'high' and pFN stimulation led to up-regulation in the blue and brown modules and down-regulation of the turquoise module. LPS 'low' also triggered up-regulation in the blue and brown module and down-regulation in the turquoise, but to a lesser extent. The meaning of this inversion (down-regulation in turquoise module compared to up-regulation in the blue and brown module) and the respective support by experimental data of our group will be discussed later. To give a first perspective, the module reflects also proliferative activity, including DNA synthesis. According to the transcriptome data, TLR4 stimulation would suppress these functions—which is actually the case, when measuring cell division and DNA content directly (Gertig et al. unpublished).
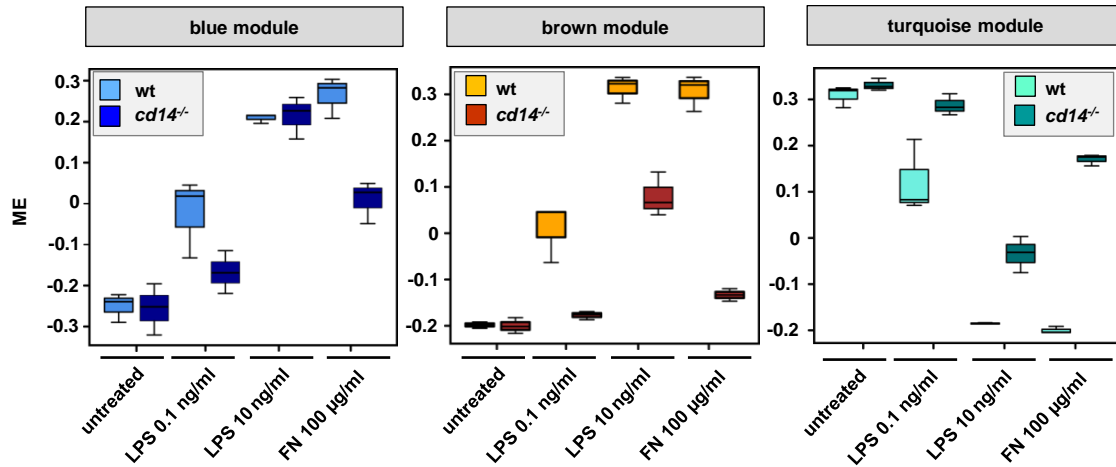
Figure 4.32: Microglia respond similarly to high amounts of LPS and FN only in the functional presence of CD14.
Wt or *cd14*^{-/-} microglia were stimulated with Re-LPS (0.1 ng/ml as 'low', 10 ng/ml as 'high'), mouse pFN (100 µg/ml) or left untreated for 3 h. The cells were processed and the analysis was further performed as described in Table 2. Figure shows expression of Module EigenGene (ME), as the first principal component, across different conditions.

Clearly different outcomes of LPS 'high' and pFN treatment were observed in the absence of CD14. In the blue module, which was significantly enriched in genes relating to NF-κB and TNF signaling and thus to the MyD88-dependent pathway of TLR signaling, LPS 'high' responses were the same in wt as well as in *cd14*^{-/-} cells. On the contrary, a pFN-triggered activation was clearly impaired in *cd14*^{-/-} microglia, agreeing with all our related experiments. Similarly, the activation by pFN turned out to be far more dependent on CD14 in the brown module. This module was found to be enriched in the genes relating to IFNβ signaling and antigen presentation, which both depend on the TRIF pathway. We had previously published that the MHC I induction via TLR4 requires TRIF (Regen et al., 2011). While a response to LPS 'high' was decreased in *cd14*^{-/-} by half, as compared to the wt situation, CD14 absence led to a complete ablation of responses to pFN. In the turquoise module, with a main annotation to DNA repair, some lack of down-regulation occurred in the absence of functional CD14. Here, a pFN-driven response was also tightly linked to CD14. The LPS 'low' stimulation of wt microglia had always half of the efficacy of that seen with LPS 'high' and pFN, and it was completely dependent on CD14.

The similarity of LPS 'high' and pFN effects on driving the activation profiles in wt cells was further confirmed by differential gene expression analysis. No genes were found to be differentially expressed in the cells treated with LPS 'high' or pFN at the FDR < 0.01 cut off. However, 1275 genes

(below FDR p<0.01) were found to be differentially expressed in *cd14*^{-/-} microglia as stimulated with LPS 'high' and pFN.

The results of the WGCNA imply that the response to damage, in this case represented by pFN, triggers the same activation profile as organized by a high concentration of LPS, affecting especially the TRIF- and MyD88-dependent pathways in TLR4 signaling. A CD14 knockout resulted in still intact responses within the blue module, containing TLR:NF-κB signaling, for the MyD88-dependent pathway, and especially for high concentrations of LPS. However, while pFN activation via the TRIF pathway—culminating in IFNβ signaling—was highly dependent on CD14 presence, activation upon LPS "high" treatment was not affected. This further suggests that CD14 is more important for IFNβ signaling than for the NF-κB (and MyD88) part of TLR signaling, confirming previous reports (Zanoni et al., 2011).

4.24 CD14 contains CXCL1 production via a TRIF-dependent mechanism

The observation that CD14 is important for especially TRIF-mediated signaling, which is happening from the intracellular endosomes, was thus strongly corroborated by the analysis of deep sequencing data. While the MyD88-dependent pathway (blue module) activated upon LPS (high) stimulation stayed largely intact in the absence of CD14, the response leading through the TRIF-dependent pathway (reflected by the brown module) was substantially reduced (Fig. 4.32). These observations also fueled a concept of the mechanism underlying the sophisticated control of pro-inflammatory gene inductions by CD14. While the TLR4-driven CXCL1 synthesis was kept in a moderate range in wt microglia, deficiency in CD14 expression or function would unleash a massive over-production, mirrored by the excessive neutrophil influx to the CNS upon LPS delivery. Yet the mechanistic link between CD14 and such a negative control remained obscure. We first developed a model in which exaggerated MyD88 signaling was in the focus.

Combining the various facts from our previous experiments and taking also the bioinformatic approach into consideration, CD14 assistance could prevent an otherwise overshooting reaction by enabling for the efficient internalization of the TLR4/LPS complex and for a concomitant termination (interruption) of the transmembrane signaling to MyD88, which is the essential pathway for CXCL1. Upon a loss of CD14 function, high levels of LPS would continue with MyD88 signaling, due to a failure in the TLR4 endocytosis and thus resulting in an exaggerated CXCL1 induction. This would not only lead to an excessive production of CXCL1, but also affect other strictly MyD88-dependent factors, such as TNFα, IL-6 or IL-12. In contrast, cytokines and chemokines which would not exclusively rely on MyD88 but more on a mixed involvement of MyD88 and TRIF, like CCL2, CCL3, CCL5 or CXCL2, would probably stay largely unaffected. Indeed, the strict *versus* a more balanced MyD88 dependence matched the actual release

behavior upon CD14 deficiency. All the eight genes did fit to such as sorting. We postulated that simple interruption of endocytosis should then mimic the CD14 absence.
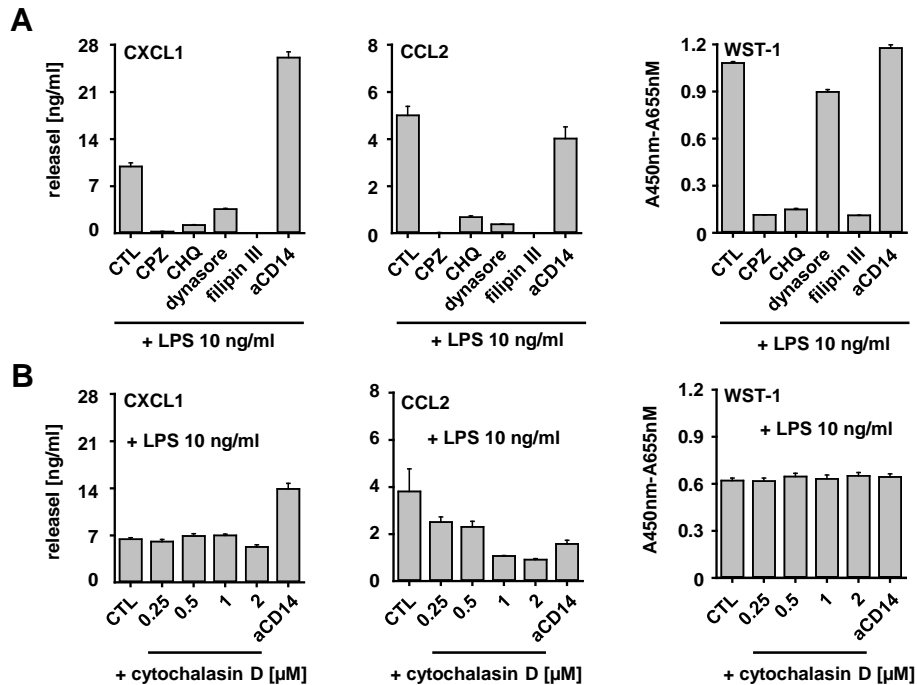
Figure 4.33: Selected inhibitors of internalization do not phenocopy the release pattern induced by CD14 blocking antibody.
Microglia (wt) were stimulated with Re-LPS (10 ng/ml) in the absence or presence of chlorpromazine (CPZ) (10 μg/ml), chloroquine (CHQ) (20 μg/ml), dynasore (80 μM) or filipin III (5 μg/ml) as inhibitors of clathrin dependent endocytosis, endosomal maturation, dynamin, and raft/caveloar endocytosis, respectively, for 18 h (with a pre-incubation of the cells with the inhibitors for 1 h). As a control was used CD14 blocking antibody (4C1, 10 μg/ml). Chemokine levels were determined in the supernatants by ELISA. Vitality/metabolic activity of the cells was determined by WST-1 test. Data are mean ± SEM of n=6 from 1 experiment. **(B)** Microglia were stimulated with Re-LPS (10 ng/ml) in the absence or presence of increasing dose of cytochalasin D as an inhibitor of actin polymerization or CD14 blocking antibody (4C1, 10 μg/ml) for 18 h (with a pre-incubation of the cells with the inhibitor/antibody for 30 min). Chemokine levels were determined in the supernatants by ELISA. Vitality/metabolic activity of the cells was determined by WST-1 test. Data are mean ± SEM of n=8 from 1 experiment.

In order to test this hypothesis, microglia were stimulated with high concentration of LPS (10 ng/ml) in the presence or absence of various inhibitors of internalization or CD14-blocking antibody as the control. After 18 h, levels of CXCL1 and CCL2 were measured in the culture supernatants, as representatives for the two groups of distinctly regulated factors. Chlorpromazine was used as an inhibitor of clathrin-dependent endocytosis, chloroquine as an inhibitor of endosomal maturation, dynasore as an inhibitor of dynamin, filipin III as an inhibitor of raft/caveolar endocytosis and cytochalasin D as an inhibitor of actin polymerization. Figures 4.33A and B show that none of these inhibitors of internalization was able

to phenocopy the release pattern caused by deficiency of CD14. While CXCL1 production triggered by LPS simulation was more than doubled by CD14 block, all the inhibitors, with the only exception of cytochalasin D, led to an ablation of the response. Similarly, no detectable or only reduced levels of CCL2 were found to be produced upon inhibition of internalization. To some extent, use of these compounds in the present work had certain limitations. The complete shut-down of chemokine production could be explained by impaired viability or affected metabolic activity of the treated cells. Data from WST-1 assays clearly indicated such a non-specific effect. Moreover, microglia treated with LPS under chlorpromazine, chloroquine or filipin III revealed a dramatically reduced ability to cleave the tetrazolium salt to its formazan product. On the other hand, neither cytochalasin D nor dynasore did reduce the viability or metabolic activity of the cells. Yet they also did not reproduce the effect as caused by the CD14-blocking antibody.

Taken together, this set of experiments could not prove our mechanistic model in which lack of TLR4 endocytosis would ultimately cause prolonged MyD88 signaling and thus enhanced production of CXCL1 (and other 'overshooting' factors). This failure could have had technical reasons—or simply indicate that the model was not appropriate. This model had focused on MyD88 signaling, taking lack of TRIF signaling simply as a side effect of non-functional endocytosis and ignoring any other contribution from this route. In an advanced concept, we still kept the idea that the regulatory influence of CD14 would target at MyD88, but we included some active component from the TRIF pathway. In other words, TRIF-derived factors could exert a negative control on the MyD88 signaling flow. Disruption of a CD14-TRIF link would deprive the system of these feedbacks.

4.25 IFNβ signaling reveals as the essential downstream element in the CD14-dependent regulation of CXCL1 production

Due to the technical issues, it was not possible to prove that the excessive release of MyD88-dependent CXCL1 in the absence of CD14 is mainly because of the disrupted CD14-dependent endocytosis, leading usually to a discontinuous MyD88 signaling. However, this view ignored the accompanying lack of TRIF signaling and thereby induced factors.

IFNβ is the best known factor induced via the TRIF-dependent pathway. Released IFNβ binds to the type I IFN receptor, which is composed of two distinct subunits, i.e. IFNAR1 and IFNAR2. IFNAR1 is associated with tyrosin kinase 2 (Tyk2), whereas IFNAR2 is associated with Janus activated kinase 1 (Jak1). Upon IFNβ binding, the receptor subunits re-arrange and dimerize, leading to autophosporylation and activation of the associated Jaks, Jak1 and Tyk2, which, in turn, regulate the phosphorylation and

activation of the signal transducer and activator of transcription (STAT) signaling pathway. Activated

STAT proteins form heterodimers (in this case STAT1/STAT2) and bind to IFN-regulatory factor 9 (IRF-9),

creating thus IFN-stimulated gene (ISG) factor 3 (ISGF3) complexes. These complexes translocate to the

nucleus and bind IFN-stimulated response elements (ISREs) in the DNA to initiate gene transcription

(Platanias, 2005).
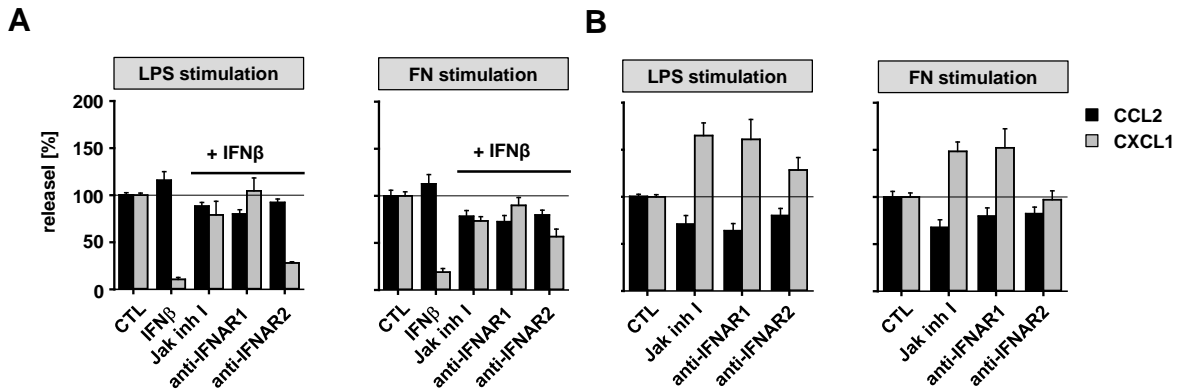
Figure 4.34: Blockade of IFNβ signaling leads to overproduction of CXCL1 by microglia stimulated with LPS or pFN.
(A) Microglia were stimulated with TLR4 agonists Re-LPS (10 ng/ml) or mouse pFN (100 µg/ml) alone (CTL) or in combinations with IFNβ (10 ng/ml) in the presence or absence of Jak inhibitor I (100 nM), anti-IFNAR1 and anti-IFNAR2 (both 10^{-5} g/ml) for 18 h (with a pre-incubation of the cells with the inhibitor and blocking Abs for 30 min). Amounts of CXCL1 and CCL2 were determined in the supernatants and expressed as a percentage of the release obtained with respective stimulations of wt cells in the absence of the inhibitor or blocking Abs. Data are mean ± SEM of n=12 from 3 experiments. **(B)** Microglia were stimulated and the release was assessed as in (A), but in the absence of IFNβ. Data are mean ± SEM of n=12 from 3 experiments.

Previous studies in microglia already showed an effect of IFNβ on the LPS-triggered production of other

cytokines and chemokines (Regen et al., 2011). It was specifically the secretion of the neutrophil

chemoattractant CXCL1 which was decreased by half, once IFNβ was added to LPS-stimulated microglia.

On the other hand, we had further observed that the pFN-triggered release of CCL2 as a monocyte

chemoattractant increased under IFNβ. To find out whether the reduction of CXCL1 levels and the

increase in CCL2 levels were due to IFNβ signaling, microglia were stimulated with LPS or pFN in the

presence of IFNβ, Jak inhibitor I or blocking antibodies against IFNAR1 or IFNAR2, or in their respective

combinations. As shown in Figure 4.34A, IFNβ dramatically decreased the LPS- and FN-triggered

production of CXCL1. The addition of Jak inhibitor I and the IFNAR1 blocking antibody was in both cases

able to restore the CXCL1 levels back to control. The blockade of IFNAR2, however, was less effective. In

comparison to CXCL1, production of CCL2 as triggered by both LPS as well as pFN was not reduced by

IFNβ (but even slightly increased). Jak inhibitor I and blocking antibodies then decreased mildly CCL2

secretion, especially in the case of a pFN stimulation. These results showed that IFNβ affects the release of CCL2 and CXCL1 by binding to its receptor IFNAR1/2 and with a subsequent use of the Jak signaling pathway.

A surprising effect was observed once the Jak inhibitor I or IFNAR1 and 2 blocking antibodies were used in the absence of additional IFNβ (Fig. 4.34B). Here, we noticed excessive production of CXCL1, especially by microglia treated with LPS. On the other hand, CCL2 levels were—by the same treatment—slightly reduced, as compared to the controls treated with TLR4 agonists alone.

This phenomenon strikingly reminded of the situation when CD14 in microglia was functionally blocked or knocked out and when cells were stimulated with high doses of LPS. To further investigate whether interference with IFNβ-triggered signaling could phenocopy the lack of CD14 and thus lead to excessive production of CXCL1, wt and $cd14^{-/-}$ microglia were stimulated with LPS in the presence of Jak inhibitor I. To find out further whether IFNβ would prevent the overshooting production of CXCL1 by $cd14^{-/-}$ cells, these microglia were stimulated with a combination of LPS and IFNβ. Figure 4.35A shows a matching pattern of CXCL1 released over a time by $cd14^{-/-}$ and wt microglia treated with Jak inhibitor I. Furthermore, the addition of IFNβ to $cd14^{-/-}$ microglia not only brought the excessive CXCL1 production down to the level of wt cells, but almost abolished it. The CCL2 release was decreased in the absence of CD14, which was rescued by addition of IFNβ. The inhibition of Jak signaling in the wt cells treated with LPS did not alter the CCL2 release.
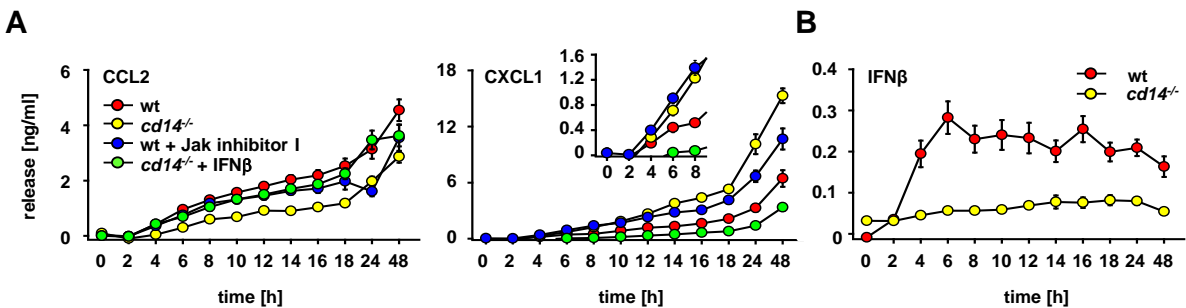
Figure 4.35: IFNβ restores the CD14 control over production of CXCL1 and CCL2 in $cd14^{-/-}$ microglia. Microglia from wt and $cd14^{-/-}$ mice were stimulated with Re-LPS (10 ng/ml) in the absence or presence of Jak inhibitor I (100 nM) or IFNβ (10 ng/ml), respectively, for the indicated time. **(A)** CXCL1 and CCL2 levels and **(B)** IFNβ levels were determined in the supernatants by ELISA. Data are mean ± SEM of n=12 from 3 experiment.

Taking these findings together, wt microglia—although expressing CD14—would reveal the overshoot phenomenon of $cd14^{-/-}$ cells once we impede IFNβ signaling, either at the receptor or the Jak level. On

the other hand, and complementing the effect, IFNβ addition to *cd14*$^{-/-}$ cells can restore a proper release control as it is functional in wt microglia. In other words, manipulating the IFNβ signaling can shift a wt situation to that of a CD14 knockout and *vice versa*. As a conclusion, the lack of CD14 will come with a lack of IFNβ production which, in turn, exerts a control over the MyD88-driven production of CXCL1.

We finally tested whether IFNβ production was actually impaired in a *cd14*$^{-/-}$ condition. Figure 4.35B shows the respective results. The dramatic drop in IFNβ release in the knockout condition nicely agreed with the former findings to suggest a CD14→TRIF→ IFNβ →IFNAR→Jak chain of command in the release regulation of CXCL1. Interestingly, the time period in which normal (wt) cells would establish IFNβ release, namely the first 6 h, matched our studies on the time dependence for establishing control of the LPS-triggered CXCL1 production, i.e. the prevention of an overshoot upon high LPS challenges. In *cd14*$^{-/-}$ microglia, this critical regulator would be absent. Of course, and as outlined in the discussion, there are more signaling elements which can impose negative control during TLR (4) signaling events. Yet as to the CXCL1 and CCL2 regulation, IFNβ could account for the essential effects by the direction of control (i.e. up- *versus* down-regulation) as well as by the magnitude of the impact. IFNβ could, indeed, serve a mechanistic explanation. It thus represented the 'missing link' in our model.

5. Discussion

Every year, hundreds thousands of people die of infectious diseases of the CNS, such as meningitis. This number is, however, surpassed by the amount of people that suffer or die due to other CNS diseases, including stroke, trauma, autoimmune and neurodegenerative diseases, such as MS, AD or PD. Indeed, non-communicable chronic diseases with components of sterile inflammation are a rising major thread to health (Lukens et al., 2012). Considering the dual role of TLR4 in sensing both gram-negative bacteria as well as a plethora of self-derived factors, cases in which the receptor only serves in anti-infectious measures could be outnumbered by those which rather develop from cell and tissue impairments of diverse etiology in the absence of an obvious microbial involvement. In all these cases, a TLR4-mediated immune response may play an important role, and in some of them it has been already strongly indicated by experimental findings.

The major reason for assuming such a critical involvement is that TLR4 has proven more than a receptor for bacterial LPS. Its ability to recognize a range of disparate endogenous molecules, which gain the meaning of a DAMP upon their translocation from physiological to abnormal compartments or by structural modification, can initiate signaling in tissue-resident and infiltrating immune cells. These cells either participate in anti-microbial responses, wound healing and tissue repair or—unfortunately—in a further aggravation of destructive cascades. Considering such a role in recognition of and responses to tissue damage and cell impairment, TLR4 could turn out to be one of the central sensors and effectors of any neuropathological event—directly upon gram-negative infection and indirectly by being recruited through DAMPs. Yet it is still enigmatic how a single receptor could manage interaction with so many different agonists. A clue to the understanding derives from the interaction of TLR4 with numerous other TLR and non-TLR molecules and the versatile options created by such complexes to bind and signal in a highly variable fashion.

This work focused on CD14 as the prototypical TLR4 co-receptor, especially in microglia as the principal innate immune cells of the CNS, and on its surprisingly sophisticated control of TLR4 responses to bacterial LPS as the established PAMP and to FN as a representative of DAMPs. The data obtained in this work describe crucial regulatory actions of CD14 at a molecular and cellular level as well as their consequences in animal models of CNS infection, mechanical injury and ischemic stroke. They also led to a mechanistic model in which CD14 organizes a control of microglial responses through a TRIF-IFNβ link.

Essentially, CD14 is shown here to organize for an increased sensitivity of microglia to PAMPs of the LPS type, a function it also exerts in other macrophage populations, but to a far lesser degree. The

gain in sensing low amounts of LPS is orders of magnitude larger compared to extraneural macrophages. On the other hand, CD14 is shown to prevent excessive responses upon massive PAMP challenges, a feature that is not shared by all cells. As a function of the PAMP agonist concentration, CD14 can thus promote as well as contain microglial reactions to an infectious confrontation, thereby organizing for responses which stay within a suitable and tolerable window. This would render microglia cells more alerted to a still barely recognizable assault while avoiding the potentially devastating consequences of an unbridled defense action. Finally, as a third and probably the most intriguing function identified in this work, CD14 functions as a gate keeper for TLR4-activating DAMPs. Demonstrated for FN as a feasible representative, but even more impressively documented in models of mechanical trauma and ischemic stroke, CD14 gives way to a microglial recruitment and functional involvement by damage-associated endogenous factors. After all, this role may determine the access to microglial engagements in a vast variety of CNS complications, exceeding by frequency the number of cases with a typical, i.e. infectious implication of TLR4. CD14 thus proves to be an *éminence grise* dictating the actions of TLR4 as a versatile sensor of infectious and non-infectious threats.

5.1   CD14 protects against hyperinflammation upon CNS infection with *E.coli*

TLR4, together with LBP and the co-receptor CD14, recognize LPS as a key component that discloses the presence of Gram-negative infection (Kawai and Akira, 2010; Wright et al., 1990). Binding of LPS to TLR4 triggers a cascade of events, which culminate in immune responses, such as production of pro-inflammatory cyto- and chemokines recruiting immune cells to the site of infection. In bacterial infections of the CNS, the infiltrating peripheral immune cells and local CNS cells are necessary for a successful eradication of the invading pathogens. However, an excessive inflammation may lead to tissue impairment. Consequently, it must be kept under a tight control.

The role of the TLR4 co-receptor CD14 during Gram-negative infections has been so far described almost exclusively in the periphery (Ebong et al., 2001; Haziot et al., 1996, 2001; Wiersinga et al., 2008). In our experiments, wt and *cd14*^{-/-} mice were inoculated with *E.coli* K1 into the right frontal neocortex. Thus, *E.coli* could directly reach the brain parenchyma. Compared to the wt situation, significantly more neutrophils were recruited into the brains of mice lacking CD14. This was in agreement with a study showing higher counts of neutrophils in the CSF of *cd14*^{-/-} mice infected by *S. pneumonia,* Gram-positive bacteria that are mainly recognized by TLR2-containing complexes—and in suggested co-operation with CD14 (Echchannaoui et al., 2005; Landmann et al., 2000)*.* Furthermore, we observed higher numbers of

neutrophils and bacteremia in the blood of mice lacking CD14, and the mice were accordingly less vital, compared to wt animals. This finding was consistent with the impaired *E.coli* phagocytosis by *cd14*^{-/-} microglia. While in a wt situation, microglial phagocytosis probably contributes to a reduction of the bacterial burden (Ribes et al., 2009), in *cd14*^{-/-} brains, *E.coli* could multiply and enter the circulation, which would lead to an attraction of more neutrophils in *cd14*^{-/-} mice than in the wt counterpart. In contrast, in models of septic shock, *cd14*^{-/-} mice had in general attenuated immune responses, decreased mortality and lower bacterial burden (Ebong et al., 2001; Haziot et al., 1996; Wiersinga et al., 2008). These contradictory results may imply that the contribution of CD14 in immune responses to infections can vary based on the location in the body, namely the afflicted organ and tissue.

In summary, CD14 enables for an appropriate immune response upon bacterial CNS infection by increasing the efficacy of microglial phagocytosis and, at the same time, by preventing an excessive neutrophil infiltration into the CNS.

5.2 CD14 controls neutrophil infiltration into the infected CNS by regulation of chemokines

The attraction of monocytes and neutrophils to sites of inflammation has most often being assigned to the chemokines CCL2 and CXCL1/2, respectively (Borregaard, 2010; McDonald et al., 2010; Tsou et al., 2007). We found elevated levels of CXCL1 in the circulation of mice with intracerebral *E.coli* infection, indicating its involvement in neutrophil recruitment. Even though a single injection of CXCL1 into the CNS did not lead to a recruitment of neutrophils, as it did in the periphery (Craciun et al., 2010; Rittner et al., 2006), an intravenous administration of a CXCR2-blocking antibody actually decreased the LPS-triggered neutrophil influx into the brains. These observations suggest that neutrophil infiltration as challenged by *E.coli* or LPS is largely due to the release of CXCR2 ligands (CXCL1 and CXCL2).

Conceivably, different expression levels of CXCR2 on neutrophils could have been a reason for variable neutrophil attraction to the challenged brains in *cd14*^{-/-} animals. However, *cd14*^{-/-} neutrophils expressed similar levels of CXCR2 as wt cells, and the CXCR2 levels were not significantly different in both genotypes 24 hours upon intracerebral injection of LPS, in contrast to CXCR2 up-regulation upon CNS infection with *S. pneumoniae* (Echchannaoui et al., 2005).

Neutrophils also express CD14 themselves. Their functions could be thus directly affected in a *cd14*^{-/-} situation. Indeed, *cd14*^{-/-} neutrophils displayed decreased migration *in vitro*, following a CXCL2 gradient (Echchannaoui et al., 2005). However, chemotaxis *in vitro* may also not reflect the situation *in vivo* and CXCL2 was found not to be relevant for our studies, as it did not show the critical overshoot induction by microglia (as discussed in the following section). Moreover, functions of *cd14*^{-/-} neutrophils

in vivo were not clearly impaired compared to the wt counterparts (McAvoy et al., 2011). All these results together pointed to the increased release of CXCR2 ligands from the infected brains of *cd14*^{-/-} animals as the main reason for the augmented neutrophil infiltration.

To further narrow down on the CNS cells that could contribute to the CD14-related mechanisms, we excluded neurons from our study. They do not express CD14, as shown by others (Lehnardt et al., 2003). Furthermore, we have also shown, in contrast to others (Lehnardt et al., 2002), that the large population of astrocytes does not express CD14, whereas microglia do express significant levels of CD14, as demonstrated by us as well as by others (Gautier et al., 2012). Thus, microglia are apparently the most relevant immune cells in the brain, which will be affected under *cd14*^{-/-} conditions. Of course, other cell populations, such as perivascular cells, could still have an impact. However, they account for a relatively small number of macrophage-like cells and they are more relevant for skin infections (Abtin et al., 2014). Finally, endothelial cells could also play a role, especially with regard to their function in the formation of the BBB. Yet they rather employ soluble CD14 from the circulation and do not express the membrane-bound version (Pugin et al., 1993). We can show that it is the membrane insertion that accounts for the regulatory activity of CD14.

In summary, microglia, as the cells expressing CD14 and producing significant amounts of CXCL1 upon sensing bacterial LPS (Regen et al., 2011; Scheffel et al., 2012) are most likely responsible for the attraction of neutrophils into the brains as challenged by bacterial infection. Accordingly, a dysregulation of microglial chemokine induction will most likely lead to the dysregulation of immune cell infiltration.

5.3 CD14 makes microglia extremely sensitive to LPS as compared to BMDM and peritoneal macrophages

Microglial cells as well as peripheral macrophages, namely peritoneal macrophages and BMDM, express substantial levels of CD14. However, these macrophages are of different origin and they are localized in completely different body compartments than microglia, which leads probably to specific adaptations in their behavior.

Indeed, microglia were clearly the most sensitive cells, both in terms of lowest concentrations of S-LPS needed to trigger a response and in terms of concentrations required to reach a response plateau, supporting and further supplementing our previous observations (Regen et al., 2011). Ten and hundred-fold higher LPS concentrations were required by BMDM and peritoneal macrophages, respectively, to trigger a saturated response, relative to microglia. This sensitivity depended on the presence of CD14. In its absence, all three types of macrophages had the same (lower) sensitivity. Thus, microglia were the

cells that benefited the most from expressing CD14, and the presence of this molecule established a dramatic difference in the sensory characteristics of their TLR4 complexes.

In contrast, all the macrophages needed basically the same concentration of Re-LPS to reach a maximal response. Compared to microglia, peritoneal macrophages and BMDM were shown to be clearly less dependent on CD14 in triggering a response to Re-LPS, which is in agreement with previous studies (Gangloff et al., 2005; Jiang et al., 2005; Regen et al., 2011). Considering that all microglia, BMDM and peritoneal macrophages express high levels of CD14, these findings indicate a cell type-specific employment of CD14. The contributions of CD14 to TLR4-triggered responses could be linked to the environment in which the cells have been developing and operating.

The peritoneal macrophages get probably more often into contact with LPS, which can be spilled from the intestinal microbiota into the peritoneal cavity. Thus, high sensitivity could lead to a chronic inflammation. On the other hand, microglia and BMDM are, during their lifespan, separated from the rest of the body, residing in compartments where infections (or exposure to LPS) rarely occur, and if so, where already traces need to be sensed. This common feature of BMDM and microglia is then probably reflected by their higher (and similar) responsiveness.

Taken together, the functional availability of CD14 makes a dramatic difference in responses of microglia and macrophages to LPS. In particular, CD14 renders microglia *a priori* extremely sensitive, more than BMDM and—even more—than peritoneal macrophages.

5.4   CD14 is used by microglia and BMDM for a dual control of LPS-triggered responses, but not by peritoneal macrophages

BMDM and microglia deficient in CD14 showed a nearly similar induction pattern, which was completely different from peritoneal macrophages. While microglia and BMDM needed CD14 to enhance their sensitivity to low amounts of LPS and to suppress their overreaction to high amounts of LPS, peritoneal macrophages used CD14 only as a supporter of their response to LPS, irrespective of the concentration.

Up to 1 ng/ml of LPS, which is the concentration at which the microglial response is saturated, CD14 presence was needed for a production of all cyto- and chemokines. Once microglial cells were stimulated with a 10-fold higher concentration (10 ng/ml), the role of CD14 changed from supportive to preventive influences, which was demonstrated by an excessive release activity by microglia lacking CD14 expression ($cd14^{-/-}$) or function (due to an antibody block). The over-produced chemokines were CXCL1, TNFα, IL-6 and IL-12p40, but only partially CXCL2, while CCL2, CCL3 and CCL5 release was not affected by CD14 absence. These observations confirm our previous results (Regen et al., 2011).

The release pattern by Re-LPS-stimulated $cd14^{-/-}$ BMDM was, indeed, comparable to that observed upon microglial stimulation, confirming the similarity of responses of BMDM and microglia. In sharp contrast, $cd14^{-/-}$ peritoneal macrophages displayed a completely different behavior. Here, CD14 only supported the release of all cyto- and chemokines, irrespective of the concentration and chemotype of LPS. There was no overshoot phenomenon at all. The only exception was a very moderate overshoot in TNFα, upon stimulation with Re-LPS, which has also been previously described (Gangloff et al., 2005). This lack of overshoot could be explained by insufficient challenge by LPS. The response to 1000 ng/ml of LPS could turn out to be still CD14-dependent, i.e. even higher concentration of LPS could reveal the suppressive role of CD14 in peritoneal macrophages. However, this possibility is unlikely given the observed plateau in the dose-response relation, as this would be an indicator for a high (enough) concentration.

Taken together, microglia and BMDM use CD14 to keep their responses to various doses of LPS in a moderate range, supporting their reactions to a low challenge and preventing excessive release upon high LPS amounts. This phenomenon is cell type-dependent, because it does not apply to the peritoneal macrophages.

5.5 BMDM and microglia use CD14 only partially for responses triggered by other TLR agonists

CD14 does not only cooperate with TLR4. It was also shown to participate in responses to ligands of TLR1, 2, 3, 6, 7 and 9 (Baumann et al., 2010; Lee et al., 2006; Yoshimura et al., 1999; Zanoni and Granucci, 2013b). We thus determined, whether and how CD14 absence could affect the microglial and BMDM release of selected cyto- and chemokines.

The wt microglia were far more efficient in responding to all tested compounds than BMDM. However, in contrast to results obtained upon LPS stimulation, the BMDM and microglial release induced by other TLR ligands depended only partially on CD14.

Contrary to previous studies which showed CD14 as a co-receptor necessary for TLR3 reactions triggered by poly(I:C) (Lee et al., 2006), responses of $cd14^{-/-}$ BMDM and microglia were mostly left intact in our experiments. Induction of CCL3 by BMDM was the only exception, which compared to microglia, required CD14. The uniqueness of CCL3 as a factor with a "strange" CD14 independency in microglia has already been observed (Regen et al., 2011). Also the release from both BMDM and microglia as triggered by CpG DNA, the specific ligand for TLR9, was independent of CD14, as described by others (Baumann et al., 2010). The contradictory results for the contribution of CD14 to both TLR3- and TLR9-triggered responses could be due to the fact that we measured different cyto- and chemokines. It can thus be

possible that CD14 is important only for selected signaling pathways leading to a production of specific factors, as seen for CD14 controls over LPS-triggered responses (release of CCL5 *versus* CXCL1).

The responses by microglia stimulated with Pam_3CSK_4 and MALP-2 were partially dependent on CD14. This did not hold true for BMDM, where CD14 was obviously not required for cyto- and chemokine induction, and where it served rather as a suppressor of excessive release. This observation was contradictory to the literature (Brandt et al., 2013). However, the authors of that study worked with human monocytes, indicating species- and cell-type specific differences.

A surprising CD14 dependency was observed for dsRNA poly(A:U), which was claimed to be a specific TLR3 ligand (Conforti et al., 2010). Compared to poly(I:C), poly(A:U) triggered a strong response by both BMDM and microglia. Both compounds were used at the same concentration. One may speculate that poly(A:U) used in our experiments was contaminated with a small amount of LPS and the triggered release by microglia as well as BMDM was abrogated in the absence of CD14. On the other hand, poly(A:U) may also not be absolutely selective, as it is the for poly(I:C), which can also act on MDA5 as a RIG-like protein (Kato et al., 2006).

Taken all together, compared to BMDM, microglia are far more sensitive as to responses to other TLR agonists. However, CD14 accounts only partially for this cell type-specific feature.

5.6 CD14 prevents hypo- and hyperinflammation in the CNS challenged with LPS

CD14 exerted a dual role in the control of a recruitment of monocytes and neutrophils into the brains upon LPS injection. Administration of low doses of LPS led to reduced infiltration of both monocytes and neutrophils into brains of $cd14^{-/-}$ mice, as compared to wt counterparts. With the increasing dose of LPS, the response turned to be independent of CD14, as manifested by the same number of infiltrating monocytes and neutrophils in both genotypes. The highest dose of LPS, however, led to an enhanced attraction of neutrophils into the brains of $cd14^{-/-}$ mice. Since we confirmed CXCL1 acting on CXCR2-expressing neutrophils and showed microglia as the main CNS cells expressing CD14, these results were highly consistent with the observed insufficient as well as excessive CXCL1 release by $cd14^{-/-}$ microglia *in vitro*, depending on the concentration of LPS. The intensity of the overshooting neutrophil influx in the brains of $cd14^{-/-}$ mice upon high LPS dose delivery, however, was not (i) as strong as in the case of *E.coli* infection and (ii) as expected from the high levels of CXCL1 produced by $cd14^{-/-}$ microglia stimulated with high amounts of LPS. This fact could be assigned to the extremely high amounts and the particular presentation of LPS as provided by intact *E.coli*, and it could additionally be due to an insufficient *E.coli* phagocytosis by $cd14^{-/-}$ microglia, causing prolonged persistence and uncontrolled spread of the bacteria.

Accordingly, the LPS dose administered in our experiments would not be high enough to mimic the full-blown infection. In addition, LPS injections penetrating the BBB would lead also to a release of DAMPs, other TLR4 ligands that, as discussed in the following sections, are recognized by microglia. In contrast to a pure LPS stimulation of microglia *in vitro*, *in vivo,* DAMPs—such as pFN—can displace LPS at the TLR4 level (Scheffel et al., unpublished). Since DAMP-triggered responses entirely depend on CD14, the displacement of LPS by DAMPs may lead to an altered response.

Very similar effects of CD14 contributions to the organization of a LPS-triggered neutrophil infiltration were also observed in the lungs upon administration of LPS intranasally (Anas et al., 2010). This suggests that alveolar cells could develop a similar CD14-dependent control over TLR4-responses as microglia do.

Taken together, on one hand, CD14 enables a stronger immune response by infiltration of more monocytes and neutrophils into the brains injected with low doses of LPS. On the other hand, CD14 halts excessive neutrophil recruitment into the brains challenged with high doses of LPS, thereby potentially preventing damage made by a high number of activated neutrophils.

5.7   CD14 serves as a mandatory receptor for responses to damage

Even in the absence of infectious stimuli, the immune system gets alarmed by recognition of DAMPs, which similarly to PAMPs, bind to TLR receptors and trigger a release of cyto- and chemokines. The subsequent immune response leads to a sterile inflammation, which is manifested—similarly to infectious scenarios—by a recruitment of immune cells to the site of the insult (Chen and Nunez, 2010; Shen et al., 2013).

Brains of *cd14*$^{-/-}$ mice showed no immune cell infiltrates as a response to tissue damage, in sharp contrast to the situation in wt animals. Thus, CD14 is shown to be very important for immune reactions to damage. We considered FN as a representative DAMP. As a plasma factor, it would usually not come into contact with microglia. However, it can enter the CNS upon vascular damage or BBB leakage. As we have already reported, microglia responded potently to increasing doses of pFN by release of various cytokines and chemokines (Goos et al., 2007; Regen et al., 2011)—however, only in the functional presence of CD14. The efficacy of cyto- and chemokine release induction in wt microglia was even comparable for LPS and pFN stimulations (Regen et al., 2011). Yet CD14 deficiency led to a complete abrogation of the pFN-triggered responses, independently of the used concentration. Notably, none of the concentrations of pFN led to an overshooting release in *cd14*$^{-/-}$ microglia, as it was observed upon stimulation with high amounts of LPS. Thus, microglial responses to pFN are dependent on CD14

presence, which differs from responses to LPS, indicating differing regulation of reactions to damage *versus* infection.

The delivery of pFN into the CNS resulted in immune responses that were halted in the absence of CD14. Both intrastriatal injections and long-term delivery of pFN led only to moderate cell infiltrates as mainly comprised of monocytes. We excluded a reduced expression of CCR2 on Ly-6C^{hi} monocytes as a reason for the abrogated monocyte infiltration in *cd14$^{-/-}$* mice. Thus, monocytes from both genotypes had the same requirements for infiltration, and it was most likely the lack of CCL2 release from *cd14$^{-/-}$* microglia which made the difference in CD14 deficiency.

Considering pFN as a potent agonist of microglial CXCL1 production, which in cell cultures can even exceed induction by LPS, the low number of infiltrating neutrophils was surprising. Conceivably, pFN deposited in the tissue is interpreted by microglia differently than LPS, which leads to an adapted response. While in bacterial infection neutrophils play a crucial role in the pathogen killing (Kielian et al., 2001), neutrophils infiltrating into CNS during a sterile inflammation contribute rather to neurotoxicity (Allen et al., 2012; Dinkel et al., 2004). In this way, microglia that sense pFN as a DAMP could organize monocyte recruitment which is rather important for tissue recovery. However, this would be impossible in the absence of CD14.

The continuous delivery of pFN into brains activated the parenchymal microglia/macrophages, as seen by up-regulation of Iba-1 and Mac3 receptors, in a CD14-dependent manner. Despite this indicated activation, pFN infusions did not lead to any additional damage in terms of interruption of myelin and axonal structure. In contrast, intracerebral LPS administration was demonstrated to cause a neurotoxicity by driving microglia to a production of pro-inflammatory and toxic factors, such as TNFα (Xing et al., 2011), and to lead to exacerbated cellular lesions and axonal damage (Carrillo-de Sauvage et al., 2013; Glezer et al., 2003a). These observations further support the concept of differential organization of immune reactions to DAMPs *versus* PAMPs.

As mentioned above, CD14 was absolutely required for the immune responses to a stab wound damage. Since in this case, also DAMPs other than pFN could be released and recognized by TLRs in co-operation with CD14, we see CD14 more as a general sensor of damage. This hypothesis is further corroborated by observations that deficiency or functional block of CD14 halts production triggered by HMGB1 and Hsp70, DAMPs released upon cell necrosis (Asea et al., 2000; Kim et al., 2013). In this case, CD14 even serves as a co-receptor of TLR2 and TLR4 (Park et al., 2004).

In summary, these results show that CD14 serves as an extremely important co-receptor for microglial responses to DAMPs. In CD14 absence, this fact is manifested by abrogated activation and

release of cyto- and chemokines by microglia and by an absence of infiltrates of immune cells upon CSN damage.

5.8 CD14 deficiency worsens the impacts of MCAO

A large spectrum of endogenous ligands is released during stroke, which is, according to the World Health Organization (WHO), the second leading cause of death worldwide. Stroke is most often caused by vessel occlusion resulting in a restriction of the blood supply. Ischemia induces rapid necrotic cell death. Restoration of the blood flow and concomitant re-oxygenation is, however, associated with exacerbation of the tissue damage. TLRs were clearly demonstrated as the receptors responsible for sensing the DAMPs which were released from necrotic cells or by ECM breakdown during stroke progression or which appeared with the restored blood flow (Buchanan et al., 2010; Wang et al., 2011).

Similarly to the other models of tissue damage, CD14 deficiency resulted in our experiments in a decreased monocyte/monocyte-derived macrophage infiltration into the brains of mice that underwent MCAO. Since release of CCL2 after ischemia correlates with influx of monocytes (Chen et al., 2003; Schilling et al., 2009), the lack of microglial release of CCL2 due to absence of CD14 may likely also here contribute to a reduction of monocyte (CD115$^+$CD11b$^+$Ly-6C^{hi}) recruitment.

The reduced monocyte infiltration in the absence of CD14 was accompanied by a larger stroke size. The $cd14^{-/-}$ mice were also more sensitive to the MCAO procedure itself, as manifested by a higher incidence of death. These results were very interesting, because $tlr2^{-/-}$ and $tlr4^{-/-}$ mice exhibited reduced infarct size, as compared to controls, which resulted in improved neurological behavior and reduced edema (Bohacek et al., 2012; Buchanan et al., 2010; Caso et al., 2007). However, CD14 may simultaneously serve as a co-receptor for various TLR agonists (Baumann et al., 2010; Lee et al., 2006; Yoshimura et al., 1999; Zanoni and Granucci, 2013b), which widens its spectrum of activities. CD14 deficiency then cannot be set equal to $tlr2^{-/-}$ or $tlr4^{-/-}$ conditions, and CD14 can likely control a larger variety of mechanisms, including those which may even protect against further damage in ischemia.

A lack of vitality and larger stroke sizes in the $cd14^{-/-}$ mice may imply a kind of beneficial role for monocytes/macrophages, since their paucity resulting from CD14 deficiency turned into negative outcomes. Such a view would be in contrast to other studies (Chen et al., 2003; Schilling et al., 2009). However, in injured retinas, monocyte-derived macrophages (CD115$^+$CD11b$^+$Ly-6C^{hi}) were shown to have also an anti-inflammatory and neuroprotective character (London et al., 2011). Furthermore, we observed a recruitment of CD115$^+$CD11b$^+$Ly-6C^{lo} monocytes already 3 days after MCAO, which were described as anti-inflammatory and which were shown to promote tissue regeneration upon infarction

of the myocardium and in an autoimmune retina disease (London et al., 2013b; Nahrendorf et al., 2007). The infiltration of these Ly-6C^{lo} monocytes, which depends on other factors than CCL2 (Donnelly et al., 2011; Nahrendorf et al., 2007), was also significantly reduced in CD14 absence, which might have contributed to an increased ischemic injury in $cd14^{-/-}$ mice during our experiments. It would thus be essential to clearly assign such a role in regeneration after stroke to CD14 in future experiments.

On the other hand, neutrophil recruitment upon MCAO, as classically linked to neurotoxic damage (Grønberg et al., 2013; Matsuo et al., 1995), was not affected by CD14 deficiency. This suggests that recruitment of neutrophils into the parenchyma upon transient MCAO and reperfusion might be more due to enhanced attachment of neutrophils to adhesive molecules, such as ICAM-1 or P-selectin on endothelial cells which are up-regulated upon ischemic injury (Connolly et al., 1996; Okada et al., 1994). This appears more likely to serve as a cause than an altered chemokine pattern.

Overall these results show a crucial role of CD14 in the response to ischemia. CD14 is required for a proper recruitment of monocytes into the brains following MCAO. Conceivably, this has beneficial potential, as manifested by a better recovery and smaller infarct size in the wt animals.

5.9 CD14, as a gate keeper of TLR-triggered responses, is itself highly regulated at expression level

Compared to peripheral macrophages, microglia express only low to moderate levels of CD14 under normal conditions (Gautier et al., 2012). However, this changes during pathological situations, such as in infections (Glezer et al., 2003a; Lacroix et al., 1998; Landmann et al., 2000).

Microglia stimulated with the TLR4 agonists LPS and pFN up-regulated CD14 expression at mRNA as well as protein level. This observation was in agreement with previous reports showing more CD14 mRNA transcripts detected in the brains of animals with peripheral or intracerebral LPS injections (Glezer et al., 2003b; Lacroix et al., 1998). Also human monocytes and macrophages were shown to increase CD14 protein levels when stimulated with LPS (Landmann et al., 1996).

Low LPS exposure would thus enhance CD14 as it is required for increased sensitivity. High dose LPS challenges would organize for sufficient CD14 also for the prevention of excessive responses. pFN would drive CD14 as the co-receptor is absolutely required. In addition to these TLR4 agonists, CD14 upregulation was initiated by Pam$_3$CSK$_4$, poly(A:U) and CpG as ligands for TLR1/2, TLR3 and TLR9. All of these TLRs were shown to be interacting with CD14 to some extent (Baumann et al., 2010; Lee et al., 2006; Yoshimura et al., 1999; Zanoni and Granucci, 2013b), which implies that microglia can be 'primed' by other TLRs in order to make them more sensitive for an induction of a CD14-depending response. As another facet of an explanation, one has to consider that CD14 presence is apparently mandatory for a

reaction to damage in general. All these TLR agonists may thus prepare the system for a response to damage, which most likely accompanies bacterial or viral infections. In other words, the damage-sensing capacity of a CD14/TLR4 complex (and beyond) could be recruited as a reaction to various PAMPs and DAMPs.

On the other hand, soluble factors like IFNγ, INFβ and IL-4, dramatically reduced the CD14 expression in a time-dependent manner, which was similarly observed for human monocytes and macrophages (Becher et al., 1996; Landmann et al., 1991; Payne et al., 1992). The Th1 and NK cell-derived IFNγ may thus shift microglial responses away from sensing damage upon infection, as high LPS would not require CD14, but DAMPs would do so. IL-4, which is mainly produced by T helper 2 (Th2) cells, shifts the system towards an anti-inflammatory state. Similarly, IFNβ may also have suppressive or more anti-inflammatory effects under specific conditions (González-Navajas et al., 2012; Trinchieri, 2010). Thus, a decrease in surface CD14 induced by both IFNβ and IL-4 in the absence of severe infection may serve as information for microglia not to alarm more peripheral cells by production of high amounts of cytokines and chemokines.

However, a presence of high amounts of LPS overwrote down-regulatory functions of IFNγ, a key cytokine of Th1 and NK cells, leading to increased expression of CD14, which exceeded the levels in untreated cells. Thus, microglia could again fully employ CD14 to control the support and containment of the TLR-driven responses.

Taken together, we showed that CD14 expression on microglia can be significantly regulated by various factors, including PAMPs, DAMPs and key cytokines. Thus, microglial functions are subject to versatile control by both CNS-resident and peripheral immune cells and can be regulated depending on the specific situation and context. The damage-sensing and response-controlling activity spectrum of CD14 could thereby by further incorporated or excluded from the reactive phenotype of microglia.

5.10 sCD14 cannot substitute for membrane-anchored CD14 to trigger immune responses by microglia and astrocytes

Peritoneal macrophages from $cd14^{-/-}$ mice can use sCD14 instead of mCD14 to trigger a response to LPS (Jiang et al., 2005; Moore et al., 2000). However, we showed that sCD14 could not substitute for the mCD14 in microglia, meaning that neither the reduction in responses to low concentrations of LPS and pFN was restored by addition of sCD14, and nor was the overshoot of CXCL1 prevented. These results further support the finding that microglia and peritoneal macrophages exhibit a cell type-specific organization of TLR4 signaling.

On the other hand, the release of chemokines by wt microglia stimulated with TLR4 agonists was increased by addition of recombinant sCD14. Similarly, sCD14 injected into the brains infected with *S. pneumonia* resulted in a markedly increased local cytokine response (Cauwels et al., 1999). Conceivably, microglia could somehow attach the sCD14 to mCD14. Indeed, we observed elevated surface-CD14 levels upon addition of recombinant sCD14. On the other hand, when the cells were simultaneously treated with TLR4 agonist and sCD14, no additional increase in CD14 was detected, which would indicate attachment of sCD14. A possible explanation of the enhanced response of wt microglia with sCD14 could be that the sCD14 binding to cell surface prevents binding of other molecules, which would otherwise prevent excessive signaling.

Endothelial and epithelial cells do not express mCD14. Instead, they employ sCD14 to trigger a response to LPS (Golenbock et al., 1995; Pugin et al., 1993). Astrocytes were shown to respond to TLR1/2/6 ligands (Bowman et al., 2003; Carpentier et al., 2005; Esen et al., 2004), whereas reports of TLR4 expression and respective responses diverge (Gorina et al., 2011; Lehnardt et al., 2002). As discussed in section 5.2, astrocytes do not express CD14. Therefore, sCD14 was considered as the missing element for a functional TLR4 signaling. However, upon addition of sCD14, still no release was observed in astrocytes stimulated with LPS or pFN. Furthermore, the unaltered cytokine production as triggered by other TLR agonists in the presence of sCD14 implies that it probably does not really play a role in a regulation of astrocytic responses to infectious stimuli. Notably, even high LPS concentrations, which were show to be CD14-independent in microglia, failed to trigger a response in astrocytes.

These findings show that even though sCD14 can be increased in the cerebral fluid during some specific circumstances, it would not play a role in the immune responses of astrocytes. Microglia require mCD14 for fully functional TLR signaling. On the other hand, microglia expressing mCD14 may probably use sCD14 to further regulate their responses.

5.11 Functional presence of CD14 is required longer to establish DAMP-triggered responses

The classical downstream signaling, which is transduced upon TLR4 ligand binding, most probably happens within the first few hours. The maximal activation of NF-kB and p38^{MAPK} occurs at 30 min after signal transduction, and after 4 h it returns to a baseline (Janova et al., unpublished). However, CD14 turned out to contribute to the organization and shaping of the TLR4-triggered reactions at later time points—with unexpected ligand discrimination. A timed block of CD14 showed that CD14 control over LPS-triggered responses, in terms of support of insufficient reaction to low LPS amounts and the containment of excessive release to high amounts of LPS, was established within the first 6 hours.

However, microglia stimulated with pFN needed the functional presence of CD14 for a time period exceeding the 6 h range, as manifested by insufficient release. These striking findings clearly imply differences in the use of CD14 to control responses to DAMP *versus* PAMP. Notably, the insufficient release by cells stimulated with pFN under functional CD14 for only 6 hours was not due to a slower onset of cyto- and chemokine production. Apart from a release of CCL2, which LPS induced at earlier time points, pFN proved to be not only similar to LPS but even faster in triggering the induction of CXCL1, TNFα and CXCL2. An explanation could be that pFN and LPS have different kinetics of CD14 induction. Accordingly, pFN would elevate CD14 expression later than LPS at high and also at low concentration. The earlier elevated CD14 levels would then also provide a full regulatory function earlier. However, pFN was actually much stronger and quicker in CD14 induction, and the levels of CD14 on the cells stimulated with pFN even exceeded those on LPS-treated microglia.

Taken together, the time needed for CD14 to control microglial responses to DAMPs and PAMPs differs. Especially in the case of DAMPs, CD14 is still required longer after the classical TLR4 signaling comes to an apparent end, suggesting additional CD14-dependent signaling events.

5.12 Syk, PLCγ2 and BTK do not play a role in a CD14 control over TLR4 signaling events

CD14 enables endocytosis of a LPS-TLR4 complex, which transduces the signaling via TRIF and TRAM (TIRAP) adaptor proteins (Kagan et al., 2008; Zanoni et al., 2011). In DCs and BMDM, this process is dependent on Syk and the downstream effector PLCγ2, as their inhibition or deficiency could largely phenocopy CD14 deficiency. In microglia, Syk inhibition did not lead to excessive production of CXCL1, as seen in CD14 deficiency and the PLC inhibition even completely prevented any CXCL1 induction. Both, Syk and PLCγ2 inhibition also did not phenocopy the induction of CCL5 in $cd14^{-/-}$ cells, which occurs in microglia to a large part by TRIF signaling (Regen et al., 2011). Similar observations were made for a TLR4-triggered induction of MHC I, which is entirely dependent on TRIF and partially on CD14 (Regen et al., 2011). These findings imply that microglia probably differ from BMDM and DCs by their involvement of downstream factors used for CD14 control over TLR4 reactions.

As a last candidate for signaling contributions in CD14-controlled processes, we chose BTK, as a kinase responsible for phosphorylation of MAL, as a MyD88 pathway-associated adaptor protein during TLR4 signal transduction (Brunner et al., 2005). Although BTK inhibition did not lead to excessive release of the MyD88-dependent CXCL1, it at least partially resembled the CD14 deficiency by moderately decreasing the release triggered by pFN or low concentrations of LPS. However, the inhibition of BTK did

not at all impair the CCL5 release as triggered by low amounts of LPS or pFN, which was seen in CD14 deficiency. Thus, BTK was also ruled out as signaling partner of CD14.

Taken together, Syk, PLCγ2 and BTK are not likely to be employed in the downstream signaling that would govern the CD14-organized release control of CXCL1 and CCL5 in microglia.

5.13 Microglia internalize only small amounts of CD14

Apart from presenting LPS to the MD2-TLR4 complex and allowing for more efficient signal transduction from the membrane, CD14 was shown to control internalization of LPS bound to MD2-TLR4 complex into the endosomal network (Zanoni et al., 2011). This step was shown to be crucial, since the translocation into an endosomal compartment allows for the TRIF-TRAM-dependent pathway, which culminates in the production of type I IFNs (IFNα/β) (Kagan et al., 2008; Kawai et al., 2001). CD14-assisted internalization of LPS-TLR4 has been so far shown only for BMDM and DCs (Zanoni et al., 2011).

In microglia, we did not observe any dramatic loss of CD14 from the microglial cell surface, as described by Zanoni et al. for BMDM (Zanoni et al., 2011). By using confocal microscopy, we could see that CD14 was distributed in a compact fashion on the surface of untreated microglia. However, we also detected pools near the nucleus, which—based on the localization—could also associate with the endoplasmatic reticulum or the Golgi apparatus. Indeed, CD14 was shown to be present in the endoplasmatic reticulum, where it is likely synthesized, and in the Golgi apparatus of peritoneal macrophages, where it is provided with its GPI anchor (Yoshioka et al., 2009). LPS stimulation led to a redistribution of the surface CD14, forming clumps and thus interrupting the previously more even arrangement. However, most of the CD14 stayed localized on the cell surface.

Both approaches used in our studies, and especially the flow cytometry, were apparently not sensitive enough to prove substantial CD14 endocytosis, which contributes to LPS-triggered TRAM-TRIF signaling from intracellular compartments. It is probably only a fraction of the CD14 which is required for such a support, and the disappearance of a small amount from the total surface pool could be easily missed in a subtractive flow-cytometry analysis. Since we proved the contribution of CD14 in TRIF-depended signaling by addressing the functionality of either the release of CCL5 or the induction of MHC I, which both rely on TRIF, we indirectly proved also CD14 endocytosis. However, in order to fully describe this phenomenon in microglia, it would be necessary to employ another technique that could clearly show the internalization of CD14. Biotin tagging of surface CD14 could be such an alternative.

5.14 CD14 deficiency reveals differences in responses to DAMPs and PAMPs at a global level

As discussed in the previous chapters, pFN and LPS as representatives for DAMPs and PAMPs, drive very similar response profiles in the functional presence of CD14. The situation completely changes once CD14 is blocked or physically absent. We addressed the differences and similarities in transcriptome profiles of microglia as stimulated with LPS or pFN. Both the differential gene analysis and the WGCNA confirmed the high similarity between the effects of both agonists at transcription level, showing that they drive the same genes under normal conditions. Also from the quantitative point of view, high concentrations of LPS and pFN up-regulated and down-regulated the same number (sets) of genes. Despite these similarities at the transcription level, and practically by the same release profiles seen *in vitro*, we observed differences in response to DAMPs and PAMPs *in vivo* (as discussed in chapter 5.7). This indicates that the outcomes upon stimulation with DAMPs and PAMPs in the tissue must be induced by supragenetic effects, like functional regulation of proteins via phosphorylation or by interactions among them, or by molecules released from other cells than microglia.

The comparisons of wt to *cd14*$^{-/-}$ microglia revealed no differences once the microglia were not stimulated, showing that CD14 absence does not lead to any other alterations at the gene regulation level (except for CD14 itself). More importantly, CD14 absence resulted in more impaired responses to DAMPs than to PAMPs. Additionally, CD14 becomes less important in microglia stimulated with high amounts of LPS. Signaling pathways related to IFN type I and antigen presentation were highly affected by CD14 absence. This confirms the previously described CD14 assistance in TRIF-dependent signaling at a global scale, namely at the transcription level. CD14 is needed for both the endocytosis of a LPS-TLR4 complex followed by IFNβ production and for TRIF-dependent induction of MHC I. On the other hand, in *cd14*$^{-/-}$ microglia, the signaling pathway related to MyD88 and NF-κB stayed more intact. Thus, also the production of inflammatory cytokines, such as TNFα or CXCL1, will be less affected in CD14 absence.

5.15 Inhibition of endocytosis does not phenocopy a *cd14*$^{-/-}$ situation in LPS-triggered responses by microglia

The functional assays together with the bioinformatics approach clearly confirmed that CD14 is especially needed for the intracellular signal transduction using the TRIF adaptor protein. Thus, excessive CD14-triggered internalization of LPS-TLR4 complex could serve as a kind of negative regulation for the signaling via MyD88. High levels of LPS, that are effective in the absence of CD14, would not be internalized to signal via TRIF, while this would simultaneously lead to a continuous transmembrane signaling via the MyD88 adaptor protein. The block of internalization would then similarly lead to an

excessive release of CXCL1 (as a representative factor under MyD88 control). However, treatment with inhibitors of internalization did not phenocopy the release effects in cells with blocked CD14. In the case of chlorpromazine, filipin III and choroquine, the reason was most probably a decrease in metabolic activity and probably also vitality. This, however, could not be an explanation for cytochalasin D and dynasore. Dynasore, a specific inhibitor of dynamin, had been used most often to prove the CD14 endocytosis (Kagan et al., 2008; Kirchhausen et al., 2008; Zanoni et al., 2011). However, dynasore loses its activity in the presence of serum, which is rich in factors (e.g. LPB) necessary for a functional LPS-triggered TLR4 signaling, culminating in cyto- and chemokine release. The failure of cytochalasin D could be due its specific inhibition of actin polymerization, which may not play role in the case of CD14-triggered LPS-TLR4 complex endocytosis, because it was shown to be regulated especially by dynamin GTPases (Husebye et al., 2006).

Taken together, we could not prove that non-functional endocytosis of LPS-CD14-TLR4 complex leads to an exaggeration of MyD88 signaling and thus to enhanced production of CXCL1, which was most likely due to technical limitations in the experimental use of inhibitors. Still, the hypothesis that CD14 lack leads to a prolonged MyD88 signaling, and thus to an exaggerated release of MyD88-controlled factors, was attractive. It was apparently supported by the fact that MyD88-dependent factors did show overshoots, whereas factors with mixed MyD88/TRIF dependence did not. Even though appealing as a concept, we found that the CD14-involving mechanism for overshoot control rather related to the TRIF signaling directly.

5.16 IFNβ signaling is the crucial regulator of CXCL1 release by LPS-stimulated microglia

CD14 deficiency would not only prolong MyD88 signaling, but prevent TRIF activation. Downstream of TRIF, some factors may exert a negative influence on MyD88-driven genes. In other words, we kept a loss of negative control as an option to explain overshooting responses. From the deep sequencing data and their bioinformatic analysis, we had learned that the IFNß system was massively impaired in $cd14^{-/-}$ cells.

Indeed, CD14 deficiency impeded the normal TRIF-dependent production of IFNβ in microglia. Accordingly, impairment of IFNβ signaling at the receptor or Jak level unleashed an excessive CXCL1 production by wt microglia as stimulated with high concentrations of LPS. Furthermore, and in turn, the addition of IFNβ to $cd14^{-/-}$ cells decreased the excessive production of CXCL1 to the levels of wt cells. Thus, by manipulating the IFNβ signaling through its receptor IFNAR and its associated Jak, we could drive dysregulated release in wt microglia as well as restore proper control in $cd14^{-/-}$ cells. The impaired IFNβ signaling in the $cd14^{-/-}$ mice is therefore most likely the main reason for both the augmented CXCL1

induction and the neutrophil infiltration upon infectious challenges. Indeed, enhanced numbers of neutrophils are infiltrating the peritoneal cavity of IFNAR1-deficient mice during septic peritonitis (Weighardt et al., 2006).

Interestingly, wt microglia with impeded IFNβ signaling and stimulated with pFN also produced higher levels of CXCL1. However, we never observed excessive production in $cd14^{-/-}$ microglia treated with pFN. The reason could be that response to pFN, compared to LPS, are far more dependent also on MyD88 signaling. Thus, in the absence of CD14, microglia do not induce IFNβ, however, they also do not properly produce the cyto- and chemokines under MyD88. There is thus no overshoot of CXCL1 since there is no real induction at all.

In contrast to CXCL1, TLR4 agonist-triggered CCL2 production was even moderately increased by addition of IFNβ. Since we and others observed that IFNβ alone can trigger CCL2 production (Lin et al., 2008), this effect seems to be most likely a consequence of synergy between LPS and IFNβ stimulations. Reduced CXCL1 release and increased CCL2 release may then result in a shifted ratio from neutrophils to monocytes.

Findings that impaired TRIF-dependent production of IFNβ leads to excessive CXCL1 production would suggest that microglia from TRIF-deficient mice should also display the same release pattern. However, this is not the case (Regen et al., 2011). The reason could be that the TRIF adaptor protein not only contributes to the production of IFNβ, but its absence then affects induction of other proteins, thereby creating a completely different signaling situation, which would then not support the excessive production of CXCL1.

Another aspect is that even though the excessive CXCL1 production by $cd14^{-/-}$ microglia was phenocopied by impairment in IFNβ signaling, the same did not apply to the release of TNFα, IL-6 and IL-12p40. In the case of these factors, other mechanisms must be considered. Possible candidates that could play a role here are suppressors of cytokine signaling (SOCSs). SOCSs are activated by TLR ligands, like LPS, and were shown to prevent a chronic production of TNFα, IL-6 and IL-12 (Yoshimura et al., 2007). Accordingly, mice deficient in SOCS were hypersensitive to LPS, leading to increases in TNFα and IL-12 production. Most importantly, CD14 deficiency and decreased negative regulation by SOCSs were already linked to excessive TNFα release as triggered by TLR1/2 ligands, i.e. triacylated lipoproteins from *Borrelia burgdorferi (B.burgdorferi*) (Sahay et al., 2009).

In summary, our results show that the lack of IFNβ due to disrupted TRIF-dependent signaling in $cd14^{-/-}$ microglia underlies the mechanism by which microglia control the LPS-triggered release of CXCL1

and CCL2 and subsequently the magnitude of neutrophil and monocyte infiltration into LPS-challenged brains.

5.17 Conclusion

We have shown here that the TLR4 co-receptor CD14 is a key organizer and versatile gate keeper in microglial responses to both bacterial LPS and endogenous factors associated with injury, as well as in immune reactions to CNS infection and damage. CD14 controls the magnitude of inflammatory responses by microglia and in the CNS according to the strength of infectious stimuli, keeping them at a moderate intensity. Upon low infectious challenges (as associating with low levels of PAMP agonists), CD14 supports microglia in their immune responses and enables appropriate immune cell infiltration into the CNS in order to readily clear the bacteria. On the other hand, CD14 also protects the CNS against hyperinflammation upon high intensity challenges by infection-related agents, at least in part based on a containment of overreactions by microglia to high doses of PAMPs. Control over the production of cytokines and chemokines is thereby translated into a control of infiltrating neutrophils and monocytes as early response elements with protective capacities as well as harmful potential. Crucial features of this CD14-dependent control as found in microglia are not equally seen in other extreneural macrophage populations, suggesting cell type-specific organizations. Unraveling the mechanism underlying the CD14-mediated control over the production of CXCL1 as a neutrophil chemoattractant, we identified IFNβ signaling as the indispensable downstream element. LPS-triggered IFNβ secretion, which is dependent on CD14, decreases CXCL1 levels and, thus, can limit a risk of uncontrolled tissue damage due to excessive neutrophil recruitment. Apart from this dual control over responses to infection, we have shown here the previously unknown function of CD14 in damage-triggered immune reactions. CD14 is revealed to be absolutely necessary for DAMP-triggered activations of microglia as well as for the mounting of immune reactions to CNS tissue trauma and ischemic injury. Enabling a sufficient monocyte entry appears to be essential for a damage-limiting response, at least in ischemic stroke. CD14 as contributing to a global DAMP sensor complex thus involves microglia in a variety of non-infectious CNS diseases and pathologies associated with TLR4-triggered sterile inflammation. Thus, we demonstrate that CD14 functions surpass by far the classically assigned role of a simple chaperon in LPS binding to TLR4. Most importantly, factors released during various pathological scenarios from CNS-resident and incoming peripheral immune cells can dramatically regulate CD14 expression and thereby control TLR4-driven functions in microglia.

Bibliography

Abtin, A., Jain, R., Mitchell, A.J., Roediger, B., Brzoska, A.J., Tikoo, S., Cheng, Q., Ng, L.G., Cavanagh, L.L., von Andrian, U.H., et al. (2014). Perivascular macrophages mediate neutrophil recruitment during bacterial skin infection. Nat. Immunol. *15*, 45–53.

Ajami, B., Bennett, J.L., Krieger, C., Tetzlaff, W., and Rossi, F.M.V. (2007). Local self-renewal can sustain CNS microglia maintenance and function throughout adult life. Nat. Neurosci. *10*, 1538–1543.

Akashi-Takamura, S., and Miyake, K. (2008). TLR accessory molecules. Curr. Opin. Immunol. *20*, 420–425.

Akira, S., Uematsu, S., and Takeuchi, O. (2006). Pathogen recognition and innate immunity. Cell *124*, 783–801.

Allen, C., Thornton, P., Denes, A., McColl, B.W., Pierozynski, A., Monestier, M., Pinteaux, E., Rothwell, N.J., and Allan, S.M. (2012). Neutrophil cerebrovascular transmigration triggers rapid neurotoxicity through release of proteases associated with decondensed DNA. J. Immunol. Baltim. Md 1950 *189*, 381–392.

Anas, A.A., Hovius, J.W.R., van 't Veer, C., van der Poll, T., and de Vos, A.F. (2010). Role of CD14 in a mouse model of acute lung inflammation induced by different lipopolysaccharide chemotypes. PloS One *5*, e10183.

Asea, A., Kraeft, S.K., Kurt-Jones, E.A., Stevenson, M.A., Chen, L.B., Finberg, R.W., Koo, G.C., and Calderwood, S.K. (2000). HSP70 stimulates cytokine production through a CD14-dependant pathway, demonstrating its dual role as a chaperone and cytokine. Nat. Med. *6*, 435–442.

Auffray, C., Fogg, D., Garfa, M., Elain, G., Join-Lambert, O., Kayal, S., Sarnacki, S., Cumano, A., Lauvau, G., and Geissmann, F. (2007). Monitoring of blood vessels and tissues by a population of monocytes with patrolling behavior. Science *317*, 666–670.

Baumann, C.L., Aspalter, I.M., Sharif, O., Pichlmair, A., Blüml, S., Grebien, F., Bruckner, M., Pasierbek, P., Aumayr, K., Planyavsky, M., et al. (2010). CD14 is a coreceptor of Toll-like receptors 7 and 9. J. Exp. Med. *207*, 2689–2701.

Becher, B., Fedorowicz, V., and Antel, J.P. (1996). Regulation of CD14 expression on human adult central nervous system-derived microglia. J. Neurosci. Res. *45*, 375–381.

Bechmann, I., Goldmann, J., Kovac, A.D., Kwidzinski, E., Simbürger, E., Naftolin, F., Dirnagl, U., Nitsch, R., and Priller, J. (2005). Circulating monocytic cells infiltrate layers of anterograde axonal degeneration where they transform into microglia. FASEB J. Off. Publ. Fed. Am. Soc. Exp. Biol. *19*, 647–649.

Beutler, B., and Rietschel, E.T. (2003). Innate immune sensing and its roots: the story of endotoxin. Nat. Rev. Immunol. *3*, 169–176.

Birdsall, H.H., Porter, W.J., Trial, J., and Rossen, R.D. (2005). Monocytes stimulated by 110-kDa fibronectin fragments suppress proliferation of anti-CD3-activated T cells. J. Immunol. Baltim. Md 1950 *175*, 3347–3353.

Block, M.L., Zecca, L., and Hong, J.-S. (2007). Microglia-mediated neurotoxicity: uncovering the molecular mechanisms. Nat. Rev. Neurosci. *8*, 57–69.

Bohacek, I., Cordeau, P., Lalancette-Hébert, M., Gorup, D., Weng, Y.-C., Gajovic, S., and Kriz, J. (2012). Toll-like receptor 2 deficiency leads to delayed exacerbation of ischemic injury. J. Neuroinflammation *9*, 191.

Borregaard, N. (2010). Neutrophils, from marrow to microbes. Immunity *33*, 657–670.

Bowman, C.C., Rasley, A., Tranguch, S.L., and Marriott, I. (2003). Cultured astrocytes express toll-like receptors for bacterial products. Glia *43*, 281–291.

Brandt, K.J., Fickentscher, C., Kruithof, E.K.O., and de Moerloose, P. (2013). TLR2 Ligands Induce NF-κB Activation from Endosomal Compartments of Human Monocytes. PLoS ONE *8*, e80743.

Brinkmann, V., Reichard, U., Goosmann, C., Fauler, B., Uhlemann, Y., Weiss, D.S., Weinrauch, Y., and Zychlinsky, A. (2004). Neutrophil extracellular traps kill bacteria. Science *303*, 1532–1535.

Brunner, C., Müller, B., and Wirth, T. (2005). Bruton's Tyrosine Kinase is involved in innate and adaptive immunity. Histol. Histopathol. *20*, 945–955.

Buchanan, M.M., Hutchinson, M., Watkins, L.R., and Yin, H. (2010). Toll-like Receptor 4 in CNS Pathologies. J. Neurochem. *114*, 13–27.

Butovsky, O., Landa, G., Kunis, G., Ziv, Y., Avidan, H., Greenberg, N., Schwartz, A., Smirnov, I., Pollack, A., Jung, S., et al. (2006). Induction and blockage of oligodendrogenesis by differently activated microglia in an animal model of multiple sclerosis. J. Clin. Invest. *116*, 905–915.

Carlin, L.M., Stamatiades, E.G., Auffray, C., Hanna, R.N., Glover, L., Vizcay-Barrena, G., Hedrick, C.C., Cook, H.T., Diebold, S., and Geissmann, F. (2013). Nr4a1-dependent Ly6C(low) monocytes monitor endothelial cells and orchestrate their disposal. Cell *153*, 362–375.

Carpentier, P.A., Begolka, W.S., Olson, J.K., Elhofy, A., Karpus, W.J., and Miller, S.D. (2005). Differential activation of astrocytes by innate and adaptive immune stimuli. Glia *49*, 360–374.

Carrillo-de Sauvage, M.Á., Maatouk, L., Arnoux, I., Pasco, M., Sanz Diez, A., Delahaye, M., Herrero, M.T., Newman, T.A., Calvo, C.F., Audinat, E., et al. (2013). Potent and multiple regulatory actions of microglial glucocorticoid receptors during CNS inflammation. Cell Death Differ. *20*, 1546–1557.

Caso, J.R., Pradillo, J.M., Hurtado, O., Lorenzo, P., Moro, M.A., and Lizasoain, I. (2007). Toll-Like Receptor 4 Is Involved in Brain Damage and Inflammation After Experimental Stroke. Circulation *115*, 1599–1608.

Cauwels, A., Frei, K., Sansano, S., Fearns, C., Ulevitch, R., Zimmerli, W., and Landmann, R. (1999). The origin and function of soluble CD14 in experimental bacterial meningitis. J. Immunol. Baltim. Md 1950 *162*, 4762–4772.

Chen, G.Y., and Nunez, G. (2010). Sterile inflammation: sensing and reacting to damage. Nat. Rev. Immunol. *10*, 826–837.

Chen, Y., Hallenbeck, J.M., Ruetzler, C., Bol, D., Thomas, K., Berman, N.E.J., and Vogel, S.N. (2003). Overexpression of monocyte chemoattractant protein 1 in the brain exacerbates ischemic brain injury and is associated with recruitment of inflammatory cells. J. Cereb. Blood Flow Metab. Off. J. Int. Soc. Cereb. Blood Flow Metab. *23*, 748–755.

Chiang, C.-Y., Veckman, V., Limmer, K., and David, M. (2012). Phospholipase C?-2 and Intracellular Calcium Are Required for Lipopolysaccharide-induced Toll-like Receptor 4 (TLR4) Endocytosis and Interferon Regulatory Factor 3 (IRF3) Activation. J. Biol. Chem. *287*, 3704–3709.

Chun, K.-H., and Seong, S.-Y. (2010). CD14 but not MD2 transmit signals from DAMP. Int. Immunopharmacol. *10*, 98–106.

Conforti, R., Ma, Y., Morel, Y., Paturel, C., Terme, M., Viaud, S., Ryffel, B., Ferrantini, M., Uppaluri, R., Schreiber, R., et al. (2010). Opposing effects of toll-like receptor (TLR3) signaling in tumors can be therapeutically uncoupled to optimize the anticancer efficacy of TLR3 ligands. Cancer Res. *70*, 490–500.

Connolly, E.S., Jr, Winfree, C.J., Springer, T.A., Naka, Y., Liao, H., Yan, S.D., Stern, D.M., Solomon, R.A., Gutierrez-Ramos, J.C., and Pinsky, D.J. (1996). Cerebral protection in homozygous null ICAM-1 mice after middle cerebral artery occlusion. Role of neutrophil adhesion in the pathogenesis of stroke. J. Clin. Invest. *97*, 209–216.

Craciun, F.L., Schuller, E.R., and Remick, D.G. (2010). Early Enhanced Local Neutrophil Recruitment in Peritonitis-Induced Sepsis Improves Bacterial Clearance and Survival. J. Immunol. *185*, 6930–6938.

Cross, A.S., Gemski, P., Sadoff, J.C., Orskov, F., and Orskov, I. (1984). The importance of the K1 capsule in invasive infections caused by Escherichia coli. J. Infect. Dis. *149*, 184–193.

Dessing, M.C., Knapp, S., Florquin, S., de Vos, A.F., and van der Poll, T. (2007). CD14 facilitates invasive respiratory tract infection by Streptococcus pneumoniae. Am. J. Respir. Crit. Care Med. *175*, 604–611.

Dinkel, K., Dhabhar, F.S., and Sapolsky, R.M. (2004). Neurotoxic effects of polymorphonuclear granulocytes on hippocampal primary cultures. Proc. Natl. Acad. Sci. U. S. A. *101*, 331–336.

Donnelly, D.J., Longbrake, E.E., Shawler, T.M., Kigerl, K.A., Lai, W., Tovar, C.A., Ransohoff, R.M., and Popovich, P.G. (2011). Deficient CX3CR1 Signaling Promotes Recovery after Mouse Spinal Cord Injury by Limiting the Recruitment and Activation of Ly6Clo/iNOS+ Macrophages. J. Neurosci. *31*, 9910–9922.

Ebong, S.J., Goyert, S.M., Nemzek, J.A., Kim, J., Bolgos, G.L., and Remick, D.G. (2001). Critical Role of CD14 for Production of Proinflammatory Cytokines and Cytokine Inhibitors during Sepsis with Failure To Alter Morbidity or Mortality. Infect. Immun. *69*, 2099–2106.

Echchannaoui, H., Frei, K., Letiembre, M., Strieter, R.M., Adachi, Y., and Landmann, R. (2005). CD14 deficiency leads to increased MIP-2 production, CXCR2 expression, neutrophil transmigration, and early death in pneumococcal infection. J. Leukoc. Biol. *78*, 705–715.

Eggen, B.J.L., Raj, D., Hanisch, U.-K., and Boddeke, H.W.G.M. (2013). Microglial phenotype and adaptation. J. Neuroimmune Pharmacol. Off. J. Soc. NeuroImmune Pharmacol. *8*, 807–823.

Ehrchen, J.M., Sunderkötter, C., Foell, D., Vogl, T., and Roth, J. (2009). The endogenous Toll-like receptor 4 agonist S100A8/S100A9 (calprotectin) as innate amplifier of infection, autoimmunity, and cancer. J. Leukoc. Biol. *86*, 557–566.

Elmore, M.R.P., Najafi, A.R., Koike, M.A., Dagher, N.N., Spangenberg, E.E., Rice, R.A., Kitazawa, M., Matusow, B., Nguyen, H., West, B.L., et al. (2014). Colony-stimulating factor 1 receptor signaling is necessary for microglia viability, unmasking a microglia progenitor cell in the adult brain. Neuron *82*, 380–397.

Esen, N., Tanga, F.Y., DeLeo, J.A., and Kielian, T. (2004). Toll-like receptor 2 (TLR2) mediates astrocyte activation in response to the Gram-positive bacterium Staphylococcus aureus. J. Neurochem. *88*, 746–758.

Fassbender, K., Walter, S., Kühl, S., Landmann, R., Ishii, K., Bertsch, T., Stalder, A.K., Muehlhauser, F., Liu, Y., Ulmer, A.J., et al. (2004). The LPS receptor (CD14) links innate immunity with Alzheimer's disease. FASEB J. Off. Publ. Fed. Am. Soc. Exp. Biol. *18*, 203–205.

Fitzner, D., Schnaars, M., van Rossum, D., Krishnamoorthy, G., Dibaj, P., Bakhti, M., Regen, T., Hanisch, U.-K., and Simons, M. (2011). Selective transfer of exosomes from oligodendrocytes to microglia by macropinocytosis. J. Cell Sci. *124*, 447–458.

Fleming, T.J., Fleming, M.L., and Malek, T.R. (1993). Selective expression of Ly-6G on myeloid lineage cells in mouse bone marrow. RB6-8C5 mAb to granulocyte-differentiation antigen (Gr-1) detects members of the Ly-6 family. J. Immunol. Baltim. Md 1950 *151*, 2399–2408.

Gangloff, S.C., Zähringer, U., Blondin, C., Guenounou, M., Silver, J., and Goyert, S.M. (2005). Influence of CD14 on ligand interactions between lipopolysaccharide and its receptor complex. J. Immunol. Baltim. Md 1950 *175*, 3940–3945.

Gautier, E.L., Shay, T., Miller, J., Greter, M., Jakubzick, C., Ivanov, S., Helft, J., Chow, A., Elpek, K.G., Gordonov, S., et al. (2012). Gene-expression profiles and transcriptional regulatory pathways that underlie the identity and diversity of mouse tissue macrophages. Nat. Immunol. *13*, 1118–1128.

Geissmann, F., Jung, S., and Littman, D.R. (2003). Blood monocytes consist of two principal subsets with distinct migratory properties. Immunity *19*, 71–82.

Gertig, U., and Hanisch, U.-K. (2014). Microglial diversity by responses and responders. Front. Cell. Neurosci. *8*, 101.

Ginhoux, F., Greter, M., Leboeuf, M., Nandi, S., See, P., Gokhan, S., Mehler, M.F., Conway, S.J., Ng, L.G., Stanley, E.R., et al. (2010). Fate mapping analysis reveals that adult microglia derive from primitive macrophages. Science *330*, 841–845.

Gioannini, T.L., Teghanemt, A., Zhang, D., Coussens, N.P., Dockstader, W., Ramaswamy, S., and Weiss, J.P. (2004). Isolation of an endotoxin–MD-2 complex that produces Toll-like receptor 4-dependent cell activation at picomolar concentrations. Proc. Natl. Acad. Sci. *101*, 4186–4191.

Glezer, I., Zekki, H., Scavone, C., and Rivest, S. (2003a). Modulation of the innate immune response by NMDA receptors has neuropathological consequences. J. Neurosci. Off. J. Soc. Neurosci. *23*, 11094–11103.

Glezer, I., Zekki, H., Scavone, C., and Rivest, S. (2003b). Modulation of the Innate Immune Response by NMDA Receptors Has Neuropathological Consequences. J. Neurosci. *23*, 11094–11103.

Glode, M.P., Sutton, A., Robbins, J.B., McCracken, G.H., Gotschlich, E.C., Kaijser, B., and Hanson, L.A. (1977). Neonatal meningitis due of Escherichia coli K1. J. Infect. Dis. *136 Suppl*, S93–97.

Golenbock, D.T., Bach, R.R., Lichenstein, H., Juan, T.S., Tadavarthy, A., and Moldow, C.F. (1995). Soluble CD14 promotes LPS activation of CD14-deficient PNH monocytes and endothelial cells. J. Lab. Clin. Med. *125*, 662–671.

González-Navajas, J.M., Lee, J., David, M., and Raz, E. (2012). Immunomodulatory functions of type I interferons. Nat. Rev. Immunol.

Goos, M., Lange, P., Hanisch, U.-K., Prinz, M., Scheffel, J., Bergmann, R., Ebert, S., and Nau, R. (2007). Fibronectin is elevated in the cerebrospinal fluid of patients suffering from bacterial meningitis and enhances inflammation caused by bacterial products in primary mouse microglial cell cultures. J. Neurochem. *102*, 2049–2060.

Gordon, S., and Taylor, P.R. (2005). Monocyte and macrophage heterogeneity. Nat. Rev. Immunol. *5*, 953–964.

Gorina, R., Font-Nieves, M., Márquez-Kisinousky, L., Santalucia, T., and Planas, A.M. (2011). Astrocyte TLR4 activation induces a proinflammatory environment through the interplay between MyD88-dependent NFκB signaling, MAPK, and Jak1/Stat1 pathways. Glia *59*, 242–255.

Goyert, S.M., Ferrero, E.M., Seremetis, S.V., Winchester, R.J., Silver, J., and Mattison, A.C. (1986). Biochemistry and expression of myelomonocytic antigens. J. Immunol. Baltim. Md 1950 *137*, 3909–3914.

Grønberg, N.V., Johansen, F.F., Kristiansen, U., and Hasseldam, H. (2013). Leukocyte infiltration in experimental stroke. J. Neuroinflammation *10*, 115.

Hanisch, U.-K. (2012). Factors Controlling Microglial Activation. In Neuroglia, H. Kettenmann, ed. (Oxford University Press),.

Hanisch, U.-K. (2013). Functional diversity of microglia – how heterogeneous are they to begin with? Front. Cell. Neurosci. *7*, 65.

Hanisch, U.-K., and Kettenmann, H. (2007). Microglia: active sensor and versatile effector cells in the normal and pathologic brain. Nat. Neurosci. *10*, 1387–1394.

Hanke, M.L., and Kielian, T. (2011). Toll-like receptors in health and disease in the brain: mechanisms and therapeutic potential. Clin. Sci. Lond. Engl. 1979 *121*, 367–387.

Hashimoto, D., Chow, A., Noizat, C., Teo, P., Beasley, M.B., Leboeuf, M., Becker, C.D., See, P., Price, J., Lucas, D., et al. (2013). Tissue-resident macrophages self-maintain locally throughout adult life with minimal contribution from circulating monocytes. Immunity *38*, 792–804.

Haziot, A., Ferrero, E., Köntgen, F., Hijiya, N., Yamamoto, S., Silver, J., Stewart, C.L., and Goyert, S.M. (1996). Resistance to endotoxin shock and reduced dissemination of gram-negative bacteria in CD14-deficient mice. Immunity *4*, 407–414.

Haziot, A., Hijiya, N., Gangloff, S.C., Silver, J., and Goyert, S.M. (2001). Induction of a novel mechanism of accelerated bacterial clearance by lipopolysaccharide in CD14-deficient and Toll-like receptor 4-deficient mice. J. Immunol. Baltim. Md 1950 *166*, 1075–1078.

Hertz, C.J., Kiertscher, S.M., Godowski, P.J., Bouis, D.A., Norgard, M.V., Roth, M.D., and Modlin, R.L. (2001). Microbial Lipopeptides Stimulate Dendritic Cell Maturation Via Toll-Like Receptor 2. J. Immunol. *166*, 2444–2450.

Hodgkinson, C.P., Patel, K., and Ye, S. (2008). Functional Toll-like receptor 4 mutations modulate the response to fibrinogen. Thromb. Haemost. *100*, 301–307.

Husebye, H., Halaas, Ø., Stenmark, H., Tunheim, G., Sandanger, Ø., Bogen, B., Brech, A., Latz, E., and Espevik, T. (2006). Endocytic pathways regulate Toll-like receptor 4 signaling and link innate and adaptive immunity. EMBO J. *25*, 683–692.

Husebye, H., Aune, M.H., Stenvik, J., Samstad, E., Skjeldal, F., Halaas, O., Nilsen, N.J., Stenmark, H., Latz, E., Lien, E., et al. (2010). The Rab11a GTPase controls Toll-like receptor 4-induced activation of interferon regulatory factor-3 on phagosomes. Immunity *33*, 583–596.

Iadecola, C., and Anrather, J. (2011). The immunology of stroke: from mechanisms to translation. Nat. Med. *17*, 796–808.

Jiang, Z., Georgel, P., Du, X., Shamel, L., Sovath, S., Mudd, S., Huber, M., Kalis, C., Keck, S., Galanos, C., et al. (2005). CD14 is required for MyD88-independent LPS signaling. Nat. Immunol. *6*, 565–570.

Kagan, J.C., Su, T., Horng, T., Chow, A., Akira, S., and Medzhitov, R. (2008). TRAM couples endocytosis of Toll-like receptor 4 to the induction of interferon-beta. Nat. Immunol. *9*, 361–368.

Kantari, C., Pederzoli-Ribeil, M., and Witko-Sarsat, V. (2008). The role of neutrophils and monocytes in innate immunity. Contrib. Microbiol. *15*, 118–146.

Katchanov, J., Harms, C., Gertz, K., Hauck, L., Waeber, C., Hirt, L., Priller, J., von Harsdorf, R., Bruck, W., Hortnagl, H., et al. (2001). Mild cerebral ischemia induces loss of cyclin-dependent kinase inhibitors and activation of cell cycle machinery before delayed neuronal cell death. J. Neurosci. Off. J. Soc. Neurosci. *21*, 5045–5053.

Kato, H., Takeuchi, O., Sato, S., Yoneyama, M., Yamamoto, M., Matsui, K., Uematsu, S., Jung, A., Kawai, T., Ishii, K.J., et al. (2006). Differential roles of MDA5 and RIG-I helicases in the recognition of RNA viruses. Nature *441*, 101–105.

Kawai, T., and Akira, S. (2010). The role of pattern-recognition receptors in innate immunity: update on Toll-like receptors. Nat. Immunol. *11*, 373–384.

Kawai, T., and Akira, S. (2011). Toll-like receptors and their crosstalk with other innate receptors in infection and immunity. Immunity *34*, 637–650.

Kawai, T., Takeuchi, O., Fujita, T., Inoue, J., Mühlradt, P.F., Sato, S., Hoshino, K., and Akira, S. (2001). Lipopolysaccharide stimulates the MyD88-independent pathway and results in activation of IFN-regulatory factor 3 and the expression of a subset of lipopolysaccharide-inducible genes. J. Immunol. Baltim. Md 1950 *167*, 5887–5894.

Kelley, S.L., Lukk, T., Nair, S.K., and Tapping, R.I. (2013). The Crystal Structure of Human Soluble CD14 Reveals a Bent Solenoid with a Hydrophobic Amino-Terminal Pocket. J. Immunol. *190*, 1304–1311.

Kempermann, G. (2008). The neurogenic reserve hypothesis: what is adult hippocampal neurogenesis good for? Trends Neurosci. *31*, 163–169.

Kettenmann, H., Hanisch, U.-K., Noda, M., and Verkhratsky, A. (2011). Physiology of microglia. Physiol. Rev. *91*, 461–553.

Kielian, T. (2009). Overview of toll-like receptors in the CNS. Curr. Top. Microbiol. Immunol. *336*, 1–14.

Kielian, T., Barry, B., and Hickey, W.F. (2001). CXC chemokine receptor-2 ligands are required for neutrophil-mediated host defense in experimental brain abscesses. J. Immunol. Baltim. Md 1950 *166*, 4634–4643.

Kierdorf, K., Erny, D., Goldmann, T., Sander, V., Schulz, C., Perdiguero, E.G., Wieghofer, P., Heinrich, A., Riemke, P., Hölscher, C., et al. (2013). Microglia emerge from erythromyeloid precursors via Pu.1- and Irf8-dependent pathways. Nat. Neurosci. *16*, 273–280.

Kim, S., Kim, S.Y., Pribis, J.P., Lotze, M., Mollen, K.P., Shapiro, R., Loughran, P., Scott, M.J., and Billiar, T.R. (2013). Signaling of high mobility group box 1 (HMGB1) through toll-like receptor 4 in macrophages requires CD14. Mol. Med. Camb. Mass *19*, 88–98.

Kim, W.G., Mohney, R.P., Wilson, B., Jeohn, G.H., Liu, B., and Hong, J.S. (2000). Regional difference in susceptibility to lipopolysaccharide-induced neurotoxicity in the rat brain: role of microglia. J. Neurosci. Off. J. Soc. Neurosci. *20*, 6309–6316.

Kirchhausen, T., Macia, E., and Pelish, H.E. (2008). Use of dynasore, the small molecule inhibitor of dynamin, in the regulation of endocytosis. Methods Enzymol. *438*, 77–93.

Knapp, S., Wieland, C.W., Florquin, S., Pantophlet, R., Dijkshoorn, L., Tshimbalanga, N., Akira, S., and van der Poll, T. (2006). Differential roles of CD14 and toll-like receptors 4 and 2 in murine Acinetobacter pneumonia. Am. J. Respir. Crit. Care Med. *173*, 122–129.

Kolaczkowska, E., and Kubes, P. (2013). Neutrophil recruitment and function in health and inflammation. Nat. Rev. Immunol. *13*, 159–175.

Lacroix, S., Feinstein, D., and Rivest, S. (1998). The bacterial endotoxin lipopolysaccharide has the ability to target the brain in upregulating its membrane CD14 receptor within specific cellular populations. Brain Pathol. Zurich Switz. *8*, 625–640.

Landmann, R., Ludwig, C., Obrist, R., and Obrecht, J.P. (1991). Effect of cytokines and lipopolysaccharide on CD14 antigen expression in human monocytes and macrophages. J. Cell. Biochem. *47*, 317–329.

Landmann, R., Knopf, H.P., Link, S., Sansano, S., Schumann, R., and Zimmerli, W. (1996). Human monocyte CD14 is upregulated by lipopolysaccharide. Infect. Immun. *64*, 1762–1769.

Landmann, R., Müller, B., and Zimmerli, W. (2000). CD14, new aspects of ligand and signal diversity. Microbes Infect. Inst. Pasteur *2*, 295–304.

Langfelder, P., and Horvath, S. (2008). WGCNA: an R package for weighted correlation network analysis. BMC Bioinformatics *9*, 559.

Lawson, L.J., Perry, V.H., Dri, P., and Gordon, S. (1990). Heterogeneity in the distribution and morphology of microglia in the normal adult mouse brain. Neuroscience *39*, 151–170.

Lee, H.-K., Dunzendorfer, S., Soldau, K., and Tobias, P.S. (2006). Double-stranded RNA-mediated TLR3 activation is enhanced by CD14. Immunity *24*, 153–163.

Lehnardt, S., Lachance, C., Patrizi, S., Lefebvre, S., Follett, P.L., Jensen, F.E., Rosenberg, P.A., Volpe, J.J., and Vartanian, T. (2002). The Toll-Like Receptor TLR4 Is Necessary for Lipopolysaccharide-Induced Oligodendrocyte Injury in the CNS. J. Neurosci. *22*, 2478–2486.

Lehnardt, S., Massillon, L., Follett, P., Jensen, F.E., Ratan, R., Rosenberg, P.A., Volpe, J.J., and Vartanian, T. (2003). Activation of innate immunity in the CNS triggers neurodegeneration through a Toll-like receptor 4-dependent pathway. Proc. Natl. Acad. Sci. U. S. A. *100*, 8514–8519.

Lin, K.L., Suzuki, Y., Nakano, H., Ramsburg, E., and Gunn, M.D. (2008). CCR2+ monocyte-derived dendritic cells and exudate macrophages produce influenza-induced pulmonary immune pathology and mortality. J. Immunol. Baltim. Md 1950 *180*, 2562–2572.

Ling, G.S., Bennett, J., Woollard, K.J., Szajna, M., Fossati-Jimack, L., Taylor, P.R., Scott, D., Franzoso, G., Cook, H.T., and Botto, M. (2014). Integrin CD11b positively regulates TLR4-induced signalling pathways in dendritic cells but not in macrophages. Nat. Commun. *5*.

Liu, Y., Walter, S., Stagi, M., Cherny, D., Letiembre, M., Schulz-Schaeffer, W., Heine, H., Penke, B., Neumann, H., and Fassbender, K. (2005). LPS receptor (CD14): a receptor for phagocytosis of Alzheimer's amyloid peptide. Brain J. Neurol. *128*, 1778–1789.

London, A., Itskovich, E., Benhar, I., Kalchenko, V., Mack, M., Jung, S., and Schwartz, M. (2011). Neuroprotection and progenitor cell renewal in the injured adult murine retina requires healing monocyte-derived macrophages. J. Exp. Med. *208*, 23–39.

London, A., Cohen, M., and Schwartz, M. (2013a). Microglia and monocyte-derived macrophages: functionally distinct populations that act in concert in CNS plasticity and repair. Front. Cell. Neurosci. *7*, 34.

London, A., Benhar, I., Mattapallil, M.J., Mack, M., Caspi, R.R., and Schwartz, M. (2013b). Functional macrophage heterogeneity in a mouse model of autoimmune central nervous system pathology. J. Immunol. Baltim. Md 1950 *190*, 3570–3578.

Matsuo, Y., Kihara, T., Ikeda, M., Ninomiya, M., Onodera, H., and Kogure, K. (1995). Role of neutrophils in radical production during ischemia and reperfusion of the rat brain: effect of neutrophil depletion on extracellular ascorbyl radical formation. J. Cereb. Blood Flow Metab. Off. J. Int. Soc. Cereb. Blood Flow Metab. *15*, 941–947.

Matzinger, P. (1994). Tolerance, danger, and the extended family. Annu. Rev. Immunol. *12*, 991–1045.

Matzinger, P. (2002). The Danger Model: A Renewed Sense of Self. Science *296*, 301–305.

McAvoy, E.F., McDonald, B., Parsons, S.A., Wong, C.H., Landmann, R., and Kubes, P. (2011). The role of CD14 in neutrophil recruitment within the liver microcirculation during endotoxemia. J. Immunol. Baltim. Md 1950 *186*, 2592–2601.

McDonald, B., Pittman, K., Menezes, G.B., Hirota, S.A., Slaba, I., Waterhouse, C.C.M., Beck, P.L., Muruve, D.A., and Kubes, P. (2010). Intravascular danger signals guide neutrophils to sites of sterile inflammation. Science *330*, 362–366.

McGettrick, A.F., and O'Neill, L.A.J. (2007). Toll-like receptors: key activators of leucocytes and regulator of haematopoiesis. Br. J. Haematol. *139*, 185–193.

Midwood, K.S., Piccinini, A.M., and Sacre, S. (2009). Targeting Toll-like receptors in autoimmunity. Curr. Drug Targets *10*, 1139–1155.

Moore, K.J., Andersson, L.P., Ingalls, R.R., Monks, B.G., Li, R., Arnaout, M.A., Golenbock, D.T., and Freeman, M.W. (2000). Divergent response to LPS and bacteria in CD14-deficient murine macrophages. J. Immunol. Baltim. Md 1950 *165*, 4272–4280.

Mosser, D.M., and Edwards, J.P. (2008). Exploring the full spectrum of macrophage activation. Nat. Rev. Immunol. *8*, 958–969.

Murray, P.J., and Wynn, T.A. (2011). Protective and pathogenic functions of macrophage subsets. Nat. Rev. Immunol. *11*, 723–737.

Nahrendorf, M., Swirski, F.K., Aikawa, E., Stangenberg, L., Wurdinger, T., Figueiredo, J.-L., Libby, P., Weissleder, R., and Pittet, M.J. (2007). The healing myocardium sequentially mobilizes two monocyte subsets with divergent and complementary functions. J. Exp. Med. *204*, 3037–3047.

Neumann, J., Gunzer, M., Gutzeit, H.O., Ullrich, O., Reymann, K.G., and Dinkel, K. (2006). Microglia provide neuroprotection after ischemia. FASEB J.

Nimmerjahn, A., Kirchhoff, F., and Helmchen, F. (2005). Resting microglial cells are highly dynamic surveillants of brain parenchyma in vivo. Science *308*, 1314–1318.

Okada, Y., Copeland, B.R., Mori, E., Tung, M.M., Thomas, W.S., and del Zoppo, G.J. (1994). P-selectin and intercellular adhesion molecule-1 expression after focal brain ischemia and reperfusion. Stroke J. Cereb. Circ. *25*, 202–211.

Opal, S.M., Palardy, J.E., Parejo, N., and Jasman, R.L. (2003). Effect of anti-CD14 monoclonal antibody on clearance of Escherichia coli bacteremia and endotoxemia. Crit. Care Med. *31*, 929–932.

Ortega-Gómez, A., Perretti, M., and Soehnlein, O. (2013). Resolution of inflammation: an integrated view. EMBO Mol. Med. *5*, 661–674.

Pagano, M., and Reboud-Ravaux, M. (2011). Cryptic activities of fibronectin fragments, particularly cryptic proteases. Front. Biosci. Landmark Ed. *16*, 698–706.

Pal, D., Dasgupta, S., Kundu, R., Maitra, S., Das, G., Mukhopadhyay, S., Ray, S., Majumdar, S.S., and Bhattacharya, S. (2012). Fetuin-A acts as an endogenous ligand of TLR4 to promote lipid-induced insulin resistance. Nat. Med. *18*, 1279–1285.

Pankov, R., and Yamada, K.M. (2002). Fibronectin at a glance. J. Cell Sci. *115*, 3861–3863.

Paolicelli, R.C., Bolasco, G., Pagani, F., Maggi, L., Scianni, M., Panzanelli, P., Giustetto, M., Ferreira, T.A., Guiducci, E., Dumas, L., et al. (2011). Synaptic Pruning by Microglia Is Necessary for Normal Brain Development. Science *333*, 1456–1458.

Park, B.S., and Lee, J.-O. (2013). Recognition of lipopolysaccharide pattern by TLR4 complexes. Exp. Mol. Med. *45*, e66.

Park, J.S., Svetkauskaite, D., He, Q., Kim, J.-Y., Strassheim, D., Ishizaka, A., and Abraham, E. (2004). Involvement of toll-like receptors 2 and 4 in cellular activation by high mobility group box 1 protein. J. Biol. Chem. *279*, 7370–7377.

Park, J.S., Gamboni-Robertson, F., He, Q., Svetkauskaite, D., Kim, J.-Y., Strassheim, D., Sohn, J.-W., Yamada, S., Maruyama, I., Banerjee, A., et al. (2006). High mobility group box 1 protein interacts with multiple Toll-like receptors. Am. J. Physiol. Cell Physiol. *290*, C917–924.

Parkhurst, C.N., Yang, G., Ninan, I., Savas, J.N., Yates, J.R., Lafaille, J.J., Hempstead, B.L., Littman, D.R., and Gan, W.-B. (2013). Microglia Promote Learning-Dependent Synapse Formation through Brain-Derived Neurotrophic Factor. Cell *155*, 1596–1609.

Pasare, C., and Medzhitov, R. (2004). Toll-dependent control mechanisms of CD4 T cell activation. Immunity *21*, 733–741.

Payne, J.B., Nichols, F.C., and Peluso, J.F. (1992). The effects of interferon-gamma and bacterial lipopolysaccharide on CD14 expression in human monocytes. J. Interferon Res. *12*, 307–310.

Pillay, J., den Braber, I., Vrisekoop, N., Kwast, L.M., de Boer, R.J., Borghans, J.A.M., Tesselaar, K., and Koenderman, L. (2010). In vivo labeling with 2H2O reveals a human neutrophil lifespan of 5.4 days. Blood *116*, 625–627.

Platanias, L.C. (2005). Mechanisms of type-I- and type-II-interferon-mediated signalling. Nat. Rev. Immunol. *5*, 375–386.

Prass, K., Meisel, C., Höflich, C., Braun, J., Halle, E., Wolf, T., Ruscher, K., Victorov, I.V., Priller, J., Dirnagl, U., et al. (2003). Stroke-induced immunodeficiency promotes spontaneous bacterial infections and is mediated by sympathetic activation reversal by poststroke T helper cell type 1-like immunostimulation. J. Exp. Med. *198*, 725–736.

Priller, J., Flügel, A., Wehner, T., Boentert, M., Haas, C.A., Prinz, M., Fernández-Klett, F., Prass, K., Bechmann, I., de Boer, B.A., et al. (2001). Targeting gene-modified hematopoietic cells to the central nervous system: Use of green fluorescent protein uncovers microglial engraftment. Nat. Med. *7*, 1356–1361.

Pugin, J., Schurer-Maly, C.C., Leturcq, D., Moriarty, A., Ulevitch, R.J., and Tobias, P.S. (1993). Lipopolysaccharide activation of human endothelial and epithelial cells is mediated by lipopolysaccharide-binding protein and soluble CD14. Proc. Natl. Acad. Sci. U. S. A. *90*, 2744–2748.

Raetz, C.R.H., and Whitfield, C. (2002). Lipopolysaccharide Endotoxins. Annu. Rev. Biochem. *71*, 635–700.

Reed-Geaghan, E.G., Savage, J.C., Hise, A.G., and Landreth, G.E. (2009). CD14 and toll-like receptors 2 and 4 are required for fibrillar A{beta}-stimulated microglial activation. J. Neurosci. Off. J. Soc. Neurosci. *29*, 11982–11992.

Regen, T., van Rossum, D., Scheffel, J., Kastriti, M.-E., Revelo, N.H., Prinz, M., Brück, W., and Hanisch, U.-K. (2011). CD14 and TRIF govern distinct responsiveness and responses in mouse microglial TLR4 challenges by structural variants of LPS. Brain. Behav. Immun. *25*, 957–970.

Ribes, S., Ebert, S., Czesnik, D., Regen, T., Zeug, A., Bukowski, S., Mildner, A., Eiffert, H., Hanisch, U.-K., Hammerschmidt, S., et al. (2009). Toll-Like Receptor Prestimulation Increases Phagocytosis of Escherichia coli DH5α and Escherichia coli K1 Strains by Murine Microglial Cells. Infect. Immun. *77*, 557–564.

Ribes, S., Adam, N., Schütze, S., Regen, T., Redlich, S., Janova, H., Borisch, A., Hanisch, U.-K., and Nau, R. (2012). The nucleotide-binding oligomerization domain-containing-2 ligand muramyl dipeptide enhances phagocytosis and intracellular killing of Escherichia coli K1 by Toll-like receptor agonists in microglial cells. J. Neuroimmunol. *252*, 16–23.

Ribes, S., Meister, T., Ott, M., Redlich, S., Janova, H., Hanisch, U.-K., Nessler, S., and Nau, R. (2014). Intraperitoneal prophylaxis with CpG oligodeoxynucleotides protects neutropenic mice against intracerebral Escherichia coli K1 infection. J. Neuroinflammation *11*, 14.

Rittner, H.L., Mousa, S.A., Labuz, D., Beschmann, K., Schäfer, M., Stein, C., and Brack, A. (2006). Selective local PMN recruitment by CXCL1 or CXCL2/3 injection does not cause inflammatory pain. J. Leukoc. Biol. *79*, 1022–1032.

Rivest, S. (2009). Regulation of innate immune responses in the brain. Nat. Rev. Immunol. *9*, 429–439.

Robinson, M.D., McCarthy, D.J., and Smyth, G.K. (2010). edgeR: a Bioconductor package for differential expression analysis of digital gene expression data. Bioinforma. Oxf. Engl. *26*, 139–140.

Roy, D.L., Padova, F.D., Adachi, Y., Glauser, M.P., Calandra, T., and Heumann, D. (2001). Critical Role of Lipopolysaccharide-Binding Protein and CD14 in Immune Responses against Gram-Negative Bacteria. J. Immunol. *167*, 2759–2765.

Rubartelli, A., and Lotze, M.T. (2007). Inside, outside, upside down: damage-associated molecular-pattern molecules (DAMPs) and redox. Trends Immunol. *28*, 429–436.

Sadik, C.D., Kim, N.D., and Luster, A.D. (2011). Neutrophils cascading their way to inflammation. Trends Immunol. *32*, 452–460.

Sahay, B., Patsey, R.L., Eggers, C.H., Salazar, J.C., Radolf, J.D., and Sellati, T.J. (2009). CD14 Signaling Restrains Chronic Inflammation through Induction of p38-MAPK/SOCS-Dependent Tolerance. PLoS Pathog *5*, e1000687.

Schafer, D.P., Lehrman, E.K., Kautzman, A.G., Koyama, R., Mardinly, A.R., Yamasaki, R., Ransohoff, R.M., Greenberg, M.E., Barres, B.A., and Stevens, B. (2012). Microglia sculpt postnatal neural circuits in an activity and complement-dependent manner. Neuron *74*, 691–705.

Scheffel, J., Regen, T., Van Rossum, D., Seifert, S., Ribes, S., Nau, R., Parsa, R., Harris, R.A., Boddeke, H.W.G.M., Chuang, H.-N., et al. (2012). Toll-like receptor activation reveals developmental reorganization and unmasks responder subsets of microglia. Glia *60*, 1930–1943.

Schilling, M., Strecker, J.-K., Schäbitz, W.-R., Ringelstein, E.B., and Kiefer, R. (2009). Effects of monocyte chemoattractant protein 1 on blood-borne cell recruitment after transient focal cerebral ischemia in mice. Neuroscience *161*, 806–812.

Schröder, N.W.J., Morath, S., Alexander, C., Hamann, L., Hartung, T., Zähringer, U., Göbel, U.B., Weber, J.R., and Schumann, R.R. (2003). Lipoteichoic Acid (LTA) of Streptococcus pneumoniaeand Staphylococcus aureus Activates Immune Cells via Toll-like Receptor (TLR)-2, Lipopolysaccharide-binding Protein (LBP), and CD14, whereas TLR-4 and MD-2 Are Not Involved. J. Biol. Chem. *278*, 15587–15594.

Schulz, C., Gomez Perdiguero, E., Chorro, L., Szabo-Rogers, H., Cagnard, N., Kierdorf, K., Prinz, M., Wu, B., Jacobsen, S.E.W., Pollard, J.W., et al. (2012). A lineage of myeloid cells independent of Myb and hematopoietic stem cells. Science *336*, 86–90.

Schwartz, M., Butovsky, O., Brück, W., and Hanisch, U.-K. (2006). Microglial phenotype: is the commitment reversible? Trends Neurosci. *29*, 68–74.

Shen, H., Kreisel, D., and Goldstein, D.R. (2013). Processes of Sterile Inflammation. J. Immunol. *191*, 2857–2863.

Shi, C., and Pamer, E.G. (2011). Monocyte recruitment during infection and inflammation. Nat. Rev. Immunol. *11*, 762–774.

Sierra, A., Encinas, J.M., Deudero, J.J.P., Chancey, J.H., Enikolopov, G., Overstreet-Wadiche, L.S., Tsirka, S.E., and Maletic-Savatic, M. (2010). Microglia shape adult hippocampal neurogenesis through apoptosis-coupled phagocytosis. Cell Stem Cell *7*, 483–495.

Sierra, A., Abiega, O., Shahraz, A., and Neumann, H. (2013). Janus-faced microglia: beneficial and detrimental consequences of microglial phagocytosis. Front. Cell. Neurosci. *7*.

Simard, A.R., Soulet, D., Gowing, G., Julien, J.-P., and Rivest, S. (2006). Bone marrow-derived microglia play a critical role in restricting senile plaque formation in Alzheimer's disease. Neuron *49*, 489–502.

Smiley, S.T., King, J.A., and Hancock, W.W. (2001). Fibrinogen stimulates macrophage chemokine secretion through toll-like receptor 4. J. Immunol. Baltim. Md 1950 *167*, 2887–2894.

Soehnlein, O., and Lindbom, L. (2010). Phagocyte partnership during the onset and resolution of inflammation. Nat. Rev. Immunol. *10*, 427–439.

Sörensen, M., Lippuner, C., Kaiser, T., Mißlitz, A., Aebischer, T., and Bumann, D. (2003). Rapidly maturing red fluorescent protein variants with strongly enhanced brightness in bacteria. FEBS Lett. *552*, 110–114.

Stewart, C.R., Stuart, L.M., Wilkinson, K., van Gils, J.M., Deng, J., Halle, A., Rayner, K.J., Boyer, L., Zhong, R., Frazier, W.A., et al. (2010). CD36 ligands promote sterile inflammation through assembly of a Toll-like receptor 4 and 6 heterodimer. Nat. Immunol. *11*, 155–161.

Stoffels, J.M.J., Jonge, J.C. de, Stancic, M., Nomden, A., Strien, M.E. van, Ma, D., Šišková, Z., Maier, O., ffrench-Constant, C., Franklin, R.J.M., et al. (2013). Fibronectin aggregation in multiple sclerosis lesions impairs remyelination. Brain *136*, 116–131.

Sunderkötter, C., Nikolic, T., Dillon, M.J., Van Rooijen, N., Stehling, M., Drevets, D.A., and Leenen, P.J.M. (2004). Subpopulations of mouse blood monocytes differ in maturation stage and inflammatory response. J. Immunol. Baltim. Md 1950 *172*, 4410–4417.

Tapping, R.I., and Tobias, P.S. (2000). Soluble CD14-mediated cellular responses to lipopolysaccharide. Chem. Immunol. *74*, 108–121.

Tasaka, S., Ishizaka, A., Yamada, W., Shimizu, M., Koh, H., Hasegawa, N., Adachi, Y., and Yamaguchi, K. (2003). Effect of CD14 blockade on endotoxin-induced acute lung injury in mice. Am. J. Respir. Cell Mol. Biol. *29*, 252–258.

Tremblay, M.-È., Stevens, B., Sierra, A., Wake, H., Bessis, A., and Nimmerjahn, A. (2011). The role of microglia in the healthy brain. J. Neurosci. Off. J. Soc. Neurosci. *31*, 16064–16069.

Triantafilou, M., and Triantafilou, K. (2002). Lipopolysaccharide recognition: CD14, TLRs and the LPS-activation cluster. Trends Immunol. *23*, 301–304.

Trinchieri, G. (2010). Type I interferon: friend or foe? J. Exp. Med. *207*, 2053–2063.

Tsou, C.-L., Peters, W., Si, Y., Slaymaker, S., Aslanian, A.M., Weisberg, S.P., Mack, M., and Charo, I.F. (2007). Critical roles for CCR2 and MCP-3 in monocyte mobilization from bone marrow and recruitment to inflammatory sites. J. Clin. Invest. *117*, 902–909.

Wake, H., Moorhouse, A.J., Jinno, S., Kohsaka, S., and Nabekura, J. (2009). Resting microglia directly monitor the functional state of synapses in vivo and determine the fate of ischemic terminals. J. Neurosci. Off. J. Soc. Neurosci. *29*, 3974–3980.

Wang, Y.-C., Lin, S., and Yang, Q.-W. (2011). Toll-like receptors in cerebral ischemic inflammatory injury. J. Neuroinflammation *8*, 134.

Wang, Y.-C., Zhou, Y., Fang, H., Lin, S., Wang, P.-F., Xiong, R.-P., Chen, J., Xiong, X.-Y., Lv, F.-L., Liang, Q.-L., et al. (2014). Toll-like receptor 2/4 heterodimer mediates inflammatory injury in intracerebral hemorrhage. Ann. Neurol. *75*, 876–889.

Weber, C., Müller, C., Podszuweit, A., Montino, C., Vollmer, J., and Forsbach, A. (2012). Toll-like receptor (TLR) 3 immune modulation by unformulated small interfering RNA or DNA and the role of CD14 (in TLR-mediated effects). Immunology *136*, 64–77.

Weighardt, H., Kaiser-Moore, S., Schlautkötter, S., Rossmann-Bloeck, T., Schleicher, U., Bogdan, C., and Holzmann, B. (2006). Type I IFN modulates host defense and late hyperinflammation in septic peritonitis. J. Immunol. Baltim. Md 1950 *177*, 5623–5630.

Wiersinga, W.J., de Vos, A.F., Wieland, C.W., Leendertse, M., Roelofs, J.J.T.H., and van der Poll, T. (2008). CD14 impairs host defense against gram-negative sepsis caused by Burkholderia pseudomallei in mice. J. Infect. Dis. *198*, 1388–1397.

Wright, S.D., Ramos, R.A., Tobias, P.S., Ulevitch, R.J., and Mathison, J.C. (1990). CD14, a receptor for complexes of lipopolysaccharide (LPS) and LPS binding protein. Science *249*, 1431–1433.

Xing, B., Bachstetter, A.D., and Eldik, L.J.V. (2011). Microglial p38α MAPK is critical for LPS-induced neuron degeneration, through a mechanism involving TNFα. Mol. Neurodegener. *6*, 84.

Yin, G.N., Jeon, H., Lee, S., Lee, H.W., Cho, J.-Y., and Suk, K. (2009). Role of soluble CD14 in cerebrospinal fluid as a regulator of glial functions. J. Neurosci. Res. *87*, 2578–2590.

Yoshimura, A., Lien, E., Ingalls, R.R., Tuomanen, E., Dziarski, R., and Golenbock, D. (1999). Cutting edge: recognition of Gram-positive bacterial cell wall components by the innate immune system occurs via Toll-like receptor 2. J. Immunol. Baltim. Md 1950 *163*, 1–5.

Yoshimura, A., Naka, T., and Kubo, M. (2007). SOCS proteins, cytokine signalling and immune regulation. Nat. Rev. Immunol. *7*, 454–465.

Yoshioka, N., Taniguchi, Y., Yoshida, A., Nakata, K., Nishizawa, T., Inagawa, H., Kohchi, C., and Soma, G.-I. (2009). Intracellular localization of CD14 protein in intestinal macrophages. Anticancer Res. *29*, 865–869.

Yu, M., Wang, H., Ding, A., Golenbock, D.T., Latz, E., Czura, C.J., Fenton, M.J., Tracey, K.J., and Yang, H. (2006). HMGB1 signals through toll-like receptor (TLR) 4 and TLR2. Shock Augusta Ga *26*, 174–179.

Zanoni, I., and Granucci, F. (2013a). Role of CD14 in host protection against infections and in metabolism regulation. Front. Cell. Infect. Microbiol. *3*.

Zanoni, I., and Granucci, F. (2013b). Role of CD14 in host protection against infections and in metabolism regulation. Front. Cell. Infect. Microbiol. *3*, 32.

Zanoni, I., Ostuni, R., Capuano, G., Collini, M., Caccia, M., Ronchi, A.E., Rocchetti, M., Mingozzi, F., Foti, M., Chirico, G., et al. (2009). CD14 regulates the dendritic cell life cycle after LPS exposure through NFAT activation. Nature *460*, 264–268.

Zanoni, I., Ostuni, R., Marek, L.R., Barresi, S., Barbalat, R., Barton, G.M., Granucci, F., and Kagan, J.C. (2011). CD14 controls the LPS-induced endocytosis of Toll-like receptor 4. Cell *147*, 868–880.

Zhan, Y., Paolicelli, R.C., Sforazzini, F., Weinhard, L., Bolasco, G., Pagani, F., Vyssotski, A.L., Bifone, A., Gozzi, A., Ragozzino, D., et al. (2014). Deficient neuron-microglia signaling results in impaired functional brain connectivity and social behavior. Nat. Neurosci. *17*, 400–406.

Acknowledgment

I would like to especially thank to my supervisor Prof. Uwe K. Hanisch. Not only was he a great boss, but also a great teacher, who has been helping to improve myself since the very beginning. I have to thank him for his endless patience that he had with me and with my rather chaotic behavior. I really do appreciate that he has been treating me (especially lately) as a truly partner, believing in me and my opinions. On the other hand, we all (our group) will probably always be his kids (another girls in addition to his family). I will never forget sitting next to him at that small stool (Hocker), discussing the new findings and listening to the great stories from his life, thinking that if "he will not become a scientist, once he grows up", he should definitely go to entertainment industry…

I also would like to thank to Prof. Wolfgang Brück as to the member of my Theses Committee and also as to the head of the Neuropathology Department for giving me the opportunity to work in his department. Special thanks also to the other member of my Thesis Committee, Prof. Hannelore Ehrenreich for the fruitful discussions and for giving me the chance to meet Prof. Uwe K. Hanisch at the workshops organized by her group.

Special thanks have to go to our team, Ulla Gertig, Nasrin Saiepour, Christin Fritsche, Elke Pralle and Susanne Kiecke who not only helped me with the laboratory work, but also supported me and were taking care of me, once the working days got a bit tougher. However, I also have to thank to the former members of our laboratory, Dr. Denise van Rossum, Dr. Tommy Regen and Dr. Christiane Menzfeld. Because of them I was able to accommodate myself in Göttingen (and not only in the laboratory☺).

Since I had the opportunity to do some experiments in Berlin at Charite, I cannot forget to thank to Prof. Josef Priller, Dr. Chotima Bötcher and Peggy Mex for the very pleasant and successful collaboration and for the wonderful job that they did for us.

I also would like to thank to Konrad Gronke and Anne-Sophie Ernst who were for a short period in our laboratory but substantially contributed to my work.

I also cannot forget to thank to the colleagues from the neuropathology department, especially to Verena Schultz, Sarah Trafffehn, Insa Damann and Sandra Ribes.

Truly great thanks must go to my family, my Daddy (Miroslav Jane) and my Mum (Hana Janova). They were always there for me, when I desperately needed them and they helped and supported me in whatever I decided to do. Especially my mother revealed to be my best friend and almost a professional coach! As almost part of my family, Jan Spiler deserves huge thanks for everything he did and how he did it. I will most probably not be where I am now without him by my side…

This work and the fruitful collaborations would not be possible without a funding from DGF – Research Unit 1336 and DFG – SFB TRR 43.

Curriculum Vitae

Education and Training

2008 – 2010	**Charles University in Prague, Faculty of Science** Prague, Czech Republic - Master's Studies program: Immunology - obtained Master's Degree
January – July 2009	**Cardiff University, School of Medicine** Cardiff, United Kingdom - Erasmus Program
2005 – 2008	**Charles University in Prague, Faculty of Science** Prague, Czech Republic - Bachelor's studies program: Molecular Biology and Biochemistry of Organisms - obtained Bachelor's Degree
1997 – 2005	**Czech Grammar School in Prague** Prague, Czech Republic - High school final exams: Czech language, English, Biology, Chemistry

Research Experience

2010 – present	**University Medical Center Göttingen, Georg-August-Universität** **Institute of Neuropathology** **Göttingen, Germany** Neuropathology Department (Supervisor: Prof. Uwe K. Hanisch) Area of research: *Organization and consequences of functional responses in microglia upon activation of the TLR4 complex.*
2007 – 2010	**Institute of Microbiology, Academy of Sciences of the Czech Republic** Prague, Czech Republic Laboratory of Molecular Biology of Bacterial Pathogens (Head of Lab: Peter Sebo, Ph.D., supervisor: Irena Adkins, PhD) Area of research: *Immunomodulation of dendritic cells by adenylate cyclase toxin from Bordetella pertussis.*
January – July 2009	**Cardiff University, School of Medicine** **Cardiff, United Kingdom** Neutrophil Signalling Group (Supervisor: Prof. Maurice Hallett) Area of research: *Change in intracellular calcium level during neutrophil phagocytosis.*
2003 – 2004	**Institute of Microbiology, Academy of Sciences of the Czech Republic** Extra-curricular high school scientific research ("Stredoskolska odborna cinnost") Area of research: *Production of heterogeneous penicillin G acylase by recombinant E. coli strain* Obtained award for excellent research project in 2004: 2nd in Prague, 6th – 7th in the Czech Republic

Publications

Hana Janova, Chotima Bötcher, Inge R. Holtman, Tommy Regen, Denise van Rossum, Alexander Götz, Anne-Sophie Ernst, Christin Fritsche, Ulla Gertig, Nasrin Saiepour, Konrad Gronke, Claudia Wrzos, Sandra Ribes, Simone Rolfes, Jonathan Weinstein, Hannelore Ehrenreich, Tobias Pukrop, Jens Kopatz, Christine Stadelmann-Nessler, Marco Prinz, Wolfgang Brück, Bart Eggen, Hendrikus W.G.M. Boddeke, Josef Priller and Uwe-Karsten Hanisch **CD14 is a key organizer in TLR4-mediated responses of microglia to CNS infection and damage** (manuscript in preparation)

Ribes, S., Meister, T., Ott, M., Redlich, S., **Janova, H**., Hanisch, U.-K., Nessler, S., and Nau, R. (2014). Intraperitoneal prophylaxis with CpG oligodeoxynucleotides protects neutropenic mice against intracerebral Escherichia coli K1 infection. J. Neuroinflammation *11*, 14. (Ribes et al., 2014)

Ribes, S., Adam, N., Schütze, S., Regen, T., Redlich, S., **Janova, H.**, Borisch, A., Hanisch, U.-K., and Nau, R. (2012). The nucleotide-binding oligomerization domain-containing-2 ligand muramyl dipeptide enhances phagocytosis and intracellular killing of Escherichia coli K1 by Toll-like receptor agonists in microglial cells. J. Neuroimmunol. *252*, 16–23. (Ribes et al., 2012)

Menzfeld, C., John M., van Rossum, D., Regen, T., Scheffel, J., **Janova, H.**, Götz, A., Ribes, S., Nau, R., Borisch, A., Boutin, P., Neumann, K., Bremes, V., Wienands, J., Reichardt, H.M., Lühder, F., Tischner, D., Waetzig, V., Herdegen, T., Teismann, P., Greig, I., Müller, M., Pukrop, T., Mildner, A., Kettenmann, H., Brück, W., Prinz, M., Rotshenker, S., Weber, M.S. and Hanisch, U.-K. (2014) Tyrphostin AG126 exerts neuroprotective effects on CNS autoimmunity and inflammation by a dual mechanism – (*for submission*)

Schaafsma, W., van Zomere,n K.C., Jacobs, S., Gorgieva, P., Wolf, S.A., Kttenmann, H., **Janova H.**, Hanisch, U.-K., van den Elsen, P.J., Brouwer, N., Boddeke, H.W.G.M., Eggen, B.J.L .(2014) LPS preconditioning-induced long-lasting inflammatory suppression in microglia is mediated by ReIB-induced epigenetic silencing –(*for submission)*

Adkins, I., Kamanova, J., Koucourkova, A., Svedova, M., Tomala, J., **Janova, H.**, Masin, J., Chladkova, B., Bumba, L., Kovar, M., Ross, J.P., Tuckova, L., Spisek, R., Mills, K.H.G. and Sebo, P. (2014) Bordetella adenylate cyclase toxin differentially modulates Toll-like receptor-stimulated activation, migration and T cell stimulatory capacity of dendritic cells– *(in press)*